# Mitigation of intrarenal pressure in retrograde intrarenal surgery with a novel isoprenaline eluting guidewire

A thesis submitted in the fulfillment
of the requirements for the degree of

## Doctor of Philosophy (Urology)

**Jeff John**
**(JHNJEF002)**
Division of Urology
Department of Surgery
Faculty of Health Sciences
University of Cape Town



Supervisor: Professor Lisa Kaestner
Co-Supervisors: Professor John Lazarus
Professor Graham Fieggen

**December 2024**

# Abstract

Urolithiasis ranks as the third most prevalent condition in urology, with statistical evidence indicating a lifetime risk of 13% in males and 7% in females, alongside a recurrence rate of 50% within a decade. The surgical care of urolithiasis is intricate, with various competing therapeutic techniques available, including retrograde intrarenal surgery (RIRS). Over the years, leading urological associations have progressively broadened the criteria for RIRS in the surgical treatment of urolithiasis. While it offers enhanced stone-free rates relative to shockwave lithotripsy and reduced patient morbidity compared to percutaneous nephrolithotomy, it is not devoid of problems, many of which are associated with intrarenal pressure (IRP).

To alleviate the challenges associated with increased IRP, surgeons may utilize diverse approaches to regulate IRP. Pharmacologic therapies in the perioperative period to mitigate IRP have been documented, although none of these strategies have been integrated into clinical practice. This thesis aims to report on the design, safety, and efficacy of an innovative isoprenaline-eluting guidewire (IsoWire), a platform guidewire intended for the administration of topical isoprenaline, a beta-receptor agonist, to the genitourinary system. This is the first study to report the delivery of isoprenaline using a drug-eluting guidewire.

This dissertation comprises six chapters. The initial five chapters each have an overview, abstract, introduction, methodology, results, discussion, and conclusion sections.

**Chapter 1** is a narrative literature review addressing the problems associated with high IRP and outlines techniques to mitigate elevated IRP in RIRS to promote safer endourological practices.

To prepare for our investigation on the porcine model, we required a simulation model to precisely outline the procedural steps. Commercially available models are expensive and not readily accessible. **Chapter 2** delineates the design and fabrication of the Frere Intrarenal Surgery Trainer (FiST) bench-top model. This chapter further elucidates its validation through the involvement of individuals with prior competence in the RIRS technique. This high-fidelity, cost-effective, portable, durable, and reusable training model is, to our knowledge, the inaugural published 3D model that integrates all components of RIRS, allowing us to meticulously optimise the procedural stages for our research.

The porcine model has frequently been utilized by researchers and urological surgeons for medical advancements. Despite the multiple advantages of this model, the specific anatomical knowledge that qualifies it as the optimal model in urology remains inadequately defined. In **Chapter 3**, we present the first reported study that precisely delineates pertinent endoscopic and CT-based urological anatomy of female Landrace pigs. The insights acquired from this research were essential for proceeding with the two studies described in Chapters 4 and 5. Furthermore, this unprecedented research will help other researchers use the porcine model to conduct research in endourology with confidence.

**Chapter 4** delineates the design of the IsoWire and examines the results of the preliminary in vitro release studies. Furthermore, we evaluated IsoWires of three distinct strengths, specifically wires that release 5 μg, 7.5 μg, and 10 μg in the first minute, respectively. Our investigation demonstrated that the IsoWire, which released 7.5 μg of isoprenaline within the initial minute, is safe, showing no alterations in mean arterial pressure (MAP), heart rate (HR), or other irregular electrocardiographic (ECG) abnormalities. Moreover, the in vitro release assays demonstrated that the IsoWire released all isoprenaline exponentially

within the initial 4 minutes.

**Chapter 5** delineates the impact of the IsoWire, which dispenses 7.5 μg of isoprenaline within the initial minute, on IRP, the duration of this effect, and its safety in a porcine model.

**Chapter 6** presents a conclusion and reflection on this thesis, emphasising its original contributions to the field of urology and addressing prospective avenues for future research.

# Declaration

I, Jeff John, solemnly declare that this thesis entitled "**Mitigation of intrarenal pressure in retrograde intrarenal surgery with a novel isoprenaline eluting guidewire**" is my original work, both in concept and execution (except where acknowledgements indicate otherwise). All sources used or quoted in the study have been indicated and acknowledged by way of complete references. Neither the whole work nor any part of it, has been, is being, or is to be submitted for another degree at this or any other university.

I confirm that I have been granted permission by the University of Cape Town's Doctoral Degrees Board to include the following publication(s) in my PhD thesis, and where co-authorships are involved, my co-authors have agreed that I may include the following publications:

1. John J, Wisniewski P, Fieggen G, Kaestner L, Lazarus J. Intrarenal pressure in retrograde intrarenal surgery: a narrative review. *Urology*. In press 2024. http://doi.org/10.1016/j.urology.2024.09.026.
2. John J, Wisniewski P, Fieggen G, Kaestner L, Lazarus J. Reply to Editorial Comment on "Intrarenal pressure in retrograde intrarenal surgery: a narrative review". *Urology*. In press 2024. http://doi.org/10.1016/j.urology.2024.10.036.
3. John J, Bosch J, Adam A, Fieggen G, Lazarus J, Kaestner L. Design and validation of a novel 3D-printed retrograde intrarenal surgery trainer. *Urology*. 2024 Sep;191:171-176. http://doi.org/10.1016/j.urology.2024.06.061.
4. John J, Wellman M, Dixon C, Kellermann T, Wisniewski P, Kopeć K, Trzciński J, Kopeć D, Ciach T, Fieggen G, Kaestner L, Lazarus J. Introducing an isoprenaline

eluting guidewire: report on its design and the results of the dose-determining pilot study. *J Endourol*. 2024 Jun;38(6):590-597. http://doi.org/10.1089/end.2023.0745.

5. John J, Wellman M, Kellermann T, Kopeć K, Ciach T, Fieggen G, Kaestner L, Lazarus J. Pharmacological modulation of intrarenal pressure in a porcine model using a novel isoprenaline-eluting guidewire. *J Endourol*. In press 2024. http://doi.org/10.1089/end.2024.0348.
6. John J, Fieggen G, Kaestner L, Lazarus J. The porcine model for urological research and training: an endoscopic and CT-based study. Submitted for publication (*World J Urol*).

I present this thesis for examination for the degree of PhD (Urology).

I grant the University of Cape Town a free license to reproduce the above thesis in whole or in part, for the purpose of research.

Signed by candidate

_____

**Dr Jeff John**

Division of Urology

Department of Surgery

Faculty of Health Sciences

University of Cape Town

Date: 1 December 2024

**Supervisor:**

Signed by candidate

_____

**Professor Lisa Kaestner**

Division of Urology

Department of Surgery

Faculty of Health Sciences

University of Cape Town

Date: 1 December 2024

**Co-supervisors:**

Signed by candidate

_____

**Professor John Lazarus**

Division of Urology

Department of Surgery

Faculty of Health Sciences

University of Cape Town

Date: 1 December 2024

Signed by candidate

_____

**Professor Graham Fieggen**

Division of Neurosurgery

Department of Surgery

Faculty of Health Sciences

University of Cape Town

Date: 1 December 2024

# Author's Contribution

The work presented in this thesis has been carried out by the author under the supervision of Professor Lisa Kaestner (Division of Urology), Professor John Lazarus (Division of Urology) and Professor Graham Fieggen (Division of Neurosurgery) from the Department of Surgery, Faculty of Health Sciences at the University of Cape Town.

The author was responsible for planning the research, designing the studies, obtaining ethics approval, collecting, managing, and analysing the data, interpreting the results, drafting and revising the manuscripts for submission to peer-reviewed journals, and composing and compiling this thesis.

As the supervisor of the thesis on which this candidature is based, I confirm that the authorship attribution statements provided above are accurate.

Signed by candidate

_____

**Professor Lisa Kaestner**
Division of Urology
Department of Surgery
Faculty of Health Sciences
University of Cape Town
Date: 1 December 2024

# Plagiarism Declaration

I am aware that plagiarism is defined at the University of Cape Town as the inclusion of another's or others' ideas, writings, works, discoveries, and inventions from any source in an assignment or research output without the due, correct and appropriate acknowledgement to the author(s) or source(s) in breach of the values, conventions, ethics and norms of the different professional, academic and research disciplines and includes unacknowledged copying from intra- and internet peers/fellow students.

I have duly and appropriately acknowledged all references and conformed to avoid plagiarism as defined by the university. I have made use of the citation and referencing style stipulated by my supervisor.

I did not and will not allow anyone to copy my work and present it as his/her own.

I am committed to upholding academic and professional integrity in academic/research activity. I am aware of the consequences of engaging in plagiarism.

This thesis has been submitted to the Turnitin module (or equivalent similarity and originality checking software) and I confirm that my supervisor has seen my report and any concerns revealed by such have been resolved with my supervisor.

Signed by candidate

_____

**Dr Jeff John**
Division of Urology
Department of Surgery
Faculty of Health Sciences
University of Cape Town
Date: 1 December 2024

# Acknowledgements

This thesis would not have been possible without the guidance and help of several individuals, who in one way or another contributed and extended their valuable assistance in the preparation and completion of this study. It is my pleasure to thank those who made it a possibility.

- To my supervisors, Professors Lisa Kaestner, John Lazarus and Graham Fieggen. Your continued guidance, unprecedented support and expertise coupled with amazing humility and grace for such distinguished academics, made this journey challenging but exciting and enjoyable. Professors John Lazarus and Lisa Kaestner have, well before this PhD, always supported my journey to become a urologist. I look forward to their continued support and mentorship.
- To Dr. Ken Kesner, the former head of the Division of Urology at Frere Hospital, who has always motivated me to keep achieving more and pushing boundaries.
- To Professor Tomasz Ciach, Kamil Kopeć, Daniel Kopeć and Jakub Trzciński from the Faculty of Chemical and Process Engineering at Warsaw University of Technology who meticulously coated the guidewire with hydrogel and loaded it with isoprenaline.
- To Pawel Wisniewski, Stephan Dijkstra, Peter Magyar, and Russell Maurer of Wismed CC for their technical support and continual optimism, confidence and perseverance despite some initial setbacks.
- To Charné Dixon and Tracy Kellerman from the Division of Clinical Pharmacology at the University of Stellenbosch for the development of the technique to quantify serum isoprenaline.
- To Shené Isaacs, for the “long-distance” administrative support at the touch of a button.

- To Rose Boltman, Helen Ilsley, Janet McCullum, John Chipangura, Tashie Makwavarara, and Thireshni Chetty at the University of Cape Town Research Animal Facility for their dedication and commitment to the project and ensuring the welfare of our animals were well looked after.
- To Val Myburgh, illustrator, and artist extraordinaire. The visual appeal created by her drawings for several of the publications from this thesis certainly took the manuscripts to another level.
- To my colleagues and friends at Frere Hospital, East London – Keri Bhana, Noma Mngqi, Kaylyn Stride, and Návan van Jaarsveld. We work under such difficult circumstances serving the most vulnerable patients in the Eastern Cape. Despite this, the pleasant environment they create gives me such energy and motivation to keep striving for more.
- Finally, to my family, for keeping me going and providing me with unfailing support throughout my years of study. This thesis stands as a testament to your unconditional love and encouragement.

# Dedication

You don’t choose your family.

They are God’s gift to you, as you are to them.

- Desmond Tutu -

# Table of Contents

# Publications arising from this research

1. John J, Wisniewski P, Fieggen G, Kaestner L, Lazarus J. Intrarenal pressure in retrograde intrarenal surgery: a narrative review. Urology. In press 2024. http://doi.org/10.1016/j.urology.2024.09.026.
2. John J, Wisniewski P, Fieggen G, Kaestner L, Lazarus J. Reply to Editorial Comment on "Intrarenal pressure in retrograde intrarenal surgery: a narrative review". Urology. In press 2024. http://doi.org/10.1016/j.urology.2024.10.036.
3. John J, Bosch J, Adam A, Fieggen G, Lazarus J, Kaestner L. Design and validation of a novel 3D-printed retrograde intrarenal surgery trainer. Urology. 2024 Sep;191:171-176. http://doi.org/10.1016/j.urology.2024.06.061.
4. John J, Wellman M, Dixon C, Kellermann T, Wisniewski P, Kopeć K, Trzciński J, Kopeć D, Ciach T, Fieggen G, Kaestner L, Lazarus J. Introducing an isoprenaline eluting guidewire: report on its design and the results of the dose-determining pilot study. J Endourol. 2024 Jun;38(6):590-597. http://doi.org/10.1089/end.2023.0745.
5. John J, Wellman M, Kellermann T, Kopeć K, Ciach T, Fieggen G, Kaestner L, Lazarus J. Pharmacological modulation of intrarenal pressure in a porcine model using a novel isoprenaline-eluting guidewire. J Endourol. In press 2024. http://doi.org/10.1089/end.2024.0348.
6. John J, Fieggen G, Kaestner L, Lazarus J. The porcine model for urological research and training: an endoscopic and CT-based study. Submitted for publication (World J Urol).

# Presentations arising from this research

## Chapter 1

**Intrarenal pressure in retrograde intrarenal surgery**

1. 43rd Congress of the Société Internationale d'Urologie (Society of International Urology – SIU), 12 October 2023 – Istanbul, Turkey
2. Combined 16th Pan African Urological Surgeons' Association Congress (PAUSA) and 34th Biennial Congress of the South African Urology Association (SAUA), 11 September 2024 – Johannesburg, South Africa

## Chapter 2

**Design and validation of a novel 3D-printed retrograde intrarenal surgery trainer**

3. University of Witwatersrand, Department of Surgery Bert Myburgh Research Forum, 10 November 2023 – Johannesburg, South Africa
4. University of Cape Town Department of Surgery Research Symposium, 1 December 2023 – Cape Town, South Africa
5. 41st World Congress of Endourology and Uro-Technology (WCET), 13 August 2024 – Seoul, South Korea
6. Combined 16th Pan African Urological Surgeons' Association Congress (PAUSA) and 34th Biennial Congress of the South African Urology Association (SAUA), 14 September 2024 – Johannesburg, South Africa

## Chapter 3

**The porcine model for urological research and training: an endoscopic and CT-based study**

7. Combined 16th Pan African Urological Surgeons' Association Congress (PAUSA) and 34th Biennial Congress of the South African Urology Association (SAUA), 11 September 2024 – Johannesburg, South Africa

## Chapter 4

**Introducing an Isoprenaline Eluting Guidewire: Report on its Design and the Results of the Dose-Determining Pilot Study**

8. 43rd Congress of the Société Internationale d'Urologie (Society of International Urology – SIU), 12 October 2023 – Istanbul, Turkey

## Chapter 5

**Pharmacological Modulation of Intrarenal Pressure in a Porcine Model Using a Novel Isoprenaline-Eluting Guidewire.**

9. 40th European Association of Urology (EAU) Congress, 6 April 2024 – Paris, France
10. 41st World Congress of Endourology and Uro-Technology (WCET), 13 August 2024 – Seoul, South Korea
11. Combined 16th Pan African Urological Surgeons' Association Congress (PAUSA) and 34th Biennial Congress of the South African Urology Association (SAUA), 14 September 2024 – Johannesburg, South Africa

# List of Tables

# List of Figures

## Chapter 1



## Chapter 2

**Figure 8:**

Photograph showing the final assembled training model.

[A] External appearance and dimensions of the model.

[B] Contents inside the case, which participants/trainees are blinded to.

[C] Setup of the entire model during simulation.

**Figure 9:**

Image showing the step-by-step validation procedure performed by the registrar. A complete video is available as an addendum for this manuscript.

[A] Cystoscopic view showing ureteric orifices.

[B] The right ureteric orifice is seen cannulated with a hydrophilic guidewire.

[C] 12/14F ureteral access sheath in position.

[D] View of the calyces seen on entering the renal pelvis.

[E] Calyx number 3 is seen during the renoscopy.

[F] Holmium laser fibre in position and ready for laser lithotripsy.

[G] Endoscopic view once dusting of stone is complete.

[H] Endoscopic view of a registrar attempting to extract a stone fragment using a stone basket.

## Chapter 3

**Figure 10:**

CT urogram and retrograde pyelogram images of the upper urinary tract showing two multirenculate, multipapillate kidneys and their corresponding ureters [A-E]. Endoscopic view of the renal pelvis from the ureteropelvic junction [F] and renal calyces [G].

**Figure 11:**

Delayed phase of CT urogram showing distal ureters (A-C) passing posterior to the bladder and emptying into the bladder (D and E) at its base. Endoscopic view of the bladder neck showing patulous ureteric orifices at the bladder neck (and no interureteric ridge) [F and G] which allowed easy passage of a 6F ureteric catheter [H].

**Figure 12:**

Graphical representation showing the genitourinary anatomy in the female [A] and male [B] porcine model and notably the position of the urethral orifice. Vaginoscopy showing both the urethral opening with [C] and without [D] a 6F ureteric catheter, and the cervical opening.

## Chapter 4

**Figure 13:**

Schematic representation of the structure of the IsoWire (A) and the hydrogel coating with (B) and without isoprenaline (C). PTFE = polytetrafluoroethylene.

**Figure 14:**

Graphical demonstration of the animal model. ECG = electrocardiogram.

**Figure 15:**

Stereomicroscopic and scanning electron microscopy images of guidewire with and without hydrogel coating.

**Figure 16:**

Isoprenaline release profile from hydrogel-coated guidewire into artificial urine solution.

**Figure 17:**

Graph showing the frictional force between the guidewire and porcine ureter. N = newton.

## Chapter 5

**Figure 18:**

Graphical representation of the mechanism of action of isoprenaline.

# Abbreviations and Terminologies

| | |
|---|---|
| IRP | intrarenal pressure |
| RIRS | retrograde intrarenal surgery |
| URS | ureteroscopy |
| mmHg | millimeters of mercury |
| $cmH_20$ | centimeters of water |
| SWL | shockwave lithotripsy |
| PCNL | percutaneous nephrolithotomy |
| UAS | ureteric access sheath |
| AKI | acute kidney injury |
| NGAL | neutrophil gelatinase-associated lipocalin |
| mL | milliliter(s) |
| Fr | French |
| RESD | ratio of the endoscope-sheath diameter |
| µg | microgram(s) |
| DICOM | Digital Imaging and Communications in Medicine |
| 3D | three-dimensional |
| SD | standard deviation |
| US | United States |
| FiST | Frere Intrarenal Surgery Trainer (FiST) |
| CT | computed tomography |
| STL | stereolithography |
| PLA | polylactic acid |
| PVC | polyvinyl chloride |

| | |
|---|---|
| USD | United States Dollar |
| UK | United Kingdom |
| kg | kilogram (s) |
| mg | milligram (s) |
| mg/kg | milligrams per kilogram |
| IM | intramuscular |
| mm | millimeter (s) |
| mL | milliliter (s) |
| SPSS | Statistical Package for the Social Sciences |
| cm | centimeter |
| SD | standard deviation |
| CV | coefficient of variation |
| cc | cubic centimetre |
| AEC | Animal Ethics Committee |
| HR | heart rate |
| bpm | beats per minute |
| MAP | mean arterial pressure |
| N | newton |
| PTFE | polytetrafluoroethylene |
| PVP | polyvinylpyrrolidone |
| SEM | scanning electron microscopy |
| mL/min | milliliter per minute |
| mL/kg/h | milliliter per kilogram per hour |
| g | gram |
| µm | micrometer |

| | |
|---|---|
| µL | microliter |
| °C | degrees Celsius |
| °F | degrees Fahrenheit |
| g/L | gram per liter |
| FDA | Federal Drug Association |
| EMA | European Medicines Agency |
| ng/mL | nanogram per milliliter |
| in | inch |
| mL/min | milliliters per minute |
| mg/mL | milligrams per milliliter |
| Gα | g-protein alpha-subunit |
| Gβ | g-protein beta-subunit |
| Gγ | g-protein gamma-subunit |
| AC | adenylyl cyclase |
| ATP | adenosine triphosphate |
| cAMP | cyclic adenosine monophosphate |
| PKA | protein kinase A |
| µg/mL | microgram per milliliter |
| s | second(s) |
| NCRD | National Center for Research Development |

# Chapter 1: Intrarenal pressure in retrograde intrarenal surgery: a narrative review

## Overview

Urolithiasis ranks as the third most prevalent condition in urology, with statistical evidence indicating a lifetime risk of 13% in males and 7% in females, alongside a recurrence rate of 50% within a decade. The surgical care of urolithiasis is intricate, with various competing therapeutic techniques available, including retrograde intrarenal surgery (RIRS). Over the years, leading urological associations have progressively broadened the indications for RIRS in the surgical management of urolithiasis. While it offers enhanced stone-free rates relative to shockwave lithotripsy (SWL) and reduced patient morbidity compared to percutaneous nephrolithotomy (PCNL), it is not devoid of problems, many of which are associated with intrarenal pressure (IRP). This chapter reviews the problems associated with high IRP and outlines techniques to mitigate elevated IRP in RIRS to promote safer endourological practices.

This narrative review was accepted for publication in Urology (Impact Factor 2.2) and at the time of submission of this thesis, it was an "article in press".

**John J,** Wisniewski P, Fieggen G, Kaestner L, Lazarus J. Intrarenal pressure in retrograde intrarenal surgery: a narrative review. *Urology*. In press 2024. http://doi.org/10.1016/j.urology.2024.09.026.

CRediT author statement:

**Jeff John**: Writing – original draft, Visualization, Methodology, Formal analysis, Data curation, Conceptualization. **Graham Fieggen**: Writing – review & editing, Supervision. **Pawel Wisniewski**: Writing – review & editing. **Lisa Kaestner**: Writing – review & editing, Supervision. **John Lazarus**: Writing – review & editing, Supervision.

# Abstract

## Objective

To review the evidence on the complications of elevated IRPs in RIRS and the strategies to mitigate the increase of IRP during surgery.

## Materials and Methods

A comprehensive literature search of PubMed, Web of Science and EBSCO research databases was conducted from inception to July 31, 2024. The analysis involved a narrative review.

## Results

Normal physiological IRP in an unobstructed kidney ranges from 0 to 15 mmHg (0-20 $cmH_2O$). During RIRS, dangerous IRPs are often reached, resulting in complications. These include pyelorenal reflux, which predisposes the patient to fever, urosepsis and postoperative pain, and forniceal rupture, which may result in intraoperative bleeding as well as acute kidney injury, postoperative pain, and fluid overload. To maintain safe IRP, outflow should be as close as possible to inflow. Minimizing the irrigation pressure by controlling the flow rate, reducing the pressure of the irrigant fluid, using a ureteral access sheath and maintaining an empty bladder during the procedure and, more recently, using real-time IRP monitoring are appropriate techniques to mitigate unsafe IRPs.

## Conclusion

Several complications of RIRS are related to elevated IRPs, which cause pyelorenal backflow and forniceal rupture. Irrigation flow and pressure dynamics drive IRP changes during RIRS. Awareness of these factors will allow urologists to institute strategies to mitigate IRP during RIRS, thereby reducing complications and improving patient outcomes.

# Introduction

The surgical management of urolithiasis is complex, and multiple competitive treatment modalities are available. Since Marshall explored the ureter with a 9F pediatric flexible cystoscope in 1964,[1] the use of flexible ureterorenoscopic devices and lasers for RIRS has become a well-established surgical modality for the management of upper urinary tract stones. It provides superior stone-free rates when compared to SWL and fewer complications in comparison to PCNL.[2,3] Technological advancements, such as the miniaturization of the endoscope, enhanced deflection mechanism, improved optical quality with digital scopes, and introduction of high-quality guidewires, baskets, and access sheaths, have led to prominent urological societies expanding the use of RIRS over the years.[4] These developments have rendered the procedure safer, more efficient, and more comfortable for both patients and surgeons.[5] However, RIRS is not without complications, many of which are related to IRP. The normal physiological IRP in an unobstructed kidney ranges from 0 to 15 mmHg (0-20 $cmH_2O$).[6] To maintain a safe IRP, fluid outflow must closely match inflow, as any discrepancy frequently leads to the surpassing of threshold pressures during RIRS.[7] Jung and Osther examined the spectrum of pressures experienced during standard RIRS without the use of a ureteric access sheath (UAS). The intraluminal renal pelvic pressure varied from 35 (±10) mmHg during uncomplicated diagnostic ureterorenoscopy to 54 (±18) mmHg during stone management. Maximum pelvic pressure peaks of 288 mmHg and 328 mmHg were seen after forced irrigation with a 20 mL syringe and the use of a holmium laser, respectively.[8] This narrative review discusses the complications of elevated IRP and the strategies to prevent elevated IRP in RIRS.

# Materials and Methods

A comprehensive literature search of PubMed, Web of Science, and EBSCO research databases was conducted from inception to July 31, 2024. Search terms included “intrarenal pressure,” “pyelorenal reflux,” “intrarenal reflux,” “retrograde intrarenal surgery,” “RIRS,” “ureteroscopy,” “URS” and “f-URS.” Boolean operators (AND and OR) were used to augment the search. In vitro human and animal studies and review articles written in English were included in the study. Relevant articles identified from the reference lists were also included. Duplicates were removed at screening. Case reports were also excluded from the full-text eligibility assessment (Figure 1).

**Figure 1**

Flow diagram of the literature search process.

# Results

Using the aforementioned search strategies, the PubMed (n=233), EBSCO (n=183), and Web of Science (n=260) databases identified 676 articles. Duplicates were removed using the EndNote Research Management Software (n=365) and manually (n=19). The remaining papers (n=292) were screened by J.J. Papers (n=39) that did not meet the inclusion criteria or were irrelevant were excluded. In total, 253 papers were retrieved and analyzed. Due to the significant degree of heterogeneity of the included studies, a systematic review or mathematical summary of the results of the selected studies was not conducted. Instead, we selected publications to conduct a narrative review, explicitly examining the complications associated with elevated IRP in RIRS, and discussing strategies to reduce IRP in RIRS. Some articles identified during the literature search were not cited due to various factors, such as limited scope, focus on specific sub-themes, or methodological choices.

## Complications associated with high intrarenal pressures

### Pyelorenal Reflux

Pyelorenal reflux is thought to be a compensatory mechanism in which the developing fetal kidney cells are shielded from excessive pressures when the developing upper urinary tract transiently experiences obstruction.[9] This compensatory mechanism has been transferred to adulthood and may follow one of five paths (Figure 2): through the interlobar veins, into the arcuate renal veins and eventually into the venous plexus (pyelovenous backflow); into the renal sinus along the infundibulae, then into the renal pelvis and proximal ureter (pyelosinous backflow); into the terminal collecting ducts (papillary ducts) in the renal medulla (pyelotubular backflow); into the medial perirenal

lymphatics (pyelolymphatic backflow); or from the renal pyramids into the subcapsular tubules in the renal interstitium (pyelointerstitial backflow).[10,11]

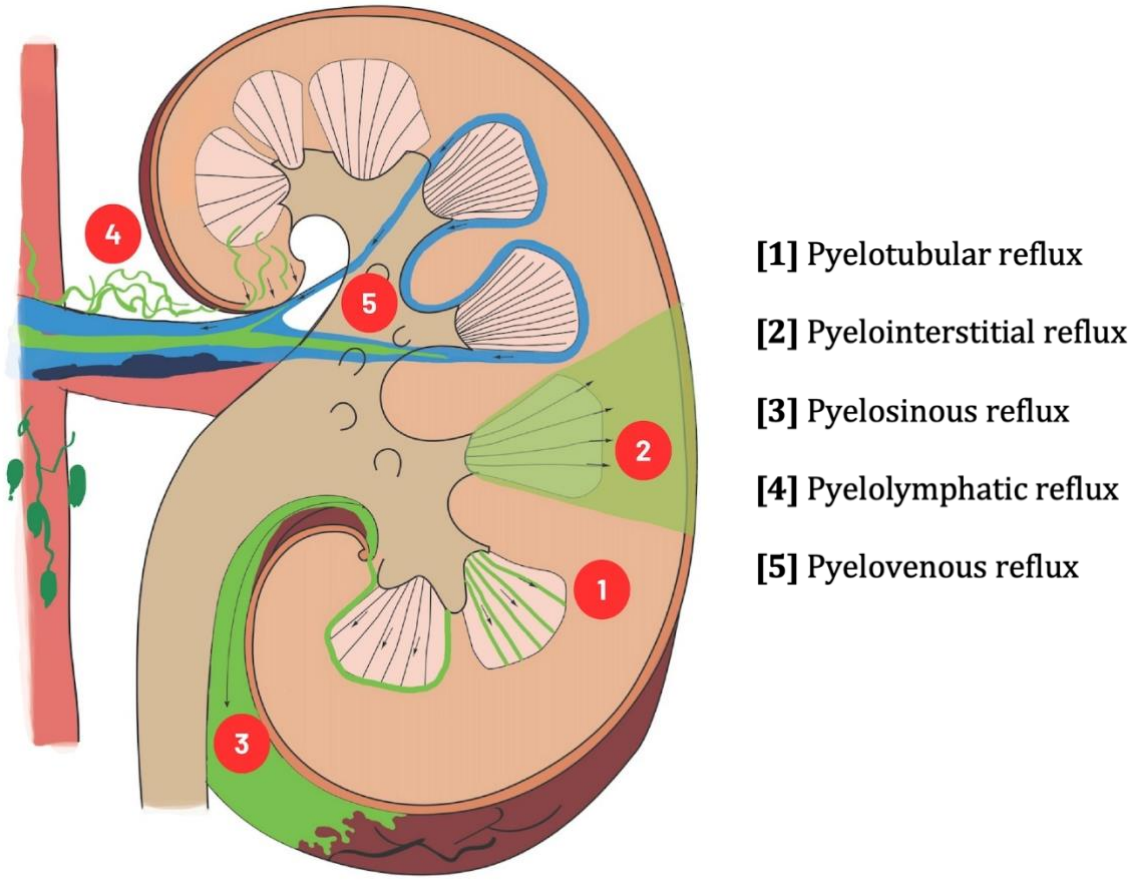


**Figure 2**

Schematic diagram of the different pathways of pyelorenal reflux.

---

In a non-perfused, cadaveric kidney, pyelotubular, and pyelovenous reflux occur when the IRP exceeds 11-15 mmHg (15-20 $cmH_20$) and 37 mmHg (50 $cmH_20$), respectively.[12] Historical data suggest that in a perfused human kidney, the threshold for pyelotubular reflux increases to 29-37 mmHg (40-50 $cmH_20$), and 44-51 mmHg (60-70 $cmH_20$) for pyelovenous reflux.[12] Further increases in the IRP result in pyelosinous and pyelolymphatic backflow.[13,14] However, recent work by Lildal et al. showed that

pyelorenal backflow may infact occur at much lower pressures than previously thought.[15] They performed a study on five female pigs. A ureteral catheter was placed in the renal pelvis and connected to gadolinium and saline solution for irrigation. Irrigation was successively regulated to maintain consistent IRP levels at 10, 20, 30, 40 and 50 mmHg. An occlusion balloon catheter was inflated at the pelvic-ureteric junction and connected to a pressure monitor. MRI scans of the kidneys were performed at five-minute intervals and showed intrarenal reflux occurring at IRPs as low as 16 mmHg (range 16-25 mmHg, mean 21 mmHg) in normal, non-hydronephrotic kidneys. This contemporary method of identifying intrarenal reflux is likely more accurate than previously used techniques, suggesting that the threshold for dangerous IRPs may need to be reconsidered.[15] Furthermore, in pathological renal units and in the presence of pre-existing factors, pyelorenal backflow may occur at even lower pressures. Patients exhibiting flattened papillae, characteristic of medullary sponge kidney, compound papillae, and papillary pitting may be predisposed to pyelorenal reflux at a lower IRP. Similarly, patients with hydronephrosis, where resultant papillary thinning and flattening undermine the antireflux mechanism, are also at risk. [10,16,17]

The clinical consequence of pyelorenal backflow is the retrograde translocation of uropathogenic bacteria and endotoxins from the urinary system into the bloodstream which predisposes patients to urosepsis.[18,19] A recent systematic review and meta-analysis of urosepsis following RIRS indicated that postoperative sepsis rates varied from 0.2% to 17.8%, resulting in prolonged hospitalization, unplanned intensive care admission, and death.[20,21] Xu et al. reported that patients subjected to elevated IRP during RIRS exhibited a markedly increased risk of postoperative urosepsis.[22] Similarly, in a prospective multi-institutional study that followed up 120 patients for 30 days it was shown that the mean

IRP (82 mmHg) was much greater in the six (5%) patients who developed postoperative urosepsis than in the controls (39 mmHg).[23]

**Forniceal Rupture**

Forniceal rupture is another complication of elevated IRP in patients with RIRS. As pressure rises within the collecting system, it dilates, placing the renal fornices under greater tension. A rapid increase in pressure causes the collecting system to rupture at the weakest point, the renal fornix (Figure 3).[24]

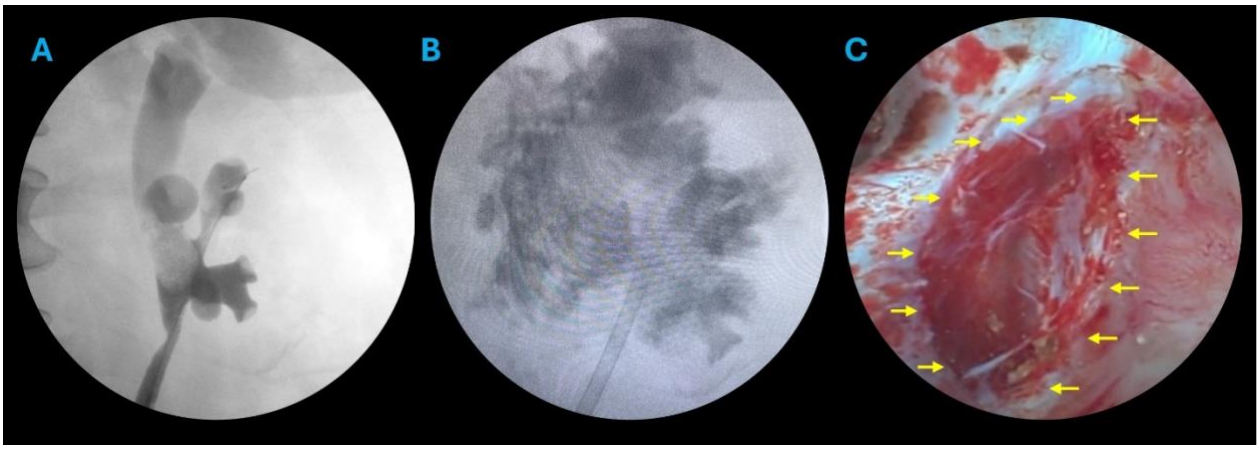


**Figure 3**

Retrograde pyelogram before (A) and after (B) the rupture of the fornix. Endoscopic image (C) during RIRS showing the rupture of the fornix.

---

An absolute pressure of 80-100 mmHg has been found to cause forniceal rupture.[25] This initiates a dangerous cycle (Figure 4). Forniceal rupture causes intraoperative bleeding and subsequently, poor vision. Surgeons may increase the rate or pressure of irrigation in the hope of improving vision, only to worsen the pressure and potentiate its consequences. Furthermore, forniceal rupture and the subsequent formation of a subcapsular or

perirenal hematoma has also been shown to account for acute flank pain after RIRS.[26,27] In addition, the extravasation of irrigation fluid, venous congestion and ureteral oedema, all of which lead to contractions of the ureter and ureteric obstruction, may also account for postoperative pain.[28] Apart from these local effects caused by the extravasation of irrigation fluid, Guzelburc et al. reported that fluid absorption during RIRS ranged from 20 mL to 573 mL.[29] This parenchymal fluid transfer places renal and cardiac failure patients at risk of postoperative systemic complications from fluid overload, and some authors have recommended the administration of diuretics to mitigate this risk.[30]

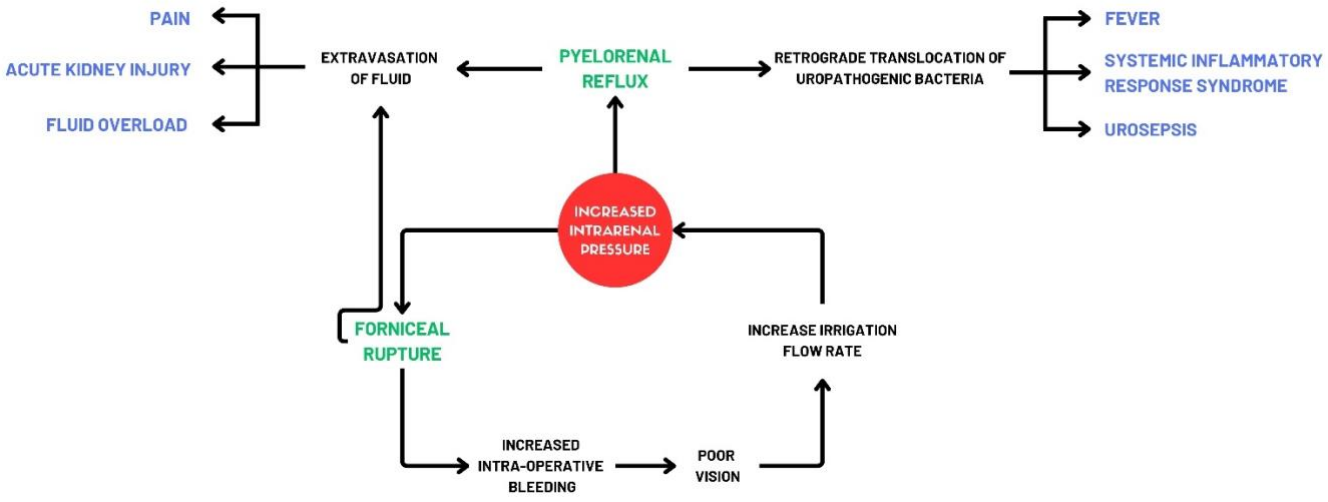


**Figure 4**

Diagram to illustrate the complications of increased intrarenal pressure.

---

Elevated IRP levels may also compromise renal function. In an experimental study, Schwalb examined the immediate and long-term effects of elevated IRP levels using freshly harvested porcine kidneys.[31] In the immediate postoperative setting, renal units subjected to high pressure showed widespread denudation and flattening of the calyceal urothelium

with submucosal edema and congestion within the calyces, vacuolization, and degeneration of the renal tubules. Four to six weeks later, widespread columnar metaplasia, subepithelial nests, and pericalyceal vasculitis were observed in the kidneys subjected to high irrigant pressure. Focal scarring was observed in five of the seven kidneys subjected to high irrigant pressure. In comparison, there was no evidence of scarring in any of the six kidneys subjected to low irrigant pressure.[31] Since human kidneys are anatomically and physiologically similar to porcine kidneys,[32,33] human kidneys subjected to elevated IRPs are likely to face similar levels of inflammation and scarring. Cruces introduced the concept of renal compartment syndrome.[34] This increase in pressure in the renal compartment results in a decrease in renal perfusion pressure, with a subsequent reduction in renal blood flow and ischemia in the outer medulla. Similar evidence of post-ureteroscopy acute kidney injury (AKI) has been observed at the biochemical level. Neutrophil gelatinase-associated lipocalin (NGAL), a 21-kDa protein expressed in neutrophils and human epithelia, is a urine biomarker for AKI.[35,36] Elevated levels of NGAL, indicative of tubular damage, have been detected as early as two hours post URS.[37] The long-term clinical consequences are uncertain.

## Strategies to reduce IRP in RIRS

Fluid irrigation during RIRS is necessary to improve visibility and distention of the upper urinary tract. However, to maintain a safe IRP during the procedure, the surgeon must maintain the outflow as close as possible to the inflow.

### Controlling the Inflow

The inflow is the volume of fluid entering the system per unit of time. It is determined by the irrigation pressure, which is determined by the flow rate and pressure of the fluid. The

flow rate is further dependent on the height of irrigation fluid in relation to the position of the kidney, and the size of the instrument that occupies the working channel of the ureteroscope.[38] To understand the effect of the height of the irrigation fluid on the flow rate, Chang et al.[38] simplified the Bernoulli[39] equation $V_2 = \sqrt[2]{z_1\ (2g)}$ . The velocity of irrigant fluid ($V_2$) at the end of the scope is proportional to the square root of the height of the irrigant bag ( $\sqrt{z_1}$). The height at which the irrigant is hung affects the driving pressure at the scope inlet and subsequent inflow. Inflow is also dependent on the resistance of the tube. Flexible ureteroscopes typically have one working channel, and flow resistance created by the occupation of the working channel by either a laser fibre or stone basket will reduce the flow rate and subsequently the irrigation pressure and IRP.[40-42] The irrigation pressure can also be affected by the pressure at which the fluid is administered. A recent study based on computed tomography pyelocalyceal system measurements reported the mean collecting system volumes of 2.9 mL in non-hydronephrotic kidneys, and 5.1 mL with diuretic distension.[43] Furthermore, a stone-filled collecting system may have a smaller capacity, and inflammation related to the stone may alter the viscoelastic properties of the collecting system, making it less distensible. On-demand flushing using a manual hand-held or foot-controlled device should be used cautiously, for fear of causing repetitive dangerous IRP spikes.[8] Therefore, gravity irrigation is the simplest and safest means of irrigation during ureteroscopy.[44]

**Improving the Outflow**

Ureteral access sheaths (UASs), developed by Takayasu and Aso in 1974,[45] have become important weapons in the armamentarium of endourologists. When the device was introduced, the success and safety of use were considered fairly low, with 19% of cases resulting in ureteric perforation.[46] However, recent technological advances in UAS, such

as the outer hydrophilic coating, an inner tapered dilator, and a hub-locking mechanism, have made it an important tool in endourology since it provides several benefits in the management of renal stones, none more than reducing the infectious complications associated with RIRS.[47,48] A recent survey of practice patterns of endourologists showed that 76% of endourologists routinely use a UAS[49] to aid in treating renal stones because it allows multiple entries and re-entries into the collecting system, providing better vision, allowing the passive efflux of small stone fragments generated during laser fragmentation, and reducing IRP.[47] The UAS reduces the IRP at various irrigant pressures[41,50,51] by improving the irrigant outflow from the collecting system by 57% to 75% during f-URS.[52] This reduction in IRP was observed during both continuous and bolus fluid administrations. Lazarus et al. demonstrated that administration of small boluses (< 5 mL) with a starting fluid height of 80 $cmH_2O$ is safe when a UAS is employed. However, in the absence of a UAS, even bolus volumes as little as 2 mL produced "unsafe" (> 40 mmHg) pressures.[51] Many variables determine the effects of the UAS on the IRP. A large calibre (12/14 Fr and 14/16 Fr) UAS allows greater outflow, and is more efficacious than a smaller UAS.[52] As the tube radius halves, the flow decreases by 16-fold (i.e. the flow is proportional to the radius of the tube to a power of 4).[53] The benefits of UAS have also been conferred to clinical practice. A prospective multicenter study of 2239 patients treated with flexible URS revealed a lower incidence of postoperative infectious complications (fever, UTI, sepsis 28.6, 18.6 and 4.3% vs. 39.1, 23.9 and 15.2% for the UAS group vs. the non-UAS group respectively).[47]

Recently, Fang et al argued that the ratio of the endoscope-sheath diameter (RESD) is more important than the individual diameter of the UAS or the flexible ureteroscope. When the RESD is ≤ 0.75, the outflow channel between the internal diameter of the UAS and

ureteroscope will be greater than four times the 3.6F inflow of the irrigation channel, which would result in an IRP <13 $cmH_2O$ (9.5 mmHg), despite the use of pressurized irrigation.[54] Based on the Hagen-Pouiselle equation, increasing the UAS length should increase the IRP by increasing the outflow channel length and delaying the outflow. However, in vitro, fresh cadaveric porcine investigations have shown that increasing the length of the UAS has minimal effect on the IRP.[54]

Increased intravesical pressure from the full bladder may be transmitted cranially, thereby affecting the IRP. This is likely related to increased ureteral outflow resistance caused by changes in the bladder wall and intramural ureter with bladder filling.[55] During ureteroscopy in a porcine model, Schwalb et al. showed that a full bladder elevated the IRP by an additional 20 to 25 mmHg.[31] While it is paramount that necessary measures to reduce IRP, as summarised in Figure 5, should be taken, the surgeon also needs to limit the length of the procedure and minimise the duration of exposure to the elevated IRP, which may predispose patients to morbidity and mortality in RIRS.[56]

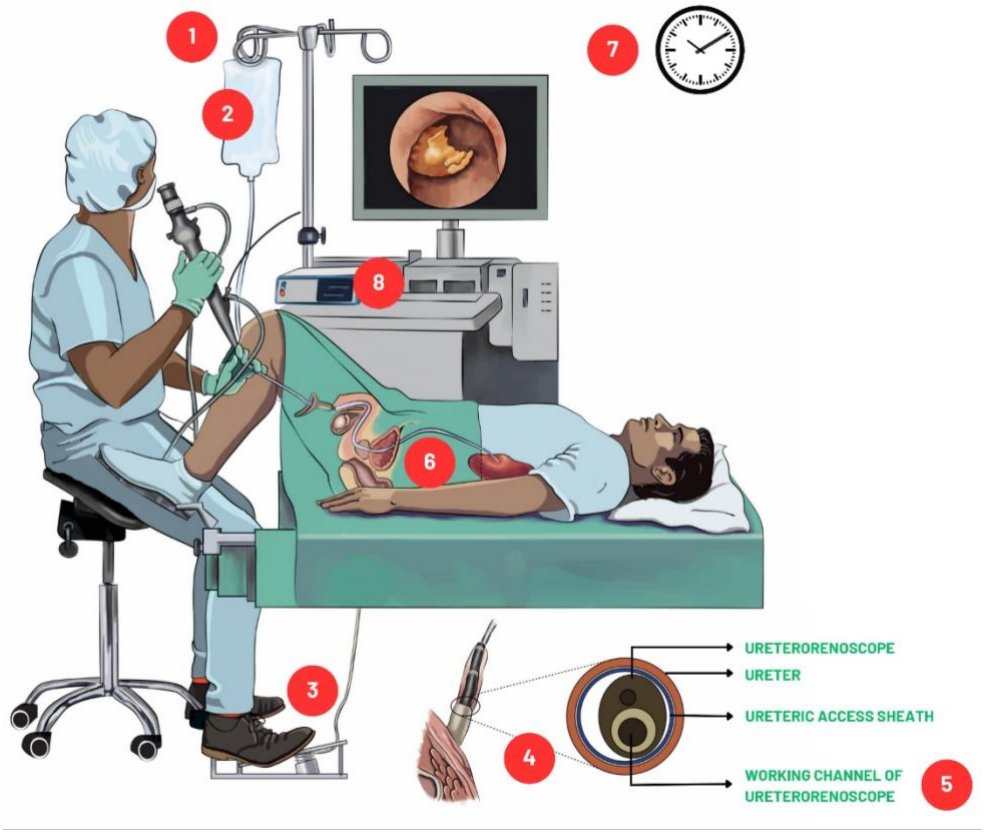


1. LIMIT THE HEIGHT OF THE IRRIGANT FLUID COLUMN
2. OPT FOR GRAVITY-BASED IRRIGATION
3. USE HAND-OPERATED OR FOOT-CONTROLLED IRRIGATION PUMPS JUDICIOUSLY
4. USE THE SMALLEST URETERIC ACCESS SHEATH AND URETERORENOSCOPE TO MAINTAIN THE RATIO ENDOSCOPE: SHEATH DIAMETER (RESD) OF ≤ 0.75
5. OCCUPY WORKING CHANNEL OF URETERORENOSCOPE
6. KEEP THE BLADDER EMPTY
7. LIMIT THE LENGTH OF THE PROCEDURE
8. CONSIDER THE USE OF REAL-TIME INTRARENAL PRESSURE MONITORING

**Figure 5**

Graphical representation of the various strategies to reduce intrarenal pressure in retrograde intrarenal surgery.

# Discussion

Urolithiasis is the third most prevalent condition in urology.[57] The increasing prevalence in recent decades can be attributed to various factors such as changes in lifestyle, diet, fluid intake, and climate. Additionally, the growing incidence of obesity, non-alcoholic fatty liver disease, diabetes, and greater utilization of abdominal imaging have contributed to this trend.[58,59] A recent systematic review that explored the global trends in the management of urolithiasis over the last two decades, showed RIRS had a 251.8% increase in the total number of treatments performed.[60] However, in the endeavour to expand the RIRS indications, one cannot overlook the potential complications of this procedure, most notably bleeding, postoperative pain, and infectious complications – all of which are related to an elevated IRP.[61] Observational studies have demonstrated that the *in vivo* IRP during RIRS is highly variable and often surpasses the traditionally quoted thresholds of 30-40 mmHg.[23,62] This review adds to the expanding body of evidence to help elucidate the role of the IRP during routine RIRS and underlines its role in the development of postoperative complications. While our review also presents strategies to mitigate increases in IRP and prevent the systemic transudation of fluid and uropathogenic bacteria, several novel technologies to reduce IRP have recently been reported. Bhojani et al. reported on the first-in-human experience using a single-use, flexible, digital ureteroscope with a built-in pressure sensor at its tip.[63] Similar innovative techniques for real-time IRP measurement using wires with a pressure sensor[64,65] or an integrated pressure-monitoring suctioning UAS have been explored.[66] Moreover, they will support additional investigations to establish precise thresholds for identifying patients who are at risk of complications. They will also provide a better understanding of whether the adverse effects associated with elevated IRP are caused by a single peak that surpasses the

pressure threshold, leading to subsequent complications, or if the complications arise from sustained high pressures.

The introduction of suctioning UASs has also shown the potential to favorably modulate IRP. In an ex-vivo porcine model, Han et al. noted that the IRP reached 30 mmHg at an irrigation fluid flow rate of 60-70 mL/min when using a standard UAS.[67] In comparison, when a suctioning UAS was used, the IRP remained at approximately 10 mmHg even with a much higher irrigation fluid flow rate of 120 mL/min.[67] Similarly, Guan et al. discovered that by utilizing 12/14F and 11/13F vacuum-assisted UAS with closed vents, the IRP was consistently maintained below 5 mmHg even at high levels of irrigation fluid flow rates of 200 cc/min.[68] This effect on IRP may be responsible for the reduced postoperative septic complications when using a suction UAS.[69,70] Yekani et al. recently piloted a novel UAS that incorporated a syphon mechanism to improve mean peak IRP.[71] The mean peak IRP following a 10 mL bolus with and without the syphon device were 71 and 104 mmHg, respectively ($p = 0.03$, SD 74 vs. 59).[71] Chen et al. conducted a study comparing IRP at different irrigation velocities when using a flexible vacuum-assisted UAS with a regular UAS in an ex vivo swine kidney model.[72] The IRP was maintained below 10 $cmH_2O$ at irrigation fluid velocities of 30, 50, and 80 mL/min using a flexible vacuum-assisted UAS. In contrast, the standard UAS resulted in a steady increase in the IRP from 26 to 99 $cmH_2O$. Despite these beneficial effects on IRP, Ostergar warned that this effect was reversed when a high vacuum rate (> 200 mmHg) was applied due to the collapse of the outflow tract. Therefore, surgeons should use lower vacuum settings for short bursts of approximately 5 seconds.[73] Recently, a novel guidewire comprising a nitinol core surrounded by a stainless-steel wire wound into a tight coil, and loaded with isoprenaline, a beta-agonist, was described. This isoprenaline-eluting guidewire, which releases 7.5 µg of isoprenaline

in the 1st minute, appears to be safe and effective in reducing the IRP.[74,75] While all these novel techniques seem promising, larger clinical trials are required to support their routine use in clinical practice.

# Conclusion

Major advances have been made in the surgical management of urinary tract stones. The pendulum has shifted away from traditional open procedures to more minimally invasive techniques such as RIRS. Many complications of RIRS are related to elevated IRPs, which cause pyelorenal backflow and forniceal rupture. Irrigation flow and pressure dynamics drive IRP changes during RIRS. Awareness of these factors will allow urologists to institute strategies to mitigate IRP during RIRS, thereby reducing complications and improving patient outcomes.

**Declaration of Competing Interest**

The authors have no conflicts of interest to disclose.

**Acknowledgment**

Saeed Bin Hamri – for providing the endoscopic image (Figure 3)

# Chapter 2: Design and validation of a novel 3D-printed retrograde intrarenal surgery trainer

## Overview

Surgical simulation models are crucial prior to research to accurately delineate the procedural steps during the investigation. However, they are expensive and not readily accessible. Moreover, they can facilitate the promotion of safer endourological practices by reducing the significant learning curve associated with RIRS, while ensuring patient safety is not compromised. This chapter delineates the design and fabrication of the Frere Intrarenal Surgery Trainer (FiST) bench-top model. This chapter further elucidates its validation through the involvement of individuals with prior competence in the RIRS technique. This high-fidelity, cost-effective, portable, durable, and reusable training model is, to our knowledge, the first published 3D model that incorporates all components of RIRS, allowing us to meticulously refine the procedural steps for the research detailed in the subsequent chapters.

This chapter was published in *Urology* (Impact Factor 2.2).

**John J,** Bosch J, Adam A, Fieggen G, Lazarus J, Kaestner L. Design and validation of a novel 3D-printed retrograde intrarenal surgery trainer. *Urology*. 2024 Sep;191:171-176. http://doi.org/10.1016/j.urology.2024.06.061.

CRediT author statement:

**Jeff John:** Writing – original draft, Visualization, Methodology, Investigation, Formal analysis, Data curation, Conceptualization. **Johan Bosch:** Writing – review and editing, Software. **Ahmed Adam:** Writing – review and editing. **Graham Fieggen:** Writing – review and editing, Supervision. **John Lazarus:** Writing – review and editing, Supervision. **Lisa Kaestner:** Writing – review and editing, Supervision.

# Abstract

**Objective:**

To report on the design of a novel 3D-printed RIRS benchtop trainer and detail its validation against real-life experiences.

**Materials and Methods:**

Digital Imaging and Communications in Medicine (DICOM) files of 2 patients with normal computed tomography of the kidney and bladder were converted into stereolithography files to create 3D triangular mesh models. These images were further refined using Autodesk Meshmixer. These 3D models were fabricated through additive manufacturing, a process commonly known as 3D printing, and assembled in a polypropylene case. After development, the model was validated by 40 experienced urologists and urology residents in their final year of training. After completion of the validation exercise, each participant was asked to rate the various components of the simulation by completing a nine-point questionnaire. The various categories assessed were each scored out of a possible ten points, with zero being 'no value' and ten being 'greatest value' score.

**Results:**

The model's value in understanding the principles of RIRS and simulating contextual anatomy had mean scores of 9.43 (standard deviation [SD] = 0.74) and 9.21 (SD = 1.03), respectively. Mean scores for specific steps in RIRS were 8.07 (SD 1.47) for cannulating the ureteric orifice, 8.61 (SD 1.24) for inserting the ureteric access sheath, 9.29 (SD 0.97) for performing a renoscopy and evaluating all the calyces, 9.46 (SD 0.87) for laser lithotripsy, and 9.17 (SD 0.94) for manual stone retrieval. Participants scored the model

with a mean score of 9.04 (SD 0.87) regarding realism and a mean score of 9.18 (SD 0.89) when evaluating its ability to enhance a trainee's confidence in RIRS.

**Conclusion:**

The model performed well for all components of RIRS. This model allows high fidelity of the simulation and is cost-effective, portable, durable, reusable, and compatible with standard ureteroscopes.

# Introduction

The prevalence of urolithiasis has increased over the past few decades. The lifetime risks are 7% and 13% in women and men, respectively,[76] with a recurrence rate of 50% within 10 years.[77] Increased prevalence leads to increased costs for both the patient and the healthcare system. Since Marshall explored the ureter with a 9F paediatric flexible cystoscope[1] in 1964, the use of flexible ureterorenoscopic devices and lasers for RIRS has gained traction. Technical improvements, including miniaturisation of the endoscope, improvements in the deflection mechanism, enhanced optical quality with digital scopes, development of disposable scopes, and the introduction of high-quality guidewires, baskets, and access sheaths, have led to prominent urological societies expanding their use in their guidelines.[4,78] One of the major advantages of RIRS is the potential to access all parts of the urinary tract, which renders stone-free rates ranging from 73.6% to 94.1%.[79] As with any surgical procedure, the results of ureteroscopy depend on the availability of equipment and surgeon's experience.[80] Surgical education and training have evolved over the past few centuries, and this change has accelerated after the publication of the landmark report by the United States (US) Institute of Medicine titled "To err is human." They reported that up to 98,000 deaths were as a result of preventable medical errors every year in US hospitals. At the time of this report, these errors accounted for more deaths, than patients who died from motor vehicle accidents, breast cancer, or HIV/AIDS, all of which receive far more public attention.[81] Therefore, the age-old Halsted apprenticeship model of "see one, do one, teach one" which had formed the backbone of surgical training,[82] has now been replaced by more pragmatic approaches. One approach is simulation-based surgical training using cadaveric models, virtual trainers, and benchtop models. An ideal simulation model for RIRS should incorporate all the steps of the procedure, available with a variety of calyceal configurations, be made of radiolucent

material, robust, portable, reusable and cheap. This study aims to report on the design and production of the Frere Intrarenal Surgery Trainer (FiST) bench-top model and detail its validation against real-life experience by enrolling participants with prior experience in the RIRS technique.

# Material and Methods

## Model Development

Written informed consent was obtained from two patients to utilize anonymized computed tomography (CT) scans. The kidney model was acquired from images of a patient with a normal CT-urogram (Figure 6A) for the evaluation of visible haematuria. The bladder model was developed from the images of a patient with a normal CT cystogram (Figure 7A) for the assessment of suspected bladder injury after blunt abdominal trauma. The Digital Imaging and Communications in Medicine (DICOM) files used in these studies were converted into stereolithography (STL) files, resulting in the creation of precise 3D triangular mesh models. This conversion process, formally referred to as segmentation, was accomplished using the freely available software, Invesalius. The software utilizes the Hounsfield unit values of the tissues and contrast medium to generate voxels of the region of interest (Figures 6B and 7B). While the segmentation process was partially automated by the software, fine-tuning and detailed refinement were performed manuallyby the operator.

*Model refinement:* The 3D models were further refined using Autodesk Meshmixer, a free mesh editing 3D software. This step involved elimination of imperfections and smoothing of the models (Figure 6C and 7C). To mimic the anatomical collecting system and facilitate

the passage of endoscopic equipment, solid calyx and bladder models were hollowed out (Figure 6D and 7C). Small openings were strategically created at the terminus of each calyx, allowing for the placement of stones in any one of the calyces, which were then sealed using specially designed plugs.

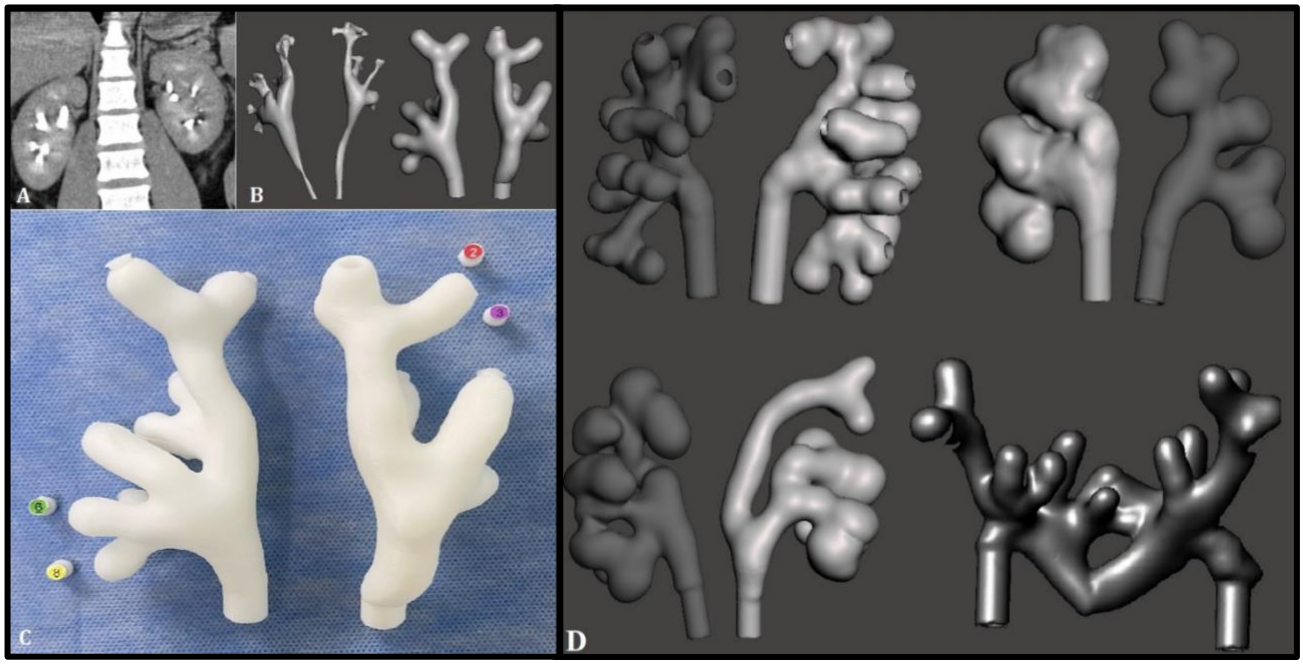


**Figure 6**

[A] Normal CT-urogram used to create the 3D model of the collecting system.

[B] Stereolithography (STL) mesh 3D model of the renal calyceal system after segmentation from the CT scan before (left) and after the smoothing and hollowing processes (right).

[C] Final 3D printed model of the right and left calyceal systems with corresponding plugs for each calyx.

[D] STL mesh 3D model of different anatomic variations of the collecting system.

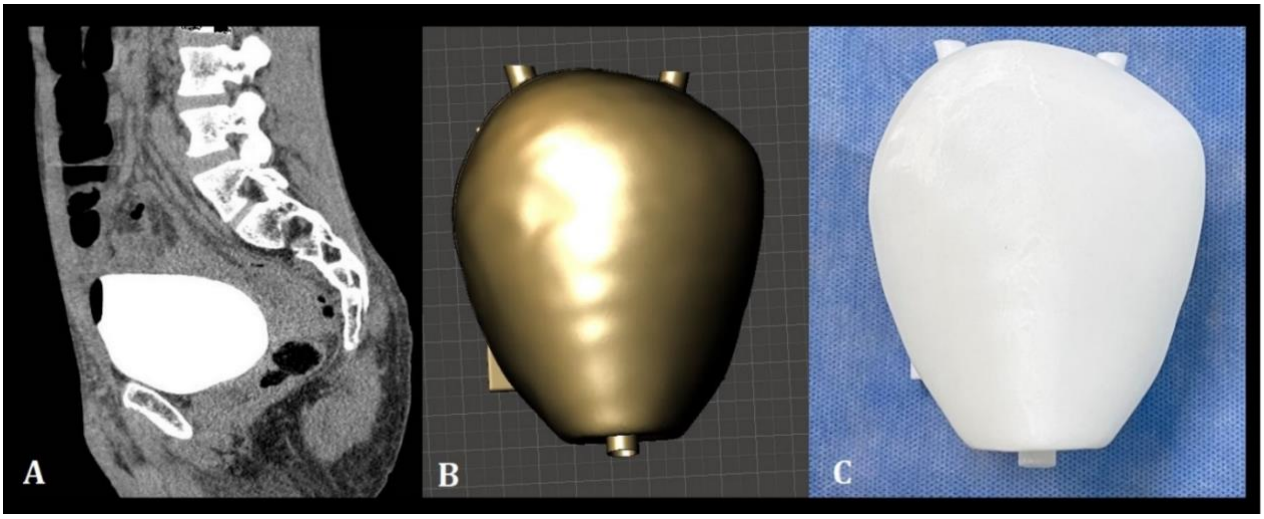


**Figure 7**

[A] Normal CT-cystogram used to create the 3D model of the bladder.

[B] STL mesh 3D model of the bladder after smoothing and hollowing with attachments for tubing that simulate the proximal urethra and distal ureters.

[C] Final 3D printed model of the bladder.

---

Numbered stickers were printed to stick onto the inside of the plugs to allow the trainee to differentiate between different calyces (Figure 6C). At the conclusion of the modelling process, the accuracy of the models in replicating the shape and size of the collecting system, as observed in the original CT images, was verified.

*Model verification:* The verification process involved digitally overlaying the final 3D model of the calyx system onto the original segmented CT data, specifically the contrast-enhanced images that defined the collecting system. We compared the inner dimensions and morphology of the 3D model to the CT-extracted anatomy to assess congruence in size and shape. It is important to note that the model reflects the static, non-distended anatomy captured during the CT scan. It does not account for dynamic changes such as calyceal

dilatation under pressure during ureteroscopy. In certain areas, the calyceal openings were intentionally enlarged during the modelling process to allow for practical passage of the ureteroscope during the simulation.

*Additive manufacturing:* These 3D models were fabricated through additive manufacturing, a process commonly known as 3D printing. This technique involves sequential deposition of thin layers of materials to construct 3D objects. To generate the printing instructions for the 3D models, the slicing software Ultimaker Cura was used. The filament material selected for printing was polylactic acid (PLA), a biodegradable and wear-resistant material known for its ease of accurate printing even in entry-level printers. The 3D printer used for this project was a Creatility Ender 3 V2 desktop hobby.

*Model assembly:* The entire model (Figure 8) was housed in a standard polypropylene case with a shallow lid, fold-down handle, and two hinged locks freely available at any supermarket or hardware store. The printed bladder was first secured to the base of the case using double-sided tape. It was then connected to clear polyvinyl chloride (PVC) tubing (8 mm in diameter) to mimic the urethra. A hole was drilled through the side of the case to externalise the tubing. We were unable to model ureters using our current method. The rigidity of the PLA material used in the study, does not replicate the flexibility of ureteric tissue, making it difficult to accurately reproduce the natural tortuosity and variable calibre of the ureter. Additionally, navigating a rigid printed ureter would not realistically simulate the endoscopic experience, as the lack of compliance would likely hinder or prevent scope advancement. We therefore used a PVC tubing, to represent the ureter. This tubing was was connected caudally to the printed bladder phantom and cranially to the kidney phantom.

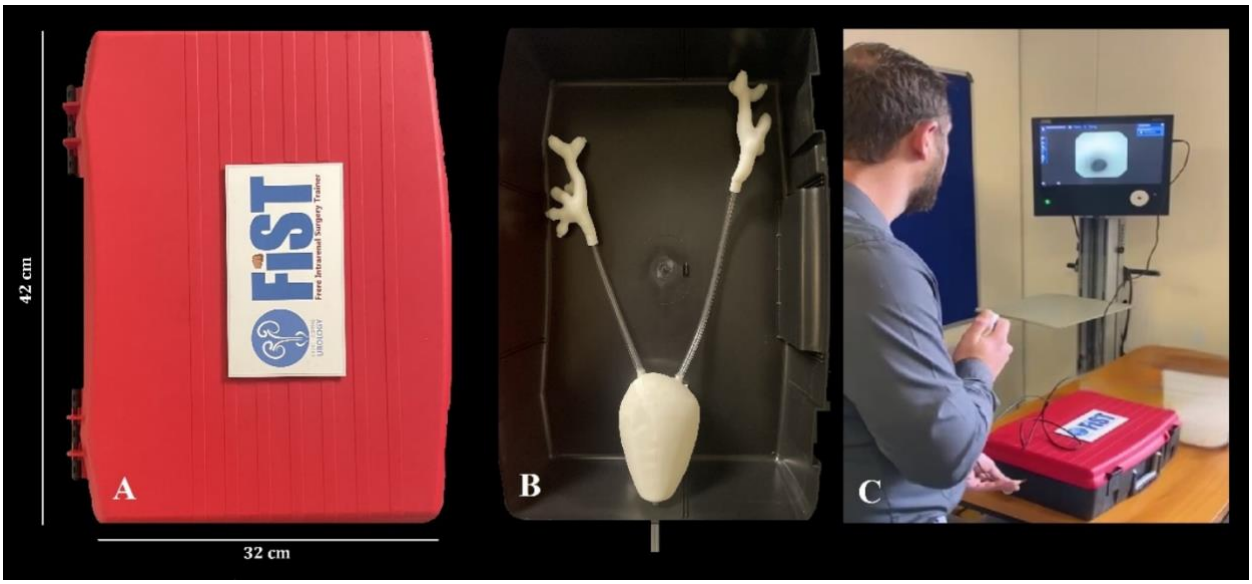


**Figure 8:**

Photograph showing the final assembled training model.

[A] External appearance and dimensions of the model.

[B] Contents inside the case, which participants/trainees are blinded to.

[C] Setup of the entire model during simulation.

---

*Operator proficiency:* It is worth highlighting that segmentation, computer-assisted design, and 3D printing of these models were executed by clinicians with no formal information technology (IT) training.

*Model costs:* The estimated total material cost for constructing each FiST model was USD 60. The total design time for a pair of kidneys and bladder was estimated to be approximately 8 hours. The total printing times for the kidneys and bladder were 8 hours and 11 hours, respectively.

## Model testing

After development, the FiST model was validated by 40 participants with experience in performing the RIRS. The validation study was approved by the Frere and Cecilia Makiwane Hospitals Research Ethics Committee - FCMHREC/A0175/2023 (Appendix 2).

Prior to the validation, the model was set up in a training room. Human stones were introduced into different calyces through small openings created at the terminus of each calyx. Once the stone was in position, specially designed plugs capped the opening. The plastic case was filled with saline solution. The lid of the case was then closed, and all participants were blinded (Figure 8).

Validation began with the participants inserting the Flex-X2 flexible ureterorenoscope (Karl Storz, Tuttlingen, Germany) into the bladder. The ureteric orifices were also identified (Figure 9A). The right orifice was cannulated (Figure 9B) with a 0.035" hydrophilic nitinol Supremo® guidewire (Allwin Medical Devices, United States), after which the ureterorenoscope was removed. A 12/14F Retrace® ureteral access sheath (Coloplast, Denmark) was inserted over the guidewire (Figure 9C). The introducer of the access sheath was removed, and the ureterorenoscope was reintroduced into the renal pelvis (Figure 9D). Participants were first asked to perform a renoscopy to identify all calyces on the right numbered 1 to 8 (Figure 9E), navigating between the upper, middle, and lower calyces as well as the anterior and posterior calyces and locating the stone. A Dormia® 1.5 Fr Nitinol stone basket (Coloplast, Denmark) was used to relocate stones to the upper pole. The stone was then fragmented or dusted at the participant's discretion using an 80 W Potent® Holmium laser equipped with a 200 µm reusable Holmium laser fiber (Figure 9F and 9G). A Dormia® 1.5 Fr Nitinol stone basket (Coloplast, Denmark) was

used again at the participant's discretion for stone fragment extraction (Figure 9H). This procedure was repeated on the right side.

After completion of the RIRS, each participant was asked to rate the various components of the simulation by completing a nine-point questionnaire. The various categories assessed were each scored out of a possible ten points with zero being ‘no value’ to ten being ‘greatest value’ score (Appendix 3).

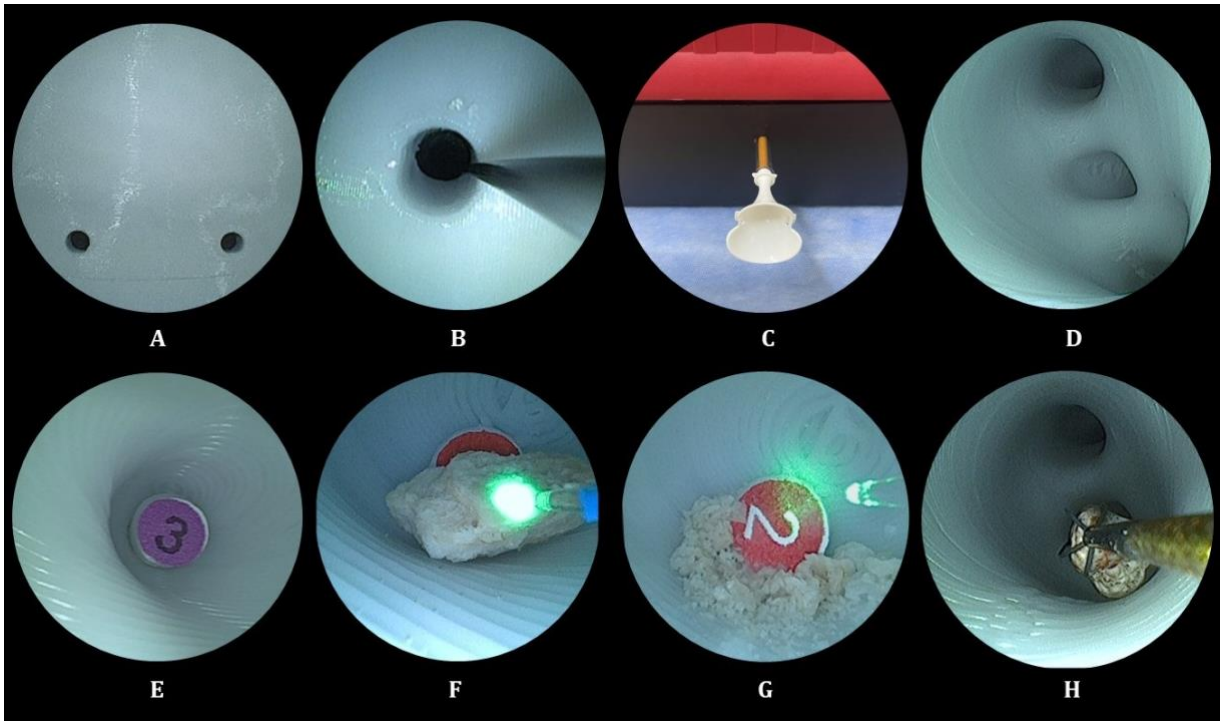


**Figure 9**

Image showing the step-by-step validation procedure performed by the registrar. A complete video is available as an addendum for this manuscript.

[A] Cystoscopic view showing ureteric orifices.

[B] The right ureteric orifice is seen cannulated with a hydrophilic guidewire.

[C] 12/14F ureteral access sheath in position.

[D] View of the calyces seen on entering the renal pelvis.

[E] Calyx number 3 is seen during the renoscopy.

[F] Holmium laser fibre in position and ready for laser lithotripsy.

[G] Endoscopic view once dusting of stone is complete.

[H] Endoscopic view of a registrar attempting to extract a stone fragment using a stone basket.

# Results

Forty participants were enrolled in the study. The distribution of participants included 15 consultants and 25 registrars in their final training year. All participants successfully completed all the RIRS steps. The FiST value in understanding the principals of RIRS had a mean score of 9.43 (standard deviation [SD] 0.74), whereas its value in simulating contextual anatomy had a mean score of 9.21 (SD 1.03). Mean scores for specific steps in RIRS were 8.07 (SD 1.47) for cannulating the ureteric orifice, 8.61 (SD 1.24) for inserting the ureteric access sheath, 9.29 (SD 0.97) for performing a renoscopy and evaluating all the calyces, 9.46 (SD 0.87) for performing laser lithotripsy, and 9.17 (SD 0.94) for performing manual stone retrieval using a stone basket. Overall, participants scored the FiST model with a mean score of 9.04 (SD 0.87) regarding realism and a mean score of 9.18 (SD 0.89) when evaluating its ability to enhance a trainee's confidence in performing RIRS.

# Discussion

The surgical learning curve represents the time taken and/or the number of procedures that an average surgeon needs before being able to perform a procedure independently and competently.[83] The learning curve includes three phases: starting point, an upward slope as skill increases, and the plateau.[84] Inexperienced surgeons operating at the early stages of their learning curve compromise patient outcomes because of the higher rate of complications and less effectiveness. Outcomes improve once technical competence has been achieved, which is represented by the steady plateau stage where the performance level has peaked and there appears to be no further improvement.[84] Evidence suggests a significant learning curve in RIRS. Numerous studies have identified a case load of 50-60 cases required to reach a plateau in terms of operative outcomes in RIRS.[85-87] In addition,

50-100 cases are needed to reduce severe operative complications.[85,88] These caseloads may not be realistically achievable outside dedicated endourology fellowships during urology training. Systematic reviews have outlined the benefits of simulation-based training for shortening surgical learning.[89,90] The integration of simulation-based learning within urology training programs could overcome the surgical caseload limitations.

Our study showed that this novel 3D-printed intrarenal surgery trainer performed well in the technical aspects of RIRS and has a number of advantages. First, the total cost of the model was only 60 USD. While we did not aim to review all available RIRS simulation models, it is worth noting that the prices of other validated, commercially available models, including the URO Mentor™ VR simulator, Uro-Scopic Trainer™ (Limbs & Things Ltd., Bristol, UK), and Scope Trainer™ (Mediskills Ltd, Edinburgh, UK), range between USD 3,700 and USD 60,000.[91] We do, however, acknowledge that the 60 USD is the direct costs involved in the production of this model. Indirect costs were not determined. Secondly, this bench-top model allows high fidelity of the simulation incorporating all aspects of RIRS starting from cystoscopy and cannulation of ureteric orifice with a guidewire, inserting a UAS, ureterorenoscopy, stone manipulation and relocation, laser lithotripsy and stone/fragment retrieval and not just certain components of the procedure. This is in contrast to the K-Box™ (Porgés-Coloplast, France) and Cook URS™ (Cook Medical, USA) simulators, which only aim to improve the trainee's movements during flexible ureteroscopy. Third, our trainer was portable, durable, and reusable. A single model was used in more than 40 cases without any apparent defects in the model from repetitive use or heat transfer from the laser fiber, which compromised its continued use. Finally, it is compatible with the standard ureteroscopes and instrumentation. This makes it an ideal

model for training courses and workshops, to upskill surgeons to reduce the caseload needed to achieve surgical competency.

Orecchia et al. also used 3D printing to create a trainer for high-fidelity simulation of RIRS.[92] There were important differences from our model. Their unvalidated model only had calyceal systems of six different kidneys 3D-printed. The models were then fitted to a commercially available Cook part-task trainer. Although their total expenditure was estimated to be USD 220-430, their costs did not include the part-task trainer. During the testing phase, human stones were not used for laser lithotripsy. Training stones were produced using suspensions of water and chalk in fixed proportions to produce soft and hard stones that best replicated real-life conditions. An advantage of their model was the use of radiotransparent polymers which would allow for the use of fluoroscopy.[92]

We acknowledge some limitations of our study. As with any benchtop model, there was less realistic tissue haptics than one would expect in biological and virtual reality models. One of the challenges in RIRS is the potential for movement of the stone within the operative field during laser lithotripsy, as the kidney moves cranially and caudally due to diaphragmatic and chest respiratory excursions in a ventilated patient. We attempted to replicate this by allowing the printed kidney to float in the submerged medium. Second, we did not use radiotransparent polymers for the upper urinary tract; therefore, fluoroscopy could not be performed. Several studies have, however, shown that RIRS can be performed safely and effectively without the use of fluoroscopy.[93,94] Furthermore, a recent systematic review and meta-analysis revealed that routine use of fluoroscopy does not influence the outcomes of RIRS.[95] Thirdly, for this validation study, our model only included one set of kidneys, which may not account for the different anatomical

complexities we expect between patients. We envisage the comprehensive training set to consist of different pairs of kidneys to account for variations among patients (Figure 6D). Although the inclusion of these other models will enhance confidence in RIRS, we recognise that the surgeon is expected to face a wider range of scenarios in real-world clinical settings, beyond what our model offers. Additionally, our model has not been able to effectively reproduce complications of RIRS, such as bleeding and perforation, nor has it successfully simulated the occurrence of an unforeseen tumour or foreign body. Despite these inherent limitations, as is with any training model, the FiST model will enhance the confidence of urology to help deal with inadvertent complications or challenging clinical scenarios. Furthermore, future improvements of this model could involve using more flexible materials, such as silicone, through techniques like casting or hybrid 3D printing. These would allow for more accurate anatomical replication and potentially enable more realistic training.

# Conclusions

The FiST model performed well for all the components of the RIRS. This benchtop model allows high fidelity of the simulation, is cost-effective and completely portable, durable, and reusable, and is compatible with standard ureteroscopes and instrumentation. We are confident that this 3D-printed RIRS model will be a valuable learning asset for urological trainees to use as an adjunct to operative training for RIRS.

**Ethical approval**

The validation study was approved by the Frere and Cecilia Makiwane Hospitals Research Ethics Committee (FCMHREC/A0175/2023).

## Declaration of Competing Interest

The authors have no conflicts of interest to disclose.

## Acknowledgment

We thank Karl Storz, NuAngle, Coloplast, and Allwin Medical Devices for making the necessary equipment and consumables available at no cost for the validation of the FiST model.

# Chapter 3: The porcine model for urological research and training: an endoscopic and CT-based study

## Overview

The porcine model has frequently been utilised by researchers and urological surgeons for medical advancements. The model has demonstrated its efficacy in understanding physiological and pathological processes, conducting preclinical trials, and facilitating robotic, laparoscopic, and endourological training. Despite the multiple advantages of this model, the specific anatomical knowledge that qualifies it as the optimal model in urology remains inadequately defined. In this chapter, we present the first reported study that precisely delineates pertinent endoscopic and CT-based urological anatomy of female Landrace pigs. The insights acquired from this research were essential for proceeding with the two studies described in Chapters 4 and 5. Furthermore, this unprecedented research will help other researchers use the porcine model to conduct research in endourology with confidence.

This chapter has been submitted to World Journal of Urology (Impact Factor: 2.8), and at the time of submission of this thesis, it was awaiting review.

**John J,** Fieggen G, Kaestner L, Lazarus J. The porcine model for urological research and training: an endoscopic and CT-based study.

CRediT author statement:

**Jeff John:** Writing – original draft, Visualization, Methodology, Formal analysis, Data curation, Conceptualization. **Graham Fieggen:** Supervision. **Lisa Kaestner:** Writing – review & editing, Supervision. **John Lazarus:** Writing – review & editing, Supervision**.**

# Abstract

**Objective:**

To describe the relevant urinary anatomy of female Landrace pigs based on endoscopy and computed tomography (CT) scans.

**Materials and Methods:**

Four white Landrace female pigs were used for the study: two for CT imaging and two for endoscopic assessment. CT-urograms were performed using a 64-channel tomography machine with 0.625 mm thick slices. For the endoscopic procedure, the intravaginal urethral meatus was cannulated using a cystoscope, followed by complete urethrocystoscopy. The ureteric orifices were then cannulated and a retrograde pyelogram was performed, followed by ureterorenoscopy.

**Results:**

CT and endoscopic findings showed two multirenculate multipapillate kidneys, each receiving blood supply from a single renal artery that is further divided into cranial and caudal branches. The delayed phase of the urogram showed distal ureters passing posterior to the bladder and emptying into the bladder at the base. Urethroscopy revealed an intravaginal urethral meatus ventral to the anus, positioned midway between the mucocutaneous junction of the vulva and the cervix. Endoscopic view of the bladder neck showing patulous ureteric orifices at the bladder neck with no distinct interureteric ridge or trigone. Retrograde pyelogram showed a Group B drainage pattern in both pigs.

**Conclusion:**

While there are numerous similarities between the urinary systems of humans and pigs, there are important subtle differences that urologists and researchers need to be mindful of before using the porcine model for urological research and training.

# Introduction

For centuries, humans have employed animal models to progress biomedical science, to understand pathological and biological processes, and to develop and test drugs, vaccines, and surgical techniques.[96] Research on cows helped create the world's first vaccine to eradicate smallpox[97]; in the 1940s and the 1950s, several monkeys died to develop the polio vaccine.[98] Professor Christian Barnard, who pioneered the first human heart transplant, initially gained expertise in orthotopic heart transplantation in canines.[98] The use of pigs in scientific studies, particularly as preclinical models, has experienced a significant surge since the early 1980s. Pigs exhibit a high degree of biological similarity to humans when considering their anatomical and physiological characteristics.[99] The porcine genome is also three times closer than the mouse genome to that of the human.[100] Furthermore, there is a wealth of information available about their unique behavioral and husbandry considerations and reproductive management.[101] They are also an economically viable and freely available model due to the widespread commercial breeding for the meat industry.[102] In the field of urology, Sampaio and his colleagues from Brazil were the pioneers in proposing that the porcine model is the most accurate representation of the human kidney.[103] This paper describes the relevant urinary anatomy of female Landrace pigs based on endoscopy and computed tomography (CT) scans. It also examines the parallels and differences between the urinary anatomy of pigs and humans.

# Materials and Methods

The local Animal Ethics Committee approved this study (020_011). Veterinary and paraveterinary specialists were employed to guarantee the well-being and clinical care of

the animals. Four white Landrace female pigs (weight 50-60 kg) were used in this study. Two were utilized for CT imaging, while an additional two were employed for endoscopic evaluation. The animals were brought to the research facility and boarded for seven days to allow a sufficient acclimatization period. The pigs were provided with a regular diet for up to 12 hours before the study, but access to water was not restricted at any point.

## Anaesthetic protocol

Identical anesthetic methods were used for both the CT scans and endoscopic procedures. Prior to the procedure, the pigs were administered a diazepam patch for pre-medication. They were then induced with a mixture of Zoletil (3 mg/kg IM), Medetomidine (0.06 mg/kg IM), and Butorphanol (0.15 mg/kg IM) then intubated, ventilated with anesthesia being maintained using isoflurane (1.5-3% in oxygen). The animals were initially hydrated with a saline bolus of 90 mL/kg, given over 5 minutes. Hydration was then maintained during the surgery by administering saline (10 mL/kg/h) through an ear vein.

## Computed tomography (CT) assessment

CT-urograms were performed using a 64-channel tomography machine with 0.625 mm thick slices. The dual-phase study included an initial 50 mL bolus of intravenous non-ionic iodinated contrast. After ten minutes, a portal venous phase enhancement study was performed using 100 mL of contrast medium to optimally evaluate the arterial and venous structures. This was followed by a delayed study performed after ten minutes for optimal evaluation of the ureters and bladder.

The following parameters were measured:

(a) Renal length: the distance measured along the long-axis of the kidney, i.e. the greatest distance between the cranial and caudal edges.

(b) Cranial and caudal pole width: from an axis, perpendicular to the length, drawn at the broadest segment of the cranial and caudal renal poles.

(c) Kidney and bladder volumes: measured using the region of interest (ROI) tool.

(d) Ureteral length: the sum of the length of the abdominal ureter (ureteropelvic junction to pelvic brim) and pelvic ureter (pelvic brim to ureterovesical junction).

## Endoscopic assessment

The pigs were positioned in the dorsal lithotomy position. A single-use cystoscope (9F, WiScope®, OTU Medical) was introduced into the vagina to locate the urethral meatus. The cystoscope was then advanced into the bladder, and following a thorough examination, the ureteral openings were located and cannulated using conventional guidewires (0.035 inch) with the assistance of fluoroscopy. The guidewire was exchanged for an open-ended ureteric catheter (6F) through which contrast was administered to completely opacify the ureter and renal collecting system (retrograde pyelogram) to determine the calyceal configuration according to the Sampaio classification. The open-ended ureteric catheter was exchanged for a standard guidewire, over which a single-use ureteroscope (7.4 Fr, WiScope®, OTU Medical) was advanced to facilitate a complete renoscopy and ureteroscopy. The procedure was then repeated on the opposite side. After completing the assessment and determining that the pig model was suitable for urological research, the researchers proceeded to use the same animals to pilot a novel drug eluting guidewire to enhance the endoscopic management of renal stones.[74,75]

## Statistical analysis

The Statistical Package for the Social Sciences (SPSS) Version 28 was utilised for all analyses, with a significance level of $p < 0.05$. The data is presented as the mean and

standard deviation. Means, standard deviations, and coefficients of variation were computed for each variable. The left and right kidney parameters were analysed by conducting independent sample t-tests and Mann-Whitney U tests.

# Results

Computed tomography (CT) and endoscopy (including retrograde pyelography) showed two multirenculate multipapillate kidneys, each receiving blood supply from a single renal artery that divides into cranial and caudal branches. In the right kidney of pig 1, there was an incidental finding of a large (2 × 2.5 cm) parapelvic cyst (Figure 10).

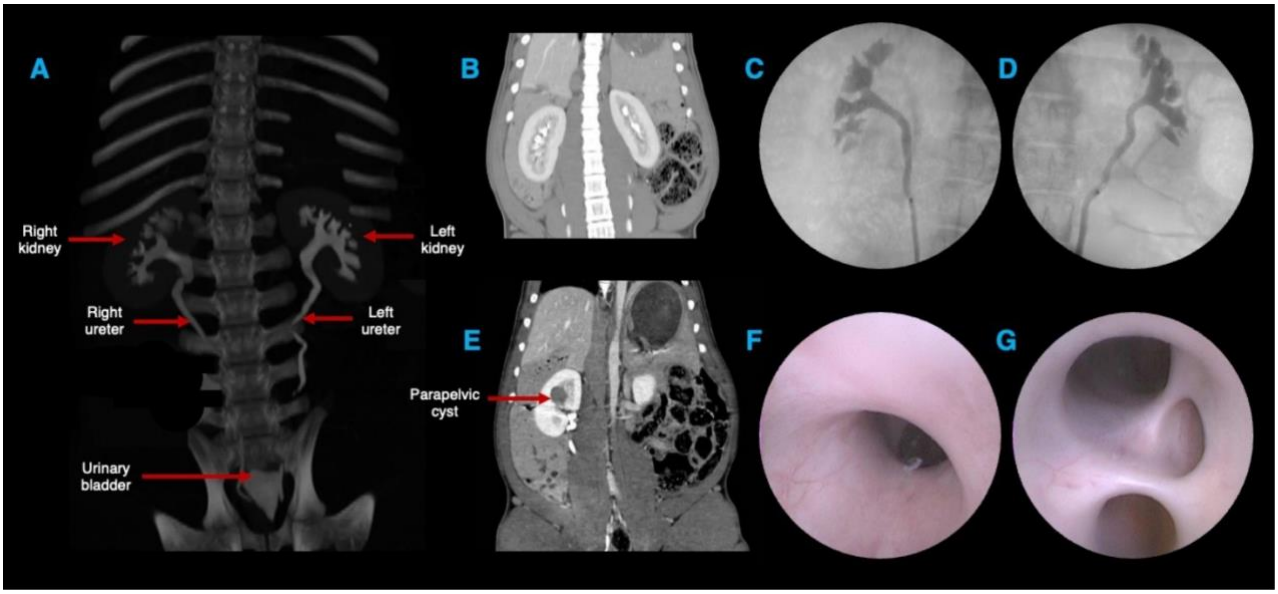


**Figure 10**

CT urogram and retrograde pyelogram images of the upper urinary tract showing two multirenculate, multipapillate kidneys and their corresponding ureters [A-E]. Endoscopic view of the renal pelvis from the ureteropelvic junction [F] and renal calyces [G].

---

CT measurements for the kidneys, ureters, and bladders of both pigs are summarized in Table 1.

**Table 1**

**CT measurements for the kidneys, ureters, and bladders of both pigs in the study**

| KIDNEYS | Pig 1 | Pig 2 | Mean | SD | CV % | p value (mean) | p value (median) |
|---|---|---|---|---|---|---|---|
| Right renal length (cm) | 10.87 | 10.50 | 10.69 | 10.69 | 2.45 | 0.534 | 0.655 |
| Left renal length (cm) | 10.79 | 12.00 | 11.40 | 11.40 | 7.51 | | |
| Right renal cranial pole width (cm) | 4.93 | 5.04 | 4.99 | 4.99 | 1.56 | 0.661 | 0.655 |
| Left renal cranial pole width (cm) | 5.21 | 3.96 | 4.59 | 4.59 | 19.28 | | |
| Right renal caudal pole width (cm) | 5.67 | 4.91 | 5.29 | 5.29 | 10.16 | 0.289 | 0.180 |
| Left renal caudal pole width (cm) | 5.45 | 4.27 | 4.86 | 4.86 | 17.17 | | |
| Right kidney volume (cc) | 164.00 | 150.00 | 157.00 | 157.00 | 6.31 | 0.033 | 0.180 |
| Left kidney volume (cc) | 155.00 | 140.00 | 147.50 | 147.50 | 7.19 | | |
| **URETERS** | **Pig 1** | **Pig 2** | **Mean** | **SD** | **CV %** | **p value (mean)** | **p value (median)** |
| Right total ureteral length (cm) | 24.00 | 25.30 | 24.65 | 24.65 | 3.73 | 0.042* | 0.180 |
| Left total ureteral length (cm) | 29.00 | 31.00 | 30.00 | 30.00 | 4.71 | | |
| Right abdominal ureteral length (cm) | 14.00 | 17.00 | 15.50 | 15.50 | 13.69 | 0.258 | 0.180 |
| Left abdominal ureteral length (cm) | 19.00 | 19.00 | 19.00 | 19.00 | 0.00 | | |
| Right pelvic ureteral length (cm) | 10.00 | 8.30 | 9.15 | 9.15 | 13.14 | 0.500 | 0.317 |
| Left pelvic ureteral length (cm) | 10.00 | 12.00 | 11.00 | 11.00 | 12.86 | | |
| **BLADDERS** | **Pig 1** | **Pig 2** | **Mean** | **Median** | **SD** | **CV %** | |
| Bladder volume (cc) | 700 | 365 | 532.50 | 236.88 | 532.50 | 44.48 | |

The length of the kidneys ranged from 10.50 to 10.87 cm on the right side, with a mean of 10.69 cm, and from 10.79 to 12.00 cm on the left side, with a mean of 11.40 cm. There was no significant difference in length between the two sides ($p = 0.534$). The width of the cranial renal pole ranged from 4.93 to 5.04 cm, with a mean of 4.99 cm on the right, and from 3.96 to 5.21 cm, with a mean of 4.59 cm on the left. There was no significant difference in width between the two sides ($p = 0.661$). The width of the caudal renal pole ranged from 4.91 to 5.67 cm, with a mean of 5.29 cm on the right side, and from 4.27 to 5.45 cm, with a mean of 4.86 cm on the left side. There was no significant difference in width between the two sides ($p = 0.289$). The right renal volume ranged from 150 to 164

$cm^3$, with an average of 157 $cm^3$, while the left renal volume ranged from 140 to 155 $cm^3$, with an average of 147.5 $cm^3$. The volume of the kidney on the right side was significantly higher ($p = 0.033$).

Both pigs exhibited a Group B pattern of drainage of the pelvi-calyceal system as revealed by the retrograde pyelogram. The overall length of the ureter ranged from 24 to 25.3 cm on the right side, with a mean of 24.65 cm, and from 29 to 31 cm on the left side, with a mean of 30 cm. The overall length of the ureter was notably greater on the left side ($p = 0.042$). The length of the abdominal ureter ranged from 14 to 17 cm on the right side, with a mean of 15.5 cm, and was 19 cm on the left side. There was no significant difference in length between the two sides ($p = 0.258$). The length of the pelvic ureter ranged from 8.3 to 10 cm on the right side, with a mean of 9.15 cm, and from 10 to 12 cm on the left side, with a mean of 11 cm. There was no significant difference in length between the two sides ($p = 0.5$).

In the delayed CT phase, the distal ureters passed posteriorly to the bladder and were emptied into the base of the bladder. Urethroscopy and cystoscopy revealed two patulous ureteric orifices at the bladder neck, 1-3 cm apart in both pigs (Figure 11). No bladder trigones were observed. The estimated bladder volumes were 700 and 365 cc in pigs 1 and 2, respectively (Figure 11).

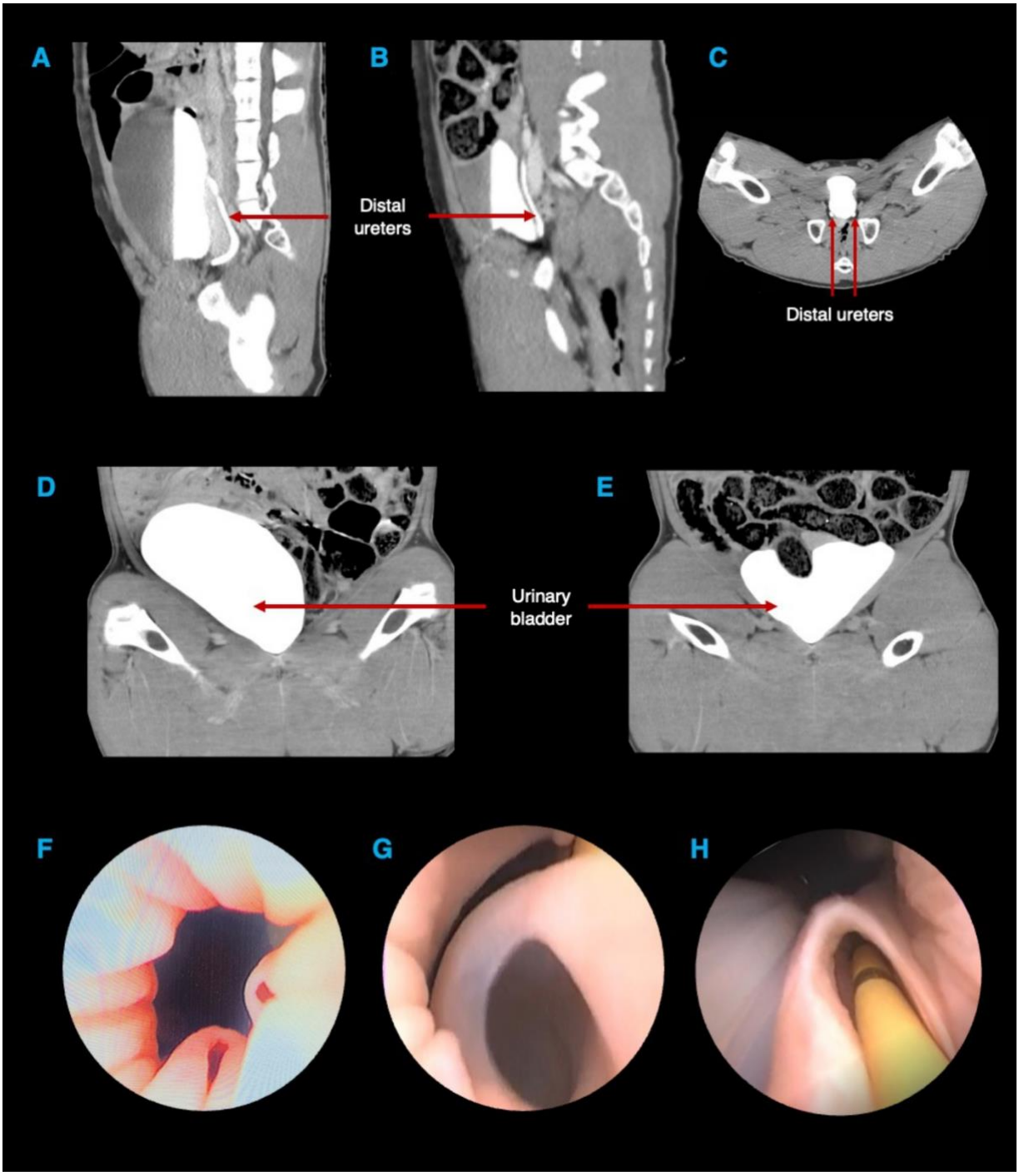


**Figure 11**

Delayed phase of CT urogram showing distal ureters (A-C) passing posterior to the bladder and emptying into the bladder (D and E) at its base. Endoscopic view of the bladder neck showing patulous ureteric orifices at the bladder neck (and no interureteric ridge) [F and G] which allowed easy passage of a 6F ureteric catheter [H].

The urethral orifice was identified intravaginally (Figure 12).

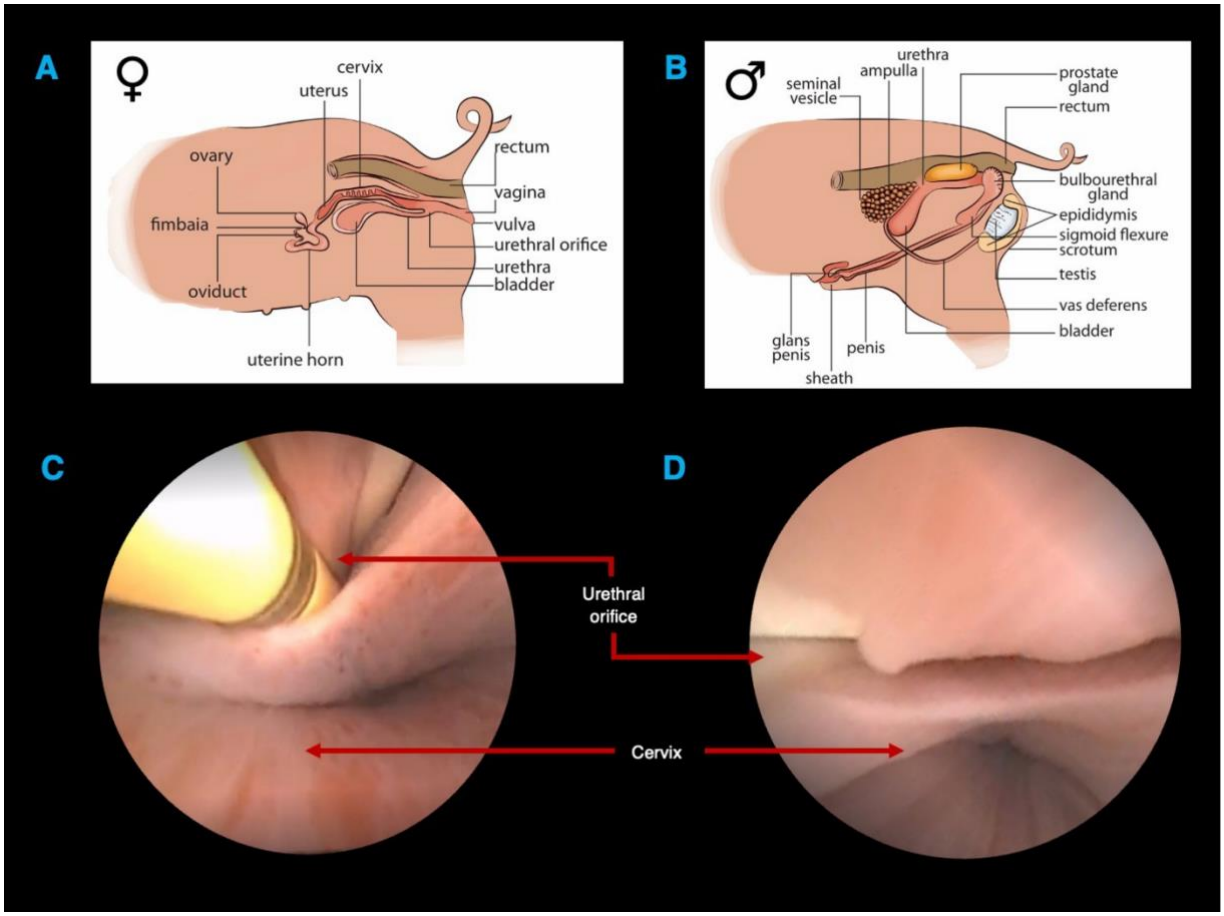


**Figure 12**

Graphical representation showing the genitourinary anatomy in the female [A] and male [B] porcine model and notably the position of the urethral orifice. Vaginoscopy showing both the urethral opening with [C] and without [D] a 6F ureteric catheter, and the cervical opening.

# Discussion

The porcine model has often been used by researchers and urological surgeons for advances in medicine. The model has proven ideal for understanding physiological and pathological processes,[15] preclinical trials[104] and robotic, laparoscopic, and endourological training.[105] Although the porcine model presents numerous benefits, precise anatomical knowledge that establishes it as the ideal model in urology remains limited. This study is the first to describe the relevant endoscopic and CT-based urological anatomy of female Landrace pigs.

In our study, the mean renal length measured from pole to pole was 10.70 cm on the right side and 11.40 cm on the left side. The measurements fall within the range of what we would expect in a human kidney.[106,107] The plausible hypotheses to account for the discrepancy in size between the two sides is similar to the explanation in humans: the presence of the liver on the right, which prevents the spatial expansion of the right kidney and there is increased blood flow to the left kidney due to a shorter left renal artery.[108] Gómez et al. and Arenas et al. reported mean renal lengths in pigs of 12 cm.[109,110] However, the lengths were determined by surgically dissecting the kidneys of various breeds that weighed much more than the pigs used in this study. In humans, the absolute renal length is considered smaller in women.[111] The mean renal lengths in our two female pigs were longer than those measured on CT, by other authors in male pigs.[112]

Talhar et al. examined the CT scans of 140 anatomically normal kidneys of 70 individuals and reported the mean renal volume to be 94.18 $cm^3$ and 98.06 $cm^3$ on the right and left, respectively.[113] The mean renal volumes in our study (157 $cm^3$ on the right, 147 $cm^3$ on the left kidney) were much larger. Furthermore, the mean renal volumes in our female

pigs were also greater than those measured on CT in male pigs (113.70 $cm^3$ on the right, 109.70 $cm^3$ on the left).[112] Surprisingly, despite the mean renal length of the left kidney being longer in our study, the mean renal volume of the right was higher. These differences are likely due to variations in the size of animals and inter-observer variability while measuring parameters. The presence of a large parapelvic cyst (2 × 2.5 cm) in the right kidney of one of our pigs could possibly also have likely influenced the measurements.

Researchers who analysed 3-dimensional endocasts of the kidneys, noted that each of the pigs had a single artery per kidney. In 93.4% of cases, this artery was divided into cranial and caudal branches, while in 6.6% of cases, it was divided into dorsal and ventral branches.[114] In contrast, humans exhibit multiple renal arteries in almost a third of cases (27-30%).[115] Prior to entering the renal hilum, the human renal artery undergoes a longitudinal division, resulting in an anterior and posterior division. Each division then divides into segmental arteries. On the other hand, Evan et al. demonstrated that the primary renal artery in pigs divides into two consistent patterns.[116] In the predominant pattern (I), the renal artery in pigs bifurcates into two polar arteries, namely upper and lower, which further divide into anterior and posterior segmental arteries. This anatomically separates the blood flow to the kidney into two separate areas that align with the top and lower sections of the kidney, namely in a transverse direction. In our investigation, we discovered a pattern where additional arteries originating from the lower polar artery also supplied the upper pole.[116] Clinically, the difference in this pattern between human and pig kidneys is important, as the avascular plane in porcine kidneys is transverse, whereas in human kidneys it is longitudinal.

The kidneys of our pigs exhibited a genuine multirenculate, multipapillate structure, like the calyceal structure found in humans. In their landmark work, Sampaio and Aragao[117] studied a porcine collecting system by injecting polyester resin into the ureter to completely fill the collecting system. The casts of the collecting system were utilised to classify the pig pelvicalyceal system into two distinct groupings. Group A exhibited two prominent calyceal groups within the pelvicalyceal system, with the draining of the mid-zone relying on either cranial or caudal calyceal drainage. In group B, the mid-zone drainage was independent on the cranial or caudal calyceal drainage. Sampaio and Aragao discovered that 40% of pig kidneys displayed Group A drainage and 60% displayed Group B drainage, while 62% of human kidneys exhibited Group A drainage and 38% exhibited Group B drainage, according to this classification. In our study, it was difficult to assess this in the delayed CT phase. However, retrograde pyelogram images suggested a Group B drainage pattern in both pigs (Figure 10 C-D). Furthermore, we noted a perpendicular minor calyx that directly drains into the renal pelvis. This particular pattern is found in 18% of pig kidneys, but it is only present in 11.4% of human kidneys.[117]

The ureteric orifices drained into the bladder at the bladder neck with a distance of roughly 1-3 cm between them. While some authors have described the ureteric orifices as tight,[118] we found them to be patulous, enabling smooth insertion of the 7.4 F ureteroscope into the renal pelvis. Endoscopically, we found that there was no bladder trigone, and this is in agreement with reports from other researchers.[119] The absence of the ureteric orifices at the trigone and, consequently, the interureteric ridge and Bell's muscle would explain this. The anatomical capacity of the bladder gradually rises with age, to a mean between 400 and 600 mL in adulthood.[120] Although our two female pigs had a comparable mean volume of 533 mL, there was a wide range, that is, 700 and 365 mL in pigs 1 and 2,

respectively, probably because of the varying degrees of bladder fullness one would expect. The porcine bladder is an intraperitoneal organ with the entire surface being covered with peritoneum, as opposed to the extraperitoneal/subperitoneal position in humans.[121] Furthermore, the bladder wall is thinner, and care should be taken during urological procedures.[122] Endoscopically and radiologically, it was difficult to confirm these findings.

The human female urethra perforates the urogenital diaphragm, and its external orifice is located right in front of the vaginal opening, making urethral catheterization straightforward. Our examination revealed that the urethral orifice in the female pig was located intravaginally, ventral to the anus, and distally positioned midway between the mucocutaneous junction of the vulva and the cervix (Figure 12). Vaginoscopy was therefore needed to identify the urethral opening and gain access to the urinary tract. In contrast, the male pig has a long, fibroelastic penis with an 'S'-shaped sigmoid flexure ventral to the pubic bone. The tip of the penis is spiral-shaped like a corkscrew, and there is a pouch-like structure called the prepeutial diverticulum on the underside of the abdomen. These anatomical features make the retrograde passage of catheters or endoscopic tools technically very challenging.[122]

As a limitation of this study, we acknowledge that only one pig breed was used, only females, and only four animals in total. This limits the wide extrapolation of these findings. Secondly, a physiological validation of this animal model was not conducted. Nevertheless, our study showed that using a porcine model is adequate for endourological research and training. While there are numerous similarities between the urinary systems of humans and pigs, comparative anatomical descriptions highlight the small but subtle differences

that urologists and researchers need to be mindful of. The authors of this study were able to use the knowledge gained from this research to conduct meaningful studies in the field of endourology to advance the surgical management of patients with kidney stones.[74,75]

**Funding source**

This work received financial assistance from the National Centre for Research and Development (Project No. M-ERA.NET2/2019/1/2020) and the Department of Science and Innovation, South Africa, as part of the 'IsoWire' project under the M-ERA.NET Program (Call2019), which is co-financed by the European Union.

**Ethical Approval for Animal Studies**

Animal studies were approved by the University of Cape Town Animal Ethics Committee (AEC 020_011).

**Declaration of Competing Interest**

The authors have no conflicts of interest to disclose.

**Acknowledgment**

(1) Peter Zilla, Rose Boltman, and Helen Ilsley of Strait Access Technologies

(2) Janet McCullum, John Chipangura, Tashie Makwavarara, and Thireshni Chetty at the University of Cape Town Research Animal Facility

(3) Michelle Henry, at the Numeracy Centre, Centre for Higher Education Development at the University of Cape Town

(4) Ivann van Der Merwe, Lettie Greef and Le Shane Heugh of SCP Radiology

(5) Val Myburgh

# Chapter 4: Introducing an isoprenaline eluting guidewire – report on its design and the results of the dose-determining pilot study

## Overview

To alleviate the challenges associated with increased IRP, surgeons may utilize diverse approaches to regulate IRP. Pharmacologic therapies in the perioperative period to mitigate IRP have been documented, although none of these strategies have been integrated into clinical practice. This chapter delineates the design of an innovative isoprenaline-eluting guidewire (IsoWire), a platform guidewire intended for the administration of topical isoprenaline, a beta-receptor agonist, to the genitourinary system. In this chapter, we discuss the findings of the initial in vitro release tests and the first animal trials. This is the first study to report the delivery of isoprenaline using a drug-eluting guidewire.

The content in this chapter was published in *Journal of Endourology* (Impact Factor 2.9).

**John J,** Wellman M, Dixon C, Kellermann T, Wisniewski P, Kopeć K, Trzciński J, Kopeć D, Ciach T, Fieggen G, Kaestner L, Lazarus J. Introducing an isoprenaline eluting guidewire: report on its design and the results of the dose-determining pilot study. J Endourol. 2024 Jun;38(6):590-597. http://doi.org/10.1089/end.2023.0745.

CRediT author statement:

**Jeff John:** Writing – original draft, Visualization, Methodology, Formal analysis, Data curation, Conceptualization. **Mark Wellman:** Investigation. **Charné Dixon:** Investigation. **Tracy Kellermann:** Investigation. **Pawel Wisniewski:** Methodology, Project Administration. **Kamil Kopeć:** Methodology, Investigation, Writing – review and editing. **Jakub Trzciński:** Investigation. **Daniel Kopeć:** Investigation. **Tomasz Ciach:** Investigation. **Graham Fieggen:** Supervision. **Lisa Kaestner:** Writing – review and editing. Supervision**. John Lazarus:** Methodology, Investigation. Writing – review and editing, Supervision.

# Abstract

**Objective:**

We aim to describe the design of a novel isoprenaline-eluting guidewire (''IsoWire'') and present the results from the first in vitro release studies and the first animal studies showing its effect on IRP.

**Materials and Methods:**

The IsoWire comprises a Nitinol core surrounded by a stainless-steel wire wound into a tight coil. The grooves created by this coil provided a reservoir for adding a hydrogel coating into which isoprenaline, a beta-agonist, was loaded. Animal studies were performed using a porcine model. For the control, IRP, heart rate (HR), and mean arterial pressure (MAP) were measured continuously for 6 minutes with a standard guidewire in place. For the experiment, the standard hydrophilic guidewire was removed, the IsoWire was inserted into the renal pelvis, and the same parameters were measured.

**Results:**

In vitro analysis of the isoprenaline release profile showed that most (63.9-5.9%) of the loaded drug mass was released in the 1st minute, and almost all of the drug was released in the first 4 minutes exponentially. Porcine studies showed a 25.1% reduction in IRP in the IsoWire that released 10 μg in the 1st minute; however, there was a marked increase in HR. The average percentage reduction in IRP was 8.95% and 21.3% in the IsoWire that released 5 and 7.5 μg of isoprenaline, respectively, with no changes in HR or MAP.

**Conclusion:**

The IsoWire, which releases 5 and 7.5 μg of isoprenaline in the 1st minute, appears to be safe and effective in reducing the IRP. Further studies are needed to establish whether the isoprenaline-induced ureteral relaxation will render easier insertion of a ureteral access sheath, reduce IRP during sheathless RIRS, or even promote the practice of sheathless RIRS.

# Introduction

Urolithiasis is considered the third most common disease in urology[57] and changes in lifestyle, diet, comorbidities, climate, and the increased use of abdominal imaging have contributed to its increased prevalence.[58,59] The pendulum has shifted from open procedures to more minimally invasive techniques such as RIRS. A flexible ureterorenoscope is inserted into the kidney to visualize the stone. If the stone is small, it may be snared and removed with a stone-extracting device. In cases where the stone is large or the diameter of the ureter is narrow, the stone can be fragmented or dusted with laser lithotripsy.

Numerous technological advancements in endoscopy have contributed to the growing popularity of RIRS, which is reflected in the recent guidelines of prominent urological societies, including the European Association of Urology (EAU) and American Urology Association (AUA), both of which have expanded the role of RIRS.[4,78]

However, RIRS is associated with complications, many of which are related to IRP. Normal physiological IRP in an unobstructed kidney ranges from 0 to 15 mmHg (0-20 $cmH_2O$).[6] During RIRS, dangerous IRPs are often encountered, resulting in complications that lead to pyelorenal reflux resulting in the retrograde translocation of uropathogenic bacteria and endotoxins from the urinary system into the bloodstream predisposing to urosepsis.[18,19] Although mortality after ureteroscopy is rare, a recent multi-institutional case series of six post-ureteroscopy mortalities revealed that four patients died due to urosepsis.[21] While the patient's age, comorbidities, stone size, positive pre-operative urine culture, and the presence of an indwelling stent contribute to the incidence of urosepsis in RIRS,[20] elevated IRP seems to be as important a risk factor.[20,123] Forniceal rupture is

another complication of elevated IRP in RIRS. As the pressure rises within the collecting system the collecting system ruptures at the renal fornix causing intraoperative bleeding and subsequently, poor vision for the surgeon.[24] Postoperative pain, acute kidney injury, and fluid overload are other complications of increased IRP that have been reported.[18,19] To mitigate these complications, surgeons can employ various techniques to control IRP. Perioperative pharmacological interventions using intravenous or endoluminal isoprenaline, a β-receptor agonist, and intravenous parecoxib, a selective cyclooxygenase-2 (COX-2) inhibitor, have been shown to reduce IRP.[26,104,124,125] However, despite promising results, neither intervention has formed part of clinical practice.

This paper describes in detail the design of a novel isoprenaline-eluting guidewire ("IsoWire") and presents the results of the first in vitro release studies and the first animal studies showing its effect on IRP. Confirmation of coating lubricity, adherence, and durability and guidewire performance of the IsoWire is also presented.

# Materials and Methods

## Guidewire design (Figure 13A)

The IsoWire is composed of a central core made of nitinol. This renders the guidewire super-elastic, offers good flexibility, stability, and torque while navigating the genitourinary system, and is kink-resistant. The body of the wire surrounding the core consists of a high-quality stainless-steel wire wound into a tight coil around the core. The distal tip is a conically grounded core wire that tapers distally with an atraumatic ball at the end. The wires are coated with polytetrafluoroethylene (PTFE) polymer to decrease

the coefficient of friction and increase the lubricity. Distally, the hydrophilic coating reduces the friction during deployment and allows easier steering.

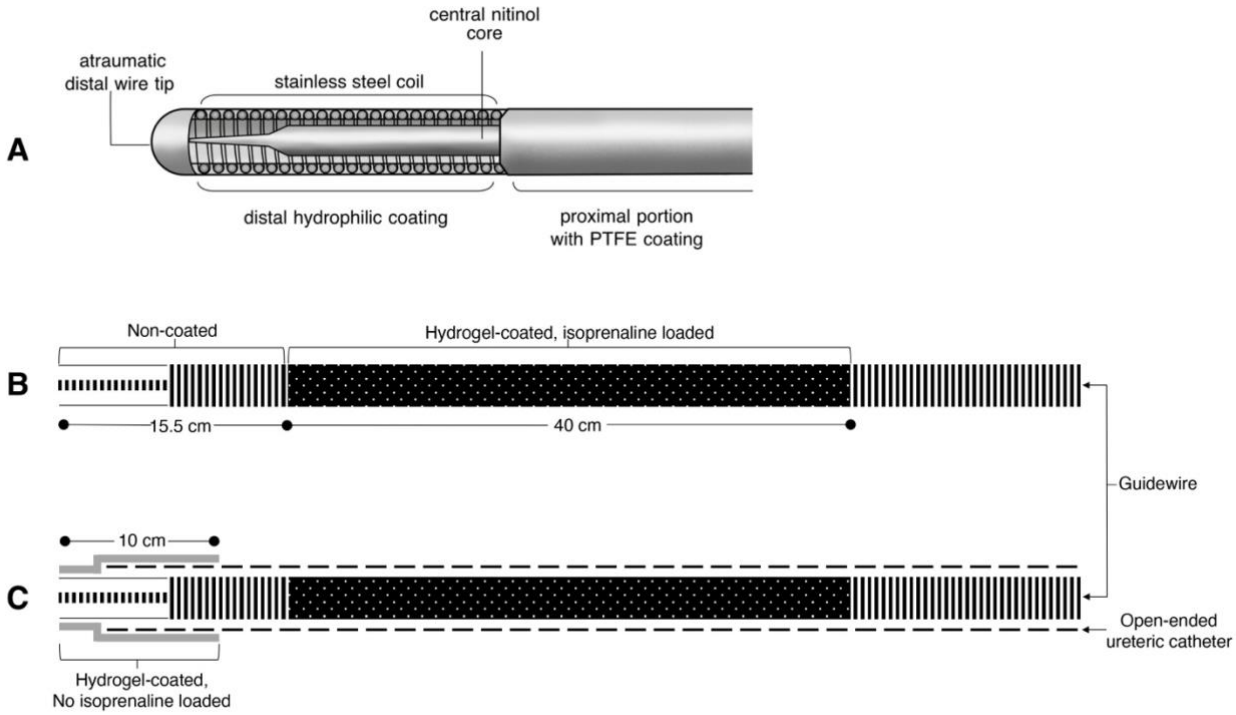


**Figure 13**

Schematic representation of the structure of the IsoWire (A) and the hydrogel coating with (B) and without isoprenaline (C). PTFE = polytetrafluoroethylene.

---

## Hydrogel-drug coating synthesis

As mentioned earlier, the stainless-steel wire is wound into a tight coil around the core. The grooves created by the coil provided a reservoir for the hydrogel. The hydrogel coating on the base wire was produced in a series of steps.

*Pre-treatment of the guidewire:* The distal 55.5 cm length of the guidewire was pre-treated by wiping it with ethanol and immersing it in hexane for two minutes (min).

*Preparation of the first hydrogel coating:* The polyvinylpyrrolidone (PVP) hydrogel coating was produced on a 40 cm length of guidewire (Figure 13B) using a method described by Butruk et al.[126] This length of guidewire, which would be in direct contact with the urothelium, was immersed in a solution of 4% cumene hydroperoxide and 5% ethylene glycol dimethylacrylate in hexane for 10 seconds and then left to dry at room temperature for 2 min to allow the solvent to evaporate. It was then immersed in a solution of 3% polyvinylpyrrolidone (average molecular weight 360 kDa), 0.05% iron (II) chloride, and 0.1% ascorbic acid in a solvent mixture of water and propylene carbonate at a volume ratio of 90:10 for 15 min. The coated product was washed in deionized water for 10 min with agitation and dried at 45°C for 30 min.

*Drug loading:* The hydrogel-coated guidewires were immersed in an aqueous isoprenaline solution for 60 min at room temperature to load isoprenaline. They were then left to dry overnight at room temperature. Based on the previously determined release profile, the isoprenaline concentration in the solution was selected to obtain the desired amount of drug released in the first minute. Guidewires with hydrogel coatings that released 5.0, 7.5 and 10.0 μg of isoprenaline in the first minute were used for animal studies. Only a 40 cm length of guidewire in direct contact with the ureteric mucosa was loaded with isoprenaline.

*Determining the release profile of isoprenaline:* Ultraviolet–visible spectroscopy was used to determine the release profile of isoprenaline from the hydrogel coating. Fragments of guidewire with a length of 10 cm and hydrogel coating loaded with different amounts of drug were placed in 10 mL of artificial urine at 37°C (98.6°F), which was transferred to a

fresh portion of artificial urine every minute for a total of 10 min. The artificial urine composition proposed by Königsberger et al.[127] was used, and the pH of this solution was adjusted to 5.5. The concentration of released isoprenaline was then determined by measuring the light absorbance at a wavelength of 291 nm using a SPECTROstar Nano instrument (BMG Labtech, Germany) in 10 × 10 mm optical path quartz glass cuvettes (Hellma Analytics, Germany). The release profile of isoprenaline was determined for samples loaded with the drug from aqueous solutions of isoprenaline at concentrations of (m:v) 1, 2.5, 4, and 5%. Measurements were performed on three independent guidewire samples for each amount of drug loaded (n = 3).

*Visualization of the guidewire surface*: The guidewire surface was visualized before and after the synthesis of the hydrogel coating, after loading the coating with isoprenaline, and after drug release using stereoscopic microscopy (Leica M125C; Leica Microsystems, Germany) and scanning electron microscopy (SEM).

Before SEM observations, samples were cut into 1 cm pieces and fixed to microscope stubs with conductive carbon adhesive tape (Agar Scientific). Next, the samples were coated with a 6 nm layer of gold-palladium (Quorum Q150 TS, Quorum Technologies Ltd). Subsequently, the samples were examined using a Hitachi SU8230 ultrahigh-resolution scanning electron microscope (Hitachi High-Technologies Corporation) with secondary electron detectors at an accelerating voltage (10 μA). The samples were imaged at a magnification of 80X.

*Determining the friction coefficients of the guidewire:* The friction coefficients between the guidewire and porcine ureter were measured using a tribometer developed for this

purpose and described elsewhere.[128] Briefly, a 20 cm long sample of guidewire was placed between two polymer elements to which the porcine ureter was glued. The device chamber was filled with artificial urine, and measurements were performed at room temperature. Before starting the measurements, each sample was immersed in deionized water for 10s. The product was set to move in a parallel plane at a constant speed of 1 cm/s. The force of friction between the sample and the animal tissue was registered using a force meter KM202 K 3N (Megatron, Munich, Germany) and acquired in a PC using an A/D converter DAQPad-6015 (National Instruments, Austin, USA). The signal from the force meter was collected using an application made in the LabView 8 (National Instruments, Austin, USA) environment for 3s before and 7s after the start of product movement. The friction coefficient was calculated as the ratio of the measured friction force to the normal force (which is the difference between the force of gravity of the pressing element and buoyancy force). The maximum friction force measured at the beginning of product movement was used to determine the static friction coefficient. The dynamic friction coefficient was determined using the mean value of the friction force after the peak at the beginning of motion. Three samples of each product were used to determine the coefficient of friction ($n = 3$). The normality of the distribution of static and dynamic friction coefficient measurement results was tested using the Kolmogorov–Smirnov test ($p < 0.05$). The difference between the mean values of measured parameters was tested in one-way ANOVA ($p < 0.05$) with post hoc Tukey's test for multiple comparisons. Statistical analysis was performed using OriginPro 8 software (OriginLab Corporation, Northampton, USA).

## IsoWire assembly

This coated isoprenaline-loaded guidewire was inserted into the 5F open-ended ureteral catheter. A 2 cm length of the atraumatic "floppy tip" was left protruding from the open-ended ureteral catheter. The distal 10 cm, which includes the "floppy tip," and the junction of the open-ended catheter and guidewire was also covered with hydrogel (Figure 13C). This prevents the inadvertent release of isoprenaline and reduces friction, allowing easier cannulation of the ureteric orifice and seamless steering into the pelvicalyceal system.

## Animal studies

### *Animal model*

Porcine studies were approved by the local animal ethics committee (AEC 020_011). Three female pigs (white, Landrace breed, weight of 50-60 kg) were transported to the study facility and housed for seven days to allow an adequate acclimatization period. The pigs were fed a standard diet for up to 12 hours before the investigation but had free access to water. They were pre-medicated with a diazepam patch then induced with zoletil (3 mg/kg IM), medetomidine (0.06 mL IM) and butorphanol (0.15 mg/kg IM), and intubated and mechanically ventilated (GE Healthcare S5 Avance). Anesthesia was maintained using isoflurane 1.5-3% in oxygen. They were pre-hydrated with an initial bolus of saline administered at 90 mL/kg/h for 5 min, and hydration was maintained throughout the procedure with saline at 10 mL/kg/h through an ear vein. A central venous catheter and femoral arterial catheter were inserted under ultrasound guidance to allow blood sampling and invasive blood pressure (BP) and heart rate (HR) monitoring (Figure 14).

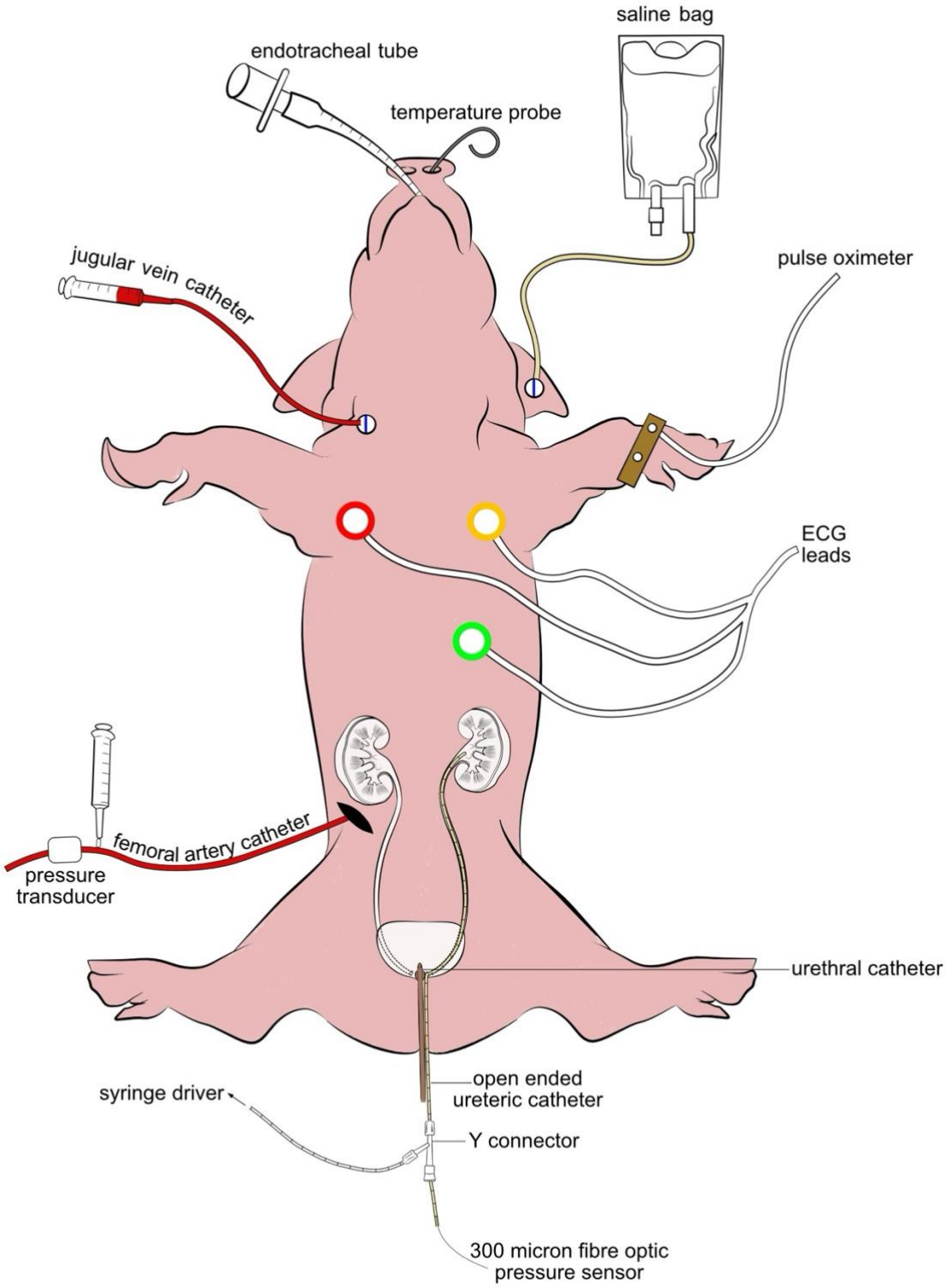


**Figure 14**

Graphical demonstration of the animal model. ECG = electrocardiogram.

*Endourological procedure*

In the lithotomy position, both ureteric orifices were cannulated with hydrophilic guidewires (0.035 in). An open-ended ureteric catheter was inserted into the left renal pelvis over the second hydrophilic guidewire. The second guidewire was removed, and a Touhy-Borst Y-connector was attached to the end of the open-ended ureteric catheter. Saline irrigation was started at 10 mL/min through the first port, and a 300 µm fiber optic pressure sensor (FISO Technologies Inc., Quebec, Canada) was inserted through the second port for continuous IRP monitoring. Size 10 French urethral catheter kept the bladder empty. As controls, IRP, HR, and MAP were measured continuously for six min during constant saline infusion. For the experiment, the standard guidewire was replaced with the IsoWire with the tip of the IsoWire positioned in the renal pelvis, confirmed on fluoroscopy. The protective ureteric catheter over the IsoWire was then removed to enable isoprenaline release. The IRP, HR, and MAP were measured continuously for six min. Blood samples were obtained to measure the plasma isoprenaline levels every minute after IsoWire insertion. Once the experiment and control were performed on one side, the same procedure was followed on the contralateral side, after ten min. Ureteroscopy was performed bilaterally to evaluate ureteric injuries.

# Results

The IsoWire surface before and after synthesizing the hydrogel coating, after loading the coating with isoprenaline, and after drug release are visualized in Figure 15. Immersing the guidewire in an artificial urine solution degraded the hydrogel coating, probably because of the ionic strength of the solution.

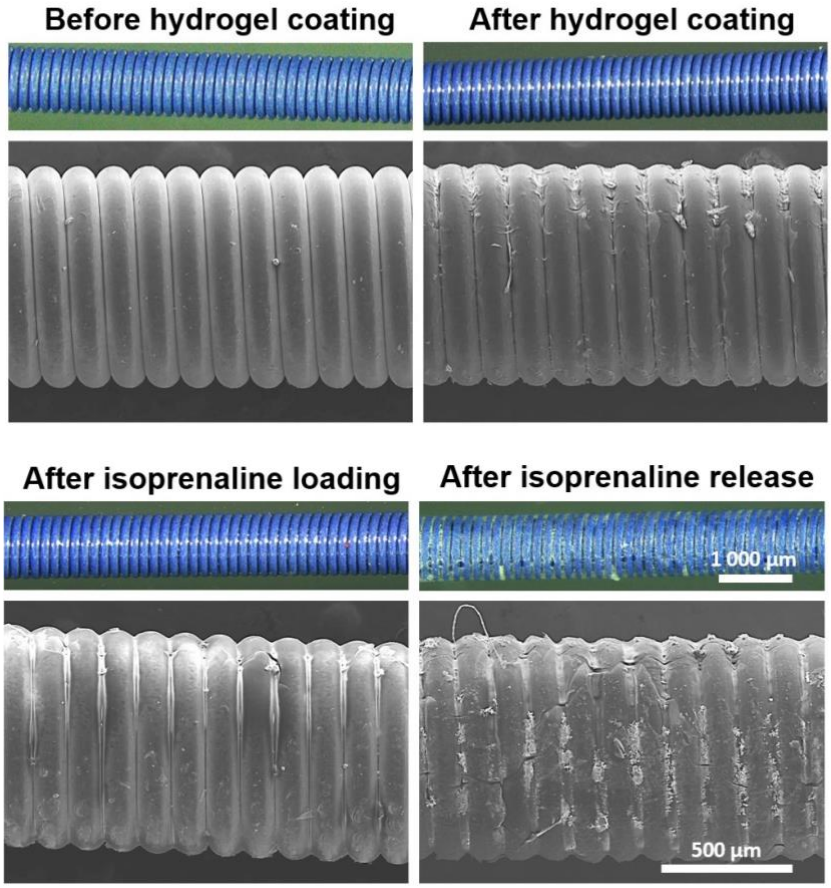


**Figure 15**

Stereomicroscopic and scanning electron microscopy images of guidewire with and without hydrogel coating.

---

Analysis of the isoprenaline release profile from the hydrogel-coated guidewire (Figure 16) showed that most (63.9 ± 5.9%) of the loaded drug mass was released in the first minute, and almost all the drug was released exponentially in the first 4 minutes. These data allowed us to determine the concentration of isoprenaline solution used to load the

drug into the hydrogel coating to obtain a given amount of drug released in the first minute.

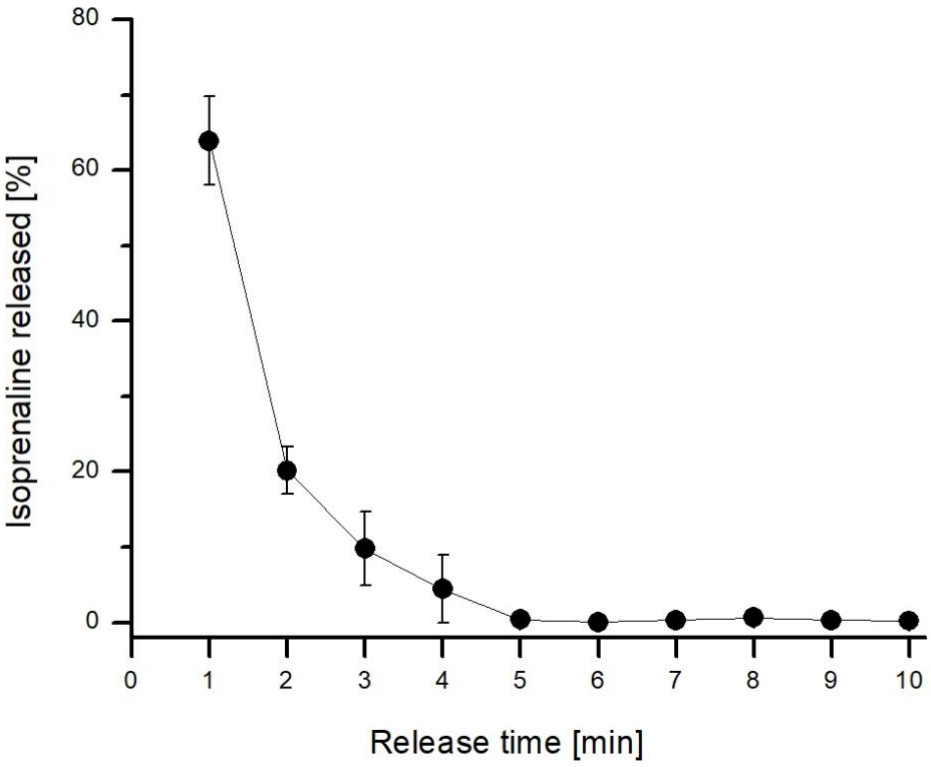


**Figure 16**

Isoprenaline release profile from hydrogel-coated guidewire into artificial urine solution.

---

The effect of the hydrogel coating on the friction between the guidewire and urinary tract tissue is shown in Figure 17. The frictional force was significantly reduced when the surface of the product was modified with hydrogel coating. The calculated static and dynamic friction coefficients were 0.084 ± 0.028 and 0.066 ± 0.020, respectively, for the guidewire without coating and 0.012 ± 0.005 and 0.006 ± 0.002, respectively, for the product with hydrogel coating. Static as well as dynamic friction coefficients were statistically different ($p < 0.05$) for the uncoated and coated guidewires. The hydrogel

coating led to a seven-fold reduction in the static friction coefficient and an eleven-fold reduction in the dynamic friction coefficient.

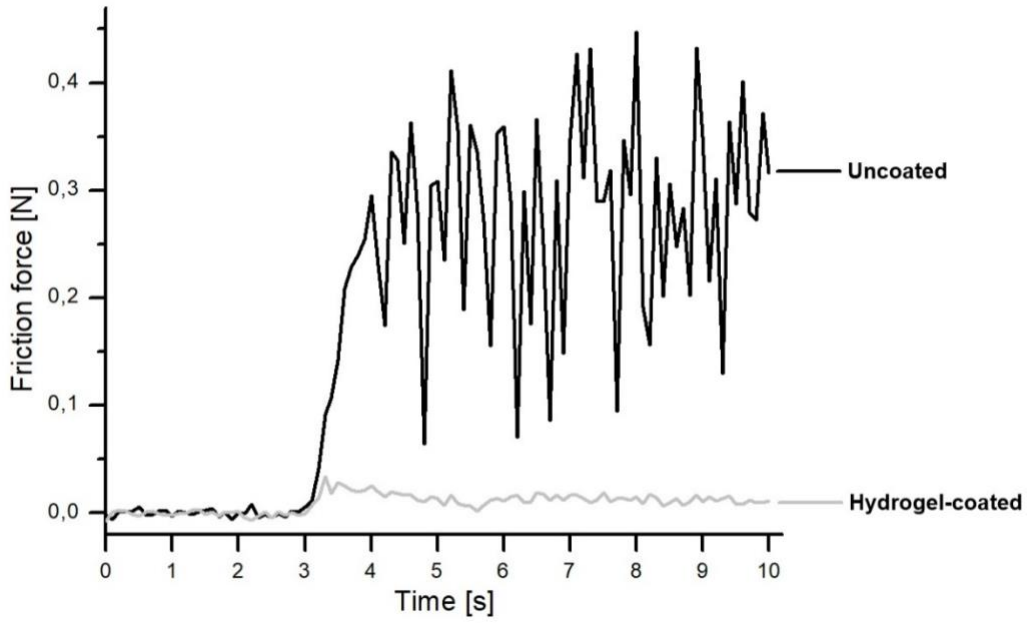


**Figure 17**

Graph showing the frictional force between the guidewire and porcine ureter. N= newton.

---

The animal study was comprised of six renal units. One renal unit was excluded because of failed access to the renal pelvis due to a tortuous proximal ureter. In this case, both the standard guidewire and the IsoWire could not be advanced into the renal pelvis and it was decided not to attempt other described techniques which may inevitably have affected the IRP readings in that renal unit. Therefore, these studies were conducted in 5 renal units. The use of the IsoWire resulted in a decrease in the IRP in all renal units (Table 2). The percentage reduction in IRP was related to the isoprenaline dose. The largest percentage reduction was observed for the IsoWire, which released 10 μg (25.1% reduction). The average percentage reduction in IRP was 8.95% and 21.3% in the IsoWire that released

5μg and 7.5 μg of isoprenaline in the first minute, respectively. In the IsoWires that released 5 μg and 7.5 μg of isoprenaline in the first minute, no changes in MAP or HR were observed. In the IsoWire, which released 10 μg of the drug in the first minute, no change in MAP was observed; however, a marked increase in HR was observed. Plasma isoprenaline levels were all below the level of quantification. No ureteric lesions were identified by ureteroscopy.

**Table 2**

**Outcome measures for the entire sample of five renal units in the pilot study**

| STUDY ID | DOSE[1] (μg) | MEAN IRP (mmHg) | | | MAP (mmHg) | | HR (bpm) | |
|---|---|---|---|---|---|---|---|---|
| | | STANDARD GUIDEWIRE | ISOWIRE | % PRESSURE REDUCTION | STANDARD GUIDEWIRE | ISOWIRE | STANDARD GUIDEWIRE | ISOWIRE |
| **1** | 10 | 43.9 | 32.9 | 25.1 | 87 | 87 | 90 | 103 |
| **2** | 5 | 26.4 | 24.4 | 8.2 | 89 | 89 | 84 | 83 |
| **3** | 5 | 33.1 | 29.9 | 9.7 | 84 | 84 | 79 | 78 |
| **4** | 7.5 | 26.4 | 19.9 | 24.6 | 71 | 70 | 91 | 91 |
| **5** | 7.5 | 27.1 | 22.2 | 18 | 72 | 72 | 94 | 94 |

[1] dose refers to the amount of isoprenaline released from the IsoWire in the first minute.

HR – heart rate; IRP – intrarenal pressure; MAP – mean arterial pressure

# Discussion

Guidewires, initially developed for vascular procedures, have become an essential tool in the armamentarium of endourologists. Many guidewires are available commercially, but they all serve a single purpose to function as a track over which catheters, ureteral stents and scopes can be passed into the collecting system of the kidney or bladder. The right

guidewire can lead to improved outcomes and reduced procedure times. Several drug-eluting implants or medical devices have been reported.[129,130] Forman et al. described the only drug-eluting guidewire. The "Adenowire" allowed for the release of pharmacologic amounts of adenosine directly into the microvasculature during a PCI procedure.[131] Here, we introduce the "IsoWire" – a platform guidewire to deliver topical isoprenaline to the genitourinary system. Isoprenaline, a drug that has a structural resemblance to epinephrine, is immediately active upon infusion and has a half-life of 2.5 to 5 minutes. Conjugation in hepatic and pulmonary tissues is the major method of metabolism. Excretion occurs via urine in the form of sulphate conjugates. [132] Stimulation of β-adrenergic receptors by isoprenaline, activates adenylate cyclase and increases cyclic adenosine monophosphate (cAMP), which in turn activates protein kinase A, causing ureteric relaxation[133] and subsequently lowering IRP.

Although a similar effect on IRP has been observed in other studies with endoluminal administration of isoprenaline, this is the first study to report the delivery of isoprenaline using a drug-eluting guidewire. Danuser et al., in 2001, showed that intravenous and endoluminal infusion of isoprenaline affected the frequency and amplitude of ureteric contractions.[125] In a porcine model, isoprenaline (0.1 mg/mL) added to the irrigation fluid significantly reduced the increase in renal pelvic pressure during ureterorenoscopy. Jakobsen et al. performed ureteroscopy in pigs while perfusing the renal pelvis at different rates (0, 4, 8, 12, 16, 25, and 33 mL/min) using either saline alone or saline mixed with isoprenaline at 0.1 μg/mL. At all irrigation rates, the perfusion with isoprenaline reduced IRP, with the maximum percentage reduction (52 mmHg to 38 mmHg - 27%, $p < 0.001$) at a 4 mL/min infusion rate.[104] A similar effect on IRP with endoluminal isoprenaline

(irrigation with isoprenaline at 0.1 mg/mL) was reproduced in humans, without any adverse effects.[134]

The in vitro results showed the ability of the hydrogel coating to load isoprenaline and release it quickly. In addition, we have shown that the hydrogel coating reduces the friction between the guidewire and urinary tract tissues. Our animal studies trialled three different doses, and we found that IRP was reduced at all three concentrations. The IsoWire that released 10 μg in the first minute, showed potential systemic effects, as reflected in an increase in HR after insertion. The IsoWire that released 5 μg and 7.5 μg in the first minute, recorded no changes in MAP, HR, ECG, or any measurable isoprenaline levels in the blood.

Apart from only reducing IRP, there are several other potential clinical applications for the IsoWire. The majority of endourologists routinely use a ureteric access sheath (UAS) in the management of renal stones.[49] Due to the failure rates of UAS insertion[135-138] and the possible ureteric injuries during UAS placement,[139,140] surgeons opt to passively dilate the ureter by pre-stenting the patient with a ureteric stent and returning one to two weeks later to manage the stone. The use of our IsoWire may result in ureteric muscle relaxation rendering easier insertion of an UAS in the first surgical sitting and therefore reducing the need to pre-stent the ureter. It may also promote the practice of sheathless RIRS.

# Conclusion

The IsoWires, which releases 5 μg and 7.5 μg of isoprenaline in the first minute, appears to be safe and effective in reducing the IRP. The IsoWires have passed bench testing for

lubricity, adherence, integrity, and tracking. Further studies are needed to establish how long this promising pressure-modulating effect will be sustained during RIRS and if the ureteric relaxation will render easier insertion of a UAS, reduce IRP during sheathless RIRS or even promote the practice of sheathless RIRS.

**Funding**

This work was supported by the National Center for Research and Development (NCRD; Project No. M-ERA.NET2/2019/1/2020) and the Department of Science and Innovation within the "IsoWire" project under the M-ERA.NET Program (Call 2019) co-financed by the European Union.

**Competing interests**

The authors declare that they have no conflict of interest.

# Chapter 5: Pharmacological modulation of intrarenal pressure in a porcine model using a novel isoprenaline-eluting guidewire

## Overview

In the preceding chapter, we introduced the design and initial in vitro release assessments of an isoprenaline-eluting guidewire (IsoWire) and its impact on IRP. This initial in vitro pilot study indicated that the IsoWire, which dispenses 7.5 µg of isoprenaline within the first minute, is safe, exhibiting no alterations in MAP, HR, or any aberrant ECG abnormalities. Additionally, the examination of the isoprenaline release profile from the hydrogel-coated guidewire indicated that the majority of the loaded drug mass was released during the initial minute, with nearly all of the drug being released exponentially during the first 4 minutes. Using the porcine model (17 renal units), this chapter goes on to further describe the effect the IsoWire, which releases 7.5 µg isoprenaline during the first minute, has on IRP, the duration of this effect, and its safety in a pig model.

The content in this chapter was published in the *Journal of Endourology* (Impact Factor 2.9), and at the time of submission of this thesis, it was an "article in-press".

**John J,** Wellman M, Kellermann T, Kopeć K, Ciach T, Fieggen G, Kaestner L, Lazarus J. Pharmacological modulation of intrarenal pressure in a porcine model using a novel isoprenaline-eluting guidewire. J Endourol. In press 2024. http://doi.org/10.1089/end.2024.0348.

CRediT author statement:

**Jeff John:** Writing – original draft, Visualization, Methodology, Formal analysis, Data curation, Conceptualization. **Mark Wellman:** Investigation. **Tracy Kellerman:** Investigation. **Kamil Kopeć:** Investigation. **Tomasz Ciach:** Investigation. **Graham Fieggen:** Supervision. **Lisa Kaestner:** Writing – review and editing. Supervision. **John Lazarus:** Methodology, Investigation. Writing – review and editing, Supervision.

# Abstract

**Objective:**

To describe the impact of an isoprenaline-eluting guidewire that releases 7.5 µg of isoprenaline in the 1st minute on the IRP and to evaluate its safety.

**Materials and Methods:**

This study was performed in 17 renal units using a porcine model. As controls, the IRP, HR, and MAP were measured for a duration of six minutes with a standard guidewire placed in the renal pelvis. For the experiment, the conventional guidewire was substituted with the IsoWire, and the same parameters were measured. Blood samples were taken at one-minute intervals to measure plasma isoprenaline levels. This procedure was repeated on the opposite side.

**Results:**

The mean intrarenal pressure reduction was 29% (95% CI: 13-53%). The mean isoprenaline effect time was 174 seconds. No changes in heart rate ($p = .908$) or mean arterial pressure ($p = .749$) were recorded after IsoWire insertion. Plasma isoprenaline levels were below the quantitation threshold. Isoprenaline concentrations in the plasma were below the quantification threshold. Ureteroscopy revealed no ureteral lesions.

**Conclusion:**

The IsoWire demonstrated a safe and effective reduction of intrarenal pressure. Additional research is necessary to determine whether ureteral smooth muscle relaxation generated by isoprenaline facilitates easier insertion of a UAS, decreases the incidence of ureteral access sheath-related ureteral lesions, or even encourage the practice of sheathless retrograde intrarenal surgery.

# Introduction

The prevalence of urolithiasis has steadily increased in the recent decades. The lifetime risk is 7 and 13% in women and men, respectively, with a recurrence rate of 50% within 10 years.[77] Increased prevalence leads to increased costs for both the patient and healthcare system. The use of flexible ureterorenoscopic devices and lasers for RIRS has gained traction, so much so that prominent urological societies, including the European Association of Urology and the American Urology Association, continue to expand its use in their guidelines.[4,78]

However, RIRS is associated with several complications. Normal physiological IRP in an unobstructed human kidney ranges from 0 to 15 mmHg (0-20 $cmH_2O$)[6] and this IRP is comparable to pressures in pigs.[141] During RIRS, intraluminal renal pelvic pressure ranges from 35 (±10) mmHg during simple diagnostic ureterorenoscopy to 54 (±18) mmHg during stone management. Maximum pelvic pressure peaks of 288 and 328 mmHg were recorded during forced irrigation with a 20 mL syringe and holmium laser use, respectively.[8] Dangerous increases in IRP beyond the safety threshold result in pyelorenal reflux and forniceal rupture. The former predisposes the patient to fever, urosepsis, and postoperative pain and was initially thought to occur when pressures exceed 30-45 mmHg.[9] However, recent work by Lildal et al. showed that intrarenal reflux may occur at IRPs as low as 16 mmHg (range 16-25 mmHg, mean 21 mmHg) in normal, non-hydronephrotic kidneys.[15]

We recently presented the design and first in vitro release tests of an isoprenaline-eluting guidewire ("IsoWire"). This IsoWire has a nitinol core and a fine stainless-steel wire twisted tightly around it. The spiral grooves created by the coil served as a reservoir for

the loading of hydrogel and isoprenaline. This hydrogel-coated isoprenaline-loaded guidewire was sheathed into a 5F open-ended ureteral catheter. Hydrogel was strategically applied to seal the junction between the open-ended catheter and guidewire to prevent the unintended release of isoprenaline, allow easy cannulation of the ureteric orifice, and allow smooth guidance into the pelvicalyceal system. After fluoroscopy confirms the accurate position, the protective sheath is removed and the drug diffuses from the coating when it becomes hydrated. Isoprenaline is a beta-agonist which stimulates beta-adrenergic receptors in the renal pelvis and ureters causing relaxation of the smooth muscle.[52]

Our preliminary in vitro pilot demonstrated that the IsoWire, which releases 7.5 µg isoprenaline during the first minute, is safe, with no changes in MAP, HR, or ECG alterations. Furthermore, analysis of the isoprenaline release profile from the hydrogel-coated guidewire showed that most (63.9 ± 5.9%) of the loaded drug mass was released in the first minute, and almost all the drug was released exponentially in the first 4 minutes. All plasma isoprenaline levels were below the quantitation limit. [74] The aim of this study was to investigate the effect the IsoWire, which release 7.5 µg isoprenaline during the first minute, has on IRP, how long this effect lasted for and to determine its safety in a porcine model.

# Material and Methods

## Ethical statement

This study adhered to the institutional protocol for animal experimentation and was approved by the Animal Ethics Committee of the Faculty of Health Sciences of the University of Cape Town (020_011).

## Study Design

### *Animal Model (Figure 14, Chapter 4)*

Nine female pigs (white, Landrace breed, weight 50-60 kg) were transferred to the study site and kept for a period of seven days to adapt to the new surroundings. The subjects were provided with a conventional pig diet for up to 12 hours before the investigation, but their access to water was unrestricted. Before transfer to the operating room, the pigs were premedicated with diazepam using a transdermal patch. They were administered Medetomidine (0.06 mg/kg IM), Zoletil (3 mg/kg IM), Medetomidine (0.06 mg/kg IM), and Butorphanol (0.15 mg/kg IM) to induce anaesthesia. Subsequently, they were intubated and ventilated using the GE Healthcare S5 Avance system. Anaesthesia was maintained with Isoflurane 1.5-3% in oxygen. To maintain proper hydration, an initial rapid infusion of saline was administered at a rate of 90 mL/kg/hour for 5 minutes. Hydration was then sustained during the procedure by administering saline solution (9 g/L sodium chloride) at a rate of 10 mL/kg/hour continuously through an ear vein. Under ultrasound guidance, a central venous catheter and a femoral arterial catheter were placed to facilitate blood sampling and monitoring of invasive blood pressure and HR. Baseline HR and MAP were measured, and any anomalies on the three-electrode ECG were documented. Blood was drawn for baseline isoprenaline levels.

### *Endourological procedure*

Both ureteral orifices were first cannulated using hydrophilic guidewires (0.035 inches). A 6F ureteric catheter was inserted over one guidewire. Retrograde pyelography was performed to identify any congenital abnormalities. Thereafter, a Y-connector was attached to the end of the ureteric catheter to allow passage of a 300 µm fibreoptic pressure measurement device (FISO Technologies, Inc., Quebec, Canada) into the renal

pelvis through one port. Saline irrigation was initiated through the second port at a rate of 10 mL/min. The bladder was kept empty using a 10F urethral catheter. In the control group, a standard guidewire was inserted into the renal pelvis on one side, and the IRP, HR, and MAP were measured continuously for six minutes. The conventional guidewire was replaced with an IsoWire for the experiments. Once the IRPs had stabilised during the exchange of guidewires and fluoroscopy confirmed that the correct position of the IsoWire was in the renal pelvis, the protective covering of the IsoWire was removed to allow for discharge of isoprenaline and exposure of the drug to the urothelium. The IRP, HR, and MAP were measured continuously for six minutes. Blood samples were obtained every minute, for six minutes to measure plasma isoprenaline levels. Once collected, they were centrifuged at 1000 × g for 15 min and stored at -80°C (-112°F) until analysis. To stabilise isoprenaline in the serum, 30 µL of an aqueous solution containing 6.5M citric acid and 0.568M ascorbic acid was added to 6700 µL of plasma. On the day of the analysis, freshly prepared working solutions in water containing 0.1% acetic acid and 1 g/L ascorbic acid were spiked into the plasma. Following a validated method[142] set by the Federal Drug Association (FDA) and European Medicines Agency (EMA), 10 µL of extracted plasma was injected for analysis using liquid chromatography-tandem mass spectrometry. This method yielded a minimum quantifiable limit of 0.488 ng/mL.

Ten minutes after the experiment and control were completed on one side, the same procedure was repeated on the contralateral side. This ten minute interval was determined after considering the short half-life of isoprenaline[143] and findings from our release profile investigations showed that almost all the drug was released exponentially in the first 4 minutes and .[74] The conclude the experiment, bilateral ureteroscopy was performed to detect any ureteric injuries.

## Statistical analysis

All analyses were performed using Statistical Package for the Social Sciences Version 28, and the significance level was set at $p < 0.05$. Data are reported as the mean, median, and standard deviation (SD). Dependent sample t-tests compared the mean pressure between the standard guidewire and IsoWire for the entire sample and each kidney. Pearson's correlation analyses were used to assess the relationship between isoprenaline effect time and pressure reduction for the whole sample and for each kidney. Dependent sample t-tests were used to compare the MAP and HR before and after IsoWire insertion.

# Results

Eighteen renal units were included in this study. Neither the standard guidewire nor the IsoWire could be advanced into the renal pelvis in one renal unit. These investigations were conducted in 17 renal units. The IRP decreased across all renal units, overall and in both the left and right kidneys ($p < 0.001$; see Table 3). The mean IRP reduction was 29% (95% CI: 13- 53%) (SD = 13%), ranging from 13 to 55%. The mean isoprenaline effect time was 174 seconds (SD = 60.6) (Table 4). There was no significant correlation between the isoprenaline effect time and pressure reduction in the whole sample ($r = -194$; $p = 456$), left ($r = -0.381$; $p = .312$), or right ($r = -0.078$; $p = .854$) kidneys. No changes in HR ($p = .908$) or MAP ($p = .749$) were recorded after the insertion of the IsoWire (see Table 3). The concentration of isoprenaline in the plasma was below the quantification threshold. Ureteroscopy revealed no ureteral lesions.

**Table 3**

Outcome measures for IRP for the entire sample, and by kidney

| | Total Sample | *t* | p | d |
|---|---|---|---|---|
| **Mean IRP: Whole Sample** | | | | |
| Standard Guidewire (mmHg) | 33.84 (6.53) | 8.56 | < .001 | 4.64 |
| IsoWire (mmHg) | 24.21 (6.83) | | | |
| **Mean IRP: Left Kidney** | | | | |
| Standard Guidewire (mmHg) | 33.42 (7.07) | 6.46 | < .001 | 4.90 |
| IsoWire (mmHg) | 22.87 (5.97) | | | |
| **Mean IRP: Right Kidney** | | | | |
| Standard Guidewire (mmHg) | 34.31 (6.31) | 5.51 | < .001 | 4.41 |
| IsoWire (mmHg) | 25.71 (7.81) | | | |

IRP – intrarenal pressure; mmHg – milimeters of mercury

---

**Table 4**

Table showing the isoprenaline effect time and percentage IRP reduction for the entire sample and by kidney

| | Total Sample | Left Kidney | Right Kidney |
|---|---|---|---|
| **Isoprenaline effect time (s)** | | | |
| Mean (SD) | 174.12 (60.60) | 168.33 (40.31) | 180.63 (80.29) |
| Range | 75-320 | 120-220 | 75-320 |
| **IRP reduction (%)** | | | |
| Mean (SD) | 28.65 % (12.53) | 31 % (12.45 %) | 26 % (12.90) |
| Range | 13- 55% | 18-55% | 13-53% |

s – seconds; SD – standard deviation, IRP – intrarenal pressure

---

# Discussion

The physiological IRP in an unobstructed kidney typically falls within the range of 0 to 15 mmHg (0-20 $cmH_2O$).[6] Harmful IRPs are frequently attained during RIRS, leading to patient morbidity. Retrograde translocation of uropathogenic bacteria, caused by pyelorenal reflux, contributes to postoperative pain, acute kidney injury, and fluid overload.[18,19] In addition, the renal fornix, which is the weakest component of the collecting system, ruptures due to the precipitous increase in pressure.[24] For the surgeon, forniceal rupture results in intraoperative bleeding and, consequently, impaired vision. Appropriate strategies for mitigating unsafe IRPs include minimising irrigation pressure by regulating the flow rate, employing a UAS, ensuring an empty bladder throughout the procedure, and more recently, utilising real-time IRP monitoring.

The pharmacological modulation of IRP using β-receptor agonists such as noradrenaline and isoprenaline has been explored. Danuser et al. demonstrated that the frequency of ureteric contractions was reduced by both intravenous (0.01 to 10 mg/kg) and endoluminal (0.1 to 200 µg/mL at a flow rate of 2 mL/minute) isoprenaline infusions. Topical administration altered the amplitude of contractions. However, both drugs exhibited adverse systemic effects.[125] Experimental data were obtained from colleagues in Denmark. Following a dose-response investigation in pigs, Jakobsen et al. concluded that smooth muscle function of the renal pelvis was inhibited by endoluminal administration of isoprenaline at a concentration of 0.1 µg/mL at a perfusion rate of 8 mL/min. Systemic adverse effects and detectable plasma isoprenaline levels were not observed.[124] The same author subsequently performed a ureteroscopy on pigs using a 7.8 F semirigid ureteroscope while perfusing the renal pelvis at various rates with either saline alone (control) or saline mixed with 0.1 µg/mL isoprenaline (experiment). Isoprenaline perfusion decreased renal pelvic pressure at all irrigation rates, with the greatest

percentage relaxation (from 52 mmHg to 38 mmHg, or 27%, $p < 0.001$) occurring at an infusion rate of 4 mL/min.[104] This effect of endoluminal isoprenaline (irrigation with isoprenaline at 0.1 µg/mL) on IRP was then replicated in humans by the same research team, with no systemic effects.[134]

In a porcine model, our study demonstrated that an isoprenaline-eluting guidewire can safely decrease the IRP. There are two potential explanations for this finding. First, it is believed that β-receptors are abundant on the luminal surface of the upper urinary tract.[144] Endoluminal stimulation of these receptors by isoprenaline, a β-agonist, induces ureteric relaxation by activating protein kinase A and adenylate cyclase, thereby increasing cAMP levels (Figure 18).[133] Secondly, Jung et al. also postulated that isoprenaline may affect the pacemaker cells of the upper urinary tract, thereby reducing the amplitude of the ureteric contractions.[134]

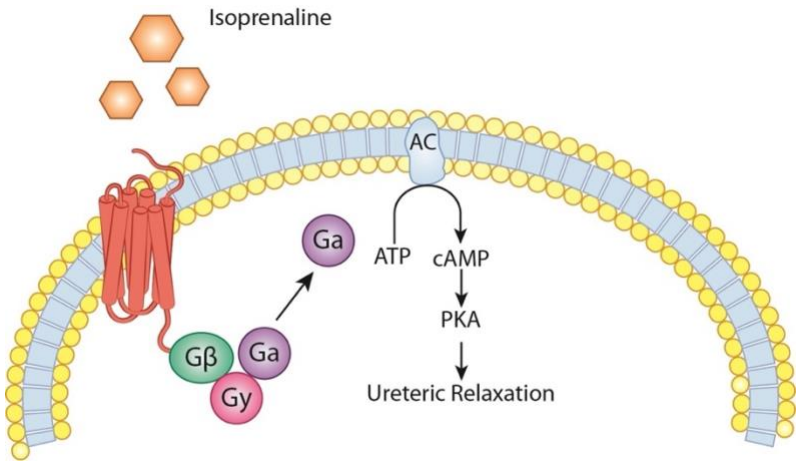


**Figure 18**

Graphical representation of the mechanism of action of isoprenaline.

Gα = g-protein alpha-subunit; Gβ = g-protein beta-subunit; Gγ = g-protein gamma-subunit AC = adenylyl cyclase; ATP = adenosine triphosphate; cAMP = cyclic adenosine monophosphate; PKA = protein kinase A

While previous studies have documented a comparable impact of topical or endoluminal isoprenaline administration on IRP, this study is the first to document the use of a drug-eluting guidewire for isoprenaline delivery.

In addition to the reduction in IRP with the use of endoluminal isoprenaline, it confers another benefit. UAS have become an important weapon in the armamentarium of endourologists. This is reflected in a recent survey of practice patterns of endourologists, which showed that 76% of endourologists routinely use a UAS to aid in treating renal stones.[49] The failure rates of UAS insertion in patients with stones have been reported to be 8.8% for 10/12 Fr UASs and 13% to 20% for 12/14 Fr UASs.[136,138] The failure rates are even higher in patients without stones.[145] Even in the case of a successful UAS insertion, there is a concern for ureteral wall injury and ureteral trauma with an excessive force of UAS insertion.[140] To limit this complication, urologists use a strategy to dilate the ureter, either passively or actively. The active form of dilatation involves the use of various ureteric dilators. These dilators produce a linear shearing force, which causes incisions in the ureteral mucosa. This results in the extravasation of urine and fluid, which can result in fibrosis.[146] A more favoured approach is passive dilatation of the ureter by pre-stenting the patient with a ureteric stent and returning one to two weeks later to manage the stone. An indwelling ureteric stent makes the ureter more distensible and subsequent RIRS easier.[147] However, this pre-stenting strategy is not without detractors. This entails a two-stage procedure, with time and cost implications. Stent-related symptoms are problematic and can result in reduced quality of life in up to 80% of patients.[148] The presence of an indwelling stent has also been shown to increase the incidence of urosepsis in RIRS.[20]

To confer this benefit of passive ureteric dilatation and simultaneously avoid the need to pre-stent a patient and return for a second procedure, Lildal et al. examined the effect of endoluminal isoprenaline on the success of UAS insertion. Pigs that had initially failed UAS insertion were randomised to endoluminal irrigation with either isoprenaline (0.1 μg/mL) or saline before a second attempt at UAS insertion by surgeons who were blinded. They observed greater success of UAS insertion in the isoprenaline group than in the saline group (63% vs. 27%).[149] Similarly, the use of our IsoWire will lead to subsequent ureteric muscle relaxation, which may facilitate easier insertion of a UAS. It may also decrease IRP during sheathless RIRS or even encourage the adoption of sheathless RIRS as a standard procedure. This finding warrants further investigation.

This study is not without its limitations. For dependent sample t-tests, with a medium effect size and power of 0.8, a sample size of 27 was suggested. With our sample size of 18, the power was only 0.65. Although the study was slightly underpowered, we found significant results with a smaller sample size. Furthermore, the researchers felt the need to adhere to the “three R" principles of animal research (i.e. replacement, reduction, and refinement).[150] These values uphold the principles and practice of using the most humane methods on the smallest number of animals that will permit valid scientific information to be acquired. As previously described, in clinical practice, IRPs can reach thresholds that promote intrarenal reflux. In our study, plasma isoprenaline levels were not detected and no changes in HR or MAP were observed. Even low doses of isoprenaline, as used in our study, can theoretically reach systemic circulation. However, considering that IsoWire releases 7.5 μg of isoprenaline in the first minute, and that the half-life of isoprenaline is brief, this seems unlikely. Lastly, due to the short half-life of isoprenaline (2-5 minutes[143]), the mean duration of the effect of eluted isoprenaline in our study was limited to 174 s,

after which the IRP seemed to return to baseline. This may not allow sufficient time to place a UAS. Further studies are needed to explore techniques to prolong this effect time or develop possible technologies for slower elution to prolong effective timeAlternatively, other exciting opportunities for further research include developing a drug-eluting guidewire with a different, longer-acting agent or developing a drug-eluting access sheath to improve peri-UAS outflow.

# Conclusion

Endoluminal isoprenaline administration using an isoprenaline-eluting guidewire (IsoWire) can safely reduce the IRP.

**Funding**

This work was supported by the National Centre for Research and Development (NCRD; Project No. MERA.NET2/2019/1/2020) and the Department of Science and Innovation within the “IsoWire” project under the M-ERA.NET Program (Call 2019) co-financed by the European Union.

**Competing interests**

The authors declare that they have no conflicts of interest.

**Acknowledgements**

We acknowledge the invaluable contribution of several individuals.

(1) Peter Zilla, Rose Boltman, and Helen Ilsley of Strait Access Technologies.

(2) Janet McCullum, John Chipangura, Tashie Makwavarara, and Thireshni Chetty at the University of Cape Town Research Animal Facility.

(3) Michelle Henry, at the Numeracy Centre, Centre for Higher Education Development at the University of Cape Town.

(4) Val Myburgh.

# Chapter 6: Conclusion and Reflection

## Overview

This provides a conclusion and reflection to this thesis highlighting the novel contributions this thesis has provided to the field of urology and touching on potential areas of future research.

Sections of this chapter has been accepted for publication in Urology (Impact Factor 2.2) and at the time of submission of this thesis, it was an “article in-press”.

John J, Wisniewski P, Fieggen G, Kaestner L, Lazarus J. Reply to Editorial Comment on "Intrarenal pressure in retrograde intrarenal surgery: a narrative review". Urology. In press 2024. http://doi.org/10.1016/j.urology.2024.10.036.

CRediT author statement:

**Jeff John**: Writing – original draft, Visualization, Methodology, Formal analysis, Data curation, Conceptualization. **Graham Fieggen**: Writing – review & editing, Supervision. **Pawel Wisniewski**: Writing – review & editing. **Lisa Kaestner**: Writing – review & editing, Supervision. **John Lazarus**: Writing – review & editing, Supervision.

IRP has recently emerged as a prominent topic in endourology for two reasons. First, while IRP and pyelorenal reflux were first described in the early 1920s,[151] we have only lately began to comprehend the clinical significance of unfavourable IRPs for our patients. In particular, despite the use of antibiotic prophylaxis and adherence to sterile methods, fever and urinary tract infections remain the most common sequelae, with the potential to progress to sepsis, which is the leading cause of mortality associated with nephrolithiasis.[21,152] Second, our ability to assess IRP in real time was limited. A systematic review by Pauchard et al. reported on existing tools available. Options include ureteral catheters connected to a pressure transducer, an IRP measuring ureteric access sheath (UAS), or pressure sensing guidewires.[153] Shu et al. also described an irrigation system for noninvasively estimating IRP during flexible ureteroscopy.[154] All of these have their inherent limitations – and therefore have failed to be incorporated into guidelines, so much so that many urologists are not even aware of their existence.[155] The United States Food and Drug Administration recently approved a scope for real-time IRP monitoring. A clinical trial comparing this pressure-monitoring ureteroscope with non-pressure-monitoring devices, with safety as the primary endpoint, is expected to be completed in June 2025.[156]

This data and data from other promising studies will continue to give us insight into many unanswered questions. Despite these challenges, a recent online survey of 522 urologists from six continents assessing their beliefs and practice patterns regarding IRP found that the majority of respondents believed IRP was clinically important, and many took appropriate measures to mitigate increases in IRP.[155]

In this thesis, we detailed how an isoprenaline-eluting guidewire (IsoWire) that releases 7.5 μg of isoprenaline is both safe and effective in lowering IRP in a porcine model. Isoprenaline, a β-agonist, stimulates endoluminal β-receptors, resulting in ureteric relaxation and reduced frequency and amplitude of contractions.[133] We further hypothesised that this would facilitate easier insertion of a UAS. While this thesis concludes, it is not the end of the IsoWire. We have submitted an application to the South African Health Products Regulatory Authority (SAHPRA) to conduct a human safety trial using the IsoWire. Once this phase is completed, we intend to progress to phase 2 trials to confirm whether the efficacy demonstrated in the porcine model can be replicated in human participants and whether it would allow easier UAS insertion. While our study has focused on lowering IRP in RIRS with this guidewire, we hope that it has paved the way for future researchers to investigate coating guidewires with different medications and compounds. This could allow for local drug delivery, thereby reducing systemic side effects and toxicity.

In addition to the IsoWire, this thesis has produced two further novel projects that will focus on increasing urological research, education, and training. In Chapter 3, we described the endoscopic and CT-based urological anatomy of female Landrace pigs. The knowledge gained from this ground-breaking study will help other researchers consider the porcine model for future endourological research. In Chapter 2, we described how we designed and validated an RIRS trainer. This low-cost, portable, long-lasting, and reusable model convincingly reproduces all RIRS components and will undoubtedly enable high-fidelity teaching in endourology. For these reasons, this trainer was utilized at the endourology workshop during the recently concluded 16th Pan African Urological Surgeons' Association Congress (PAUSA) and 34th Biennial Congress of the South African

Urology Association (SAUA) in Johannesburg, South Africa. Furthermore, since its creation, the model has been utilised to instruct at the annual South African Urology Registrars Masterclass in 2023 and 2024. This masterclass is a two-day session designed to prepare final-year residents for their urology exit exams. The College of Urology, which is affiliated with the Colleges of Medicine of South Africa, the custodian of the quality of medical care in South Africa, made a unanimous council decision to allocate funds for me to produce this RIRS trainer for each urology division in the country.

We are now entering an exciting period in endourology, and we hope that the results provided in this thesis will encourage additional research. We look forward to more data on IRP appearing in the future, both from our own work and that of others.

# References


1. Marshall VF. Fiber optics in urology. J Urol. 1964 Jan;91(1):110-4. doi:10.1016/S0022-5347(17)64066-7.
2. Shi X, Peng Y, Li X, Wang Q, Li L, Liu M, et al. Propensity score-matched analysis comparing retrograde intrarenal surgery with percutaneous nephrolithotomy for large stones in patients with a solitary kidney. J Endourol. 2018 Mar;32(3):198-204. doi:10.1089/end.2017.0482.
3. Kim CH, Chung DY, Rha KH, Lee JY, Lee SH. Effectiveness of percutaneous nephrolithotomy, retrograde intrarenal surgery, and extracorporeal shock wave lithotripsy for treatment of renal stones: a systematic review and meta-analysis. Medicina (Kaunas). 2020 Dec 30;57(1):26. doi:10.3390/medicina57010026.
4. Türk C, Neisius A, Petrik A, Seitz C, Skolarikos A, Thomas K, et al. EAU Guidelines on Urolithiasis. Arnhem, The Netherlands: EAU; 2021 [cited 18 May 2021]. Available from: https://uroweb.org/guidelines/urolithiasis
5. Inoue T, Okada S, Hamamoto S, Fujisawa M. Retrograde intrarenal surgery: past, present, and future. Investig Clin Urol. 2021 Mar;62(2):121-35. doi:10.4111/icu.20200526.
6. Oratis AT, Subasic JJ, Hernandez N, Bird JC, Eisner BH. A simple fluid dynamic model of renal pelvis pressures during ureteroscopic kidney stone treatment. PLoS One. 2018 Nov 29;13(11):e0208209. doi:10.1371/journal.pone.0208209.
7. Grinholtz D, Kamkoum H, Capretti C, Traxer O, Doizi S. Comparison of irrigation flows between different irrigation methods for flexible ureteroscopy: an in vitro study. Prog Urol. 2022 Jul;32(8-9):616-22. doi:10.1016/j.purol.2021.10.007.

8. Jung H, Osther PJS. Intraluminal pressure profiles during flexible ureterorenoscopy. Springerplus. 2015 Jul 24;4:373. doi:10.1186/s40064-015-1114-4.
9. Osther PJS, Osther SS, Hesselholt MP, Byllov S, Lildal SK, Øbro LF, et al. Understanding intrarenal backflow: intrarenal pressure during ureteroscopy and beyond. Asian J Urol. 2024 Feb 2;11(2):139-42. doi:10.1016/j.ajur.2024.01.008.
10. Angel JR, Smith TW, Roberts JA. The hydrodynamics of pyelorenal reflux. J Urol. 1979 Jul;122(1):20-6. doi:10.1016/s0022-5347(17)56234-5.
11. Nemeth AJ, Patel SK. Pyelovenous backflow seen on CT urography. AJR Am J Roentgenol 2004 Feb;182(2):532-3. doi:10.2214/ajr.182.2.1820532a.
12. Boccafoschi C, Lugnani F. Intra-renal reflux. Urol Res. 1985;13(5):253-8. doi:10.1007/BF00261587.
13. Thomsen HS, Dorph S, Olsen S. Pyelorenal backflow in rabbits following clamping of the renal vein and artery: radiologic and microscopic investigation. Acta Radiol Diagn (Stockh). 1982;23(2):143-8. doi:10.1177/028418518202300210.
14. Thomsen HS, Larsen S, Talner LB. Pyelorenal backflow during retrograde pyelography in normal and ischemic porcine kidneys: a radiologic and pathoanatomic study. Eur Urol. 1982;8(5):291-7. doi:10.1159/000473538.
15. Lildal SK, Hansen ESS, Laustsen C, Nørregaard R, Bertelsen LB, Madsen K, et al. Gadolinium-enhanced MRI visualizing backflow at increasing intra-renal pressure in a porcine model. PLoS One. 2023 Feb 16;18(2):e0281676. doi: 10.1371/journal.pone.0281676.
16. Thomsen HS, Dorph S, Olsen S. Pyelorenal backflow in normal and ischemic rabbit kidneys. Invest Radiol. 1981 May-Jun;16(3):206-14. doi:10.1097/00004424-198105000-00009.

17. Hodson CJ. The effects of disturbance of flow on the kidney. J Infect Dis. 1969 Jul;120(1):54-60. doi:10.1093/infdis/120.1.54.

18. Zhong W, Leto G, Wang L, Zeng G. Systemic inflammatory response syndrome after flexible ureteroscopic lithotripsy: a study of risk factors. J Endourol. 2015 Jan;29(1):25-8. doi:10.1089/end.2014.0409.

19. Scotland KB, Lange D. Prevention and management of urosepsis triggered by ureteroscopy. Res Rep Urol. 2018 Jul 5;10:43-9. doi:10.2147/RRU.S128071.

20. Bhojani N, Miller LE, Bhattacharyya S, Cutone B, Chew BH. Risk factors for urosepsis after ureteroscopy for stone disease: a systematic review with meta-analysis. J Endourol. 2021 Jul;35(7):991-1000. doi:10.1089/end.2020.1133.

21. Cindolo L, Castellan P, Scoffone CM, Cracco CM, Celia A, Paccaduscio A, et al. Mortality and flexible ureteroscopy: analysis of six cases. World J Urol. 2016 Mar;34(3):305-10. doi:10.1007/s00345-015-1642-0.

22. Xu Y, Min Z, Wan SP, Nie H, Duan G. Complications of retrograde intrarenal surgery classified by the modified Clavien grading system. Urolithiasis. 2018 Apr;46(2):197-202. doi:10.1007/s00240-017-0961-6.

23. Croghan SM, Cunnane EM, O'Meara S, Muheilan M, Cunnane CV, Patterson K, et al. In vivo ureteroscopic intrarenal pressures and clinical outcomes: a multi-institutional analysis of 120 consecutive patients. BJU Int. 2023 Nov;132(5):531-40. doi:10.1111/bju.16169.

24. Harvey N, Rudman H, Gall Z. Managing renal forniceal rupture secondary to ureteric calculi in line with the NICE 2019 Renal and Ureteric Stone Guidelines. J Clin Urol. 2021;14(6):514-20. doi:10.1177/2051415820961297.

25. Kohler R. Investigations on backflow in retrograde pyelography: a roentgenological and clinical study. Acta Radiol (Stockh) 1953;39(99):1-92.

26. Wu YH, Wu CT, Lin CF, Chen WH, Huang SS, Wu LSH, et al. Efficacy of parecoxib for reducing pyelovenous backflow pain during retrograde intrarenal surgery. Urol Sci. 2017; Aug. doi:10.1016/j.urols.2017.07.003.

27. Shrestha A, Gharti BB, Adhikari B. Perirenal extravasation after retrograde intrarenal surgery for renal stones: a prospective study. Cureus. 2022 Jan 16;14(1):e21283. doi:10.7759/cureus.21283.

28. Djaladat H, Tajik P, Payandemehr P, Alehashemi S. Ureteral catheterization in uncomplicated ureterolithotripsy: a randomized, controlled trial. Eur Urol. 2007 Sep;52(3):836-41. doi:10.1016/j.eururo.2007.01.042.

29. Guzelburc V, Balasar M, Colakogullari M, Guven S, Kandemir A, Ozturk A, et al. Comparison of absorbed irrigation fluid volumes during retrograde intrarenal surgery and percutaneous nephrolithotomy for the treatment of kidney stones larger than 2 cm. Springerplus. 2016 Oct 4;5(1):1707. doi:10.1186/s40064-016-3383-y.

30. Aykaç A, Baran Ö, Öner Z, Kaya Ç, Özok U, Sunay M. Simultaneous measurement of pressure in the calyces during RIRS in a human cadaver model. J Urol Surg. 2019 Sep;6(3):213-7. doi:10.4274/jus.galenos.2019.2412.

31. Schwalb DM, Eshghi M, Davidian M, Franco I. Morphological and physiological changes in the urinary tract associated with ureteral dilation and ureteropyeloscopy: an experimental study. J Urol. 1993 Jun;149(6):1576-85. doi:10.1016/s0022-5347(17)36456-x.

32. Djurhuus J. Aspects of renal pelvic function. Copenhagen: University of Copenhagen; 1980.

33. Kiil F. Pressure recordings in the upper urinary tract. Scand J Clin Lab Invest. 1953;5(4):383-4. doi:10.3109/00365515309094217.

34. Cruces P, Salas C, Lillo P, Salomon T, Lillo F, Hurtado DE. The renal compartment: a hydraulic view. Intensive Care Med Exp. 2014 Oct 23;2:26. doi:10.1186/s40635-014-0026-x.

35. Schmidt-Ott KM, Mori K, Jau YL, Kalandadze A, Cohen DJ, Devarajan P, et al. Dual action of neutrophil gelatinase-associated lipocalin. J Am Soc Nephrol. 2007 Feb;18(2):407-13. doi:10.1681/ASN.2006080882.

36. Siew ED, Ware LB, Gebretsadik T, Shintani A, Moons KGM, Wickersham N, et al. Urine neutrophil gelatinase-associated lipocalin moderately predicts acute kidney injury in critically ill adults. J Am Soc Nephrol. 2009 Aug;20(8):1823-32. doi:10.1681/ASN.2008070673.

37. Bolignano D, Lacquaniti A, Coppolino G, Donato V, Fazio MR, Nicocia G, et al. Neutrophil gelatinase-associated lipocalin as an early biomarker of nephropathy in diabetic patients. Kidney Blood Press Res. 2009;32(2):91-8. doi:10.1159/000209379.

38. Chang D, Manecksha RP, Syrrakos K, Lawrentschuk N. An investigation of the basic physics of irrigation in urology and the role of automated pump irrigation in cystoscopy. ScientificWorldJournal. 2012;2012:476759. doi:10.1100/2012/476759.

39. Hamill L. Fluids in motion. In: Understanding hydraulics. 2nd ed. New York: Palgrave; 2011.

40. Doizi S, Uzan A, Keller EX, De Coninck V, Kamkoum H, Barghouthy Y, et al. Comparison of intrapelvic pressures during flexible ureteroscopy, mini-percutaneous nephrolithotomy, standard percutaneous nephrolithotomy, and endoscopic combined intrarenal surgery in a kidney model. World J Urol. 2021 Jul;39(7):2709-17. doi:10.1007/s00345-020-03450-2.

41. Wright A, Williams K, Somani B, Rukin N. Intrarenal pressure and irrigation flow with commonly used ureteric access sheaths and instruments. Cent European J Urol. 2015;68(4):434-8. doi:10.5173/ceju.2015.604.

42. Ng YH, Somani BK, Dennison A, Kata SG, Nabi G, Brown S. Irrigant flow and intrarenal pressure during flexible ureteroscopy: the effect of different access sheaths, working channel instruments, and hydrostatic pressure. J Endourol. 2010 Dec;24(12):1915-20. doi:10.1089/end.2010.0188.

43. Sung JM, Jefferson FA, Tapiero S, Patel RM, Owyong M, Xie L, et al. Evaluation of a diuresis enhanced non-contrast computed tomography for kidney stones protocol to maximize collecting system distention. J Endourol. 2020 Mar;34(3):255-61. doi:10.1089/end.2019.0719.

44. Lopes Neto AC, Dall'Aqua V, Carrera RV, Molina WR, Glina S. Intra-renal pressure and temperature during ureteroscopy: does it matter? Int Braz J Urol. 2021 Mar-Apr;47(2):436-42. doi:10.1590/S1677-5538.IBJU.2020.0428.

45. Takayasu H, Aso Y. Recent development for pyeloureteroscopy: guide tube method for its introduction into the ureter. J Urol. 1974 Aug;112(2):176-8. doi:10.1016/s0022-5347(17)59675-5.

46. Newman RC, Hunter PT, Hawkins IF, Finlayson B. The ureteral access system: a review of the immediate results in 43 cases. J Urol. 1987 Mar;137(3):380-3. doi:10.1016/s0022-5347(17)44039-0.

47. Traxer O, Wendt-Nordahl G, Sodha H, Rassweiler J, Meretyk S, Tefekli A, et al. Differences in renal stone treatment and outcomes for patients treated either with or without the support of a ureteral access sheath: The Clinical Research Office of the Endourological Society Ureteroscopy Global Study. World J Urol. 2015 Dec;33(12):2137-44. doi:10.1007/s00345-015-1582-8.

48. Villa L, Dioni P, Candela L, Ventimiglia E, de Angelis M, Corsini C, et al. Understanding the role of ureteral access sheath in preventing post-operative infectious complications in stone patients treated with ureteroscopy and Ho:YAG laser lithotripsy: results from a tertiary care referral center. J Clin Med. 2023 Feb 12;12(4):1457. doi:10.3390/jcm12041457.

49. Zilberman DE, Lazarovich A, Winkler H, Kleinmann N. Practice patterns of ureteral access sheath during ureteroscopy for nephrolithiasis: a survey among endourologists worldwide. BMC Urol. 2019 Jul 4;19:58. doi:10.1186/s12894-019-0489-x.

50. Rehman J, Monga M, Landman J, Lee DI, Felfela T, Conradie MC, et al. Characterization of intrapelvic pressure during ureteropyeloscopy with ureteral access sheaths. Urology. 2003 Apr;61(4):713-8. doi:j10.1016/s0090-4295(02)02440-8.

51. Lazarus J, Wisniewski P, Kaestner L. Beware the bolus size: understanding intrarenal pressure during ureteroscopic fluid administration. S Afr J Surg. 2020 Dec;58(4):220.

52. Auge BK, Pietrow PK, Lallas CD, Raj GV, Santa-Cruz RW, Preminger GM. Ureteral access sheath provides protection against elevated renal pressures during routine flexible ureteroscopic stone manipulation. J Endourol. 2004 Feb;18(1):33-6. doi:10.1089/089277904322836631.

53. Pisano A. From tubes and catheters to the basis of hemodynamics: the Hagen–Poiseuille Equation. In: Physics for anesthesiologists. Cham: Springer International Publishing; 2017. p. 55-61.

54. Fang L, Xie G, Zheng Z, Liu W, Zhu J, Huang T, et al. The effect of ratio of endoscope-sheath diameter on intrapelvic pressure during flexible ureteroscopic lasertripsy. J Endourol. 2019 Feb;33(2):132-9. doi:10.1089/end.2018.0774.

55. Smyth TB, Shortliffe LMD, Constantinou CE. The effect of urinary flow and bladder fullness on renal pelvic pressure in a rat model. J Urol. 1991 Aug;146(2 Pt 2):592-6. doi:10.1016/s0022-5347(17)37864-3.

56. Tokas T, Herrmann TRW, Skolarikos A, Nagele U; Training and Research in Urological Surgery and Technology (T.R.U.S.T.) Group. Pressure matters: intrarenal pressures during normal and pathological conditions, and impact of increased values to renal physiology. World J Urol. 2019 Jan;37(1):125-31. doi:10.1007/s00345-018-2378-4.

57. Mohammed S, Yohannes B, Tegegne A, Abebe K. Urolithiasis: Presentation and surgical outcome at a tertiary care hospital in Ethiopia. Res Rep Urol. 2020 Dec 8;12:623-31. doi:10.2147/RRU.S284706.

58. Roudakova K, Monga M. The evolving epidemiology of stone disease. Indian J Urol. 2014 Jan-Mar;30(1):44-8. doi:10.4103/0970-1591.124206.

59. Aune D, Mahamat-Saleh Y, Norat T, Riboli E. Body fatness, diabetes, physical activity and risk of kidney stones: a systematic review and meta-analysis of cohort studies. Eur J Epidemiol. 2018 Nov;33(11):1033-47. doi:10.1007/s10654-018-0426-4.

60. Geraghty RM, Jones P, Somani BK. Worldwide trends of urinary stone disease treatment over the last two decades: a systematic review. J Endourol. 2017 Jun;31(6):547-56. doi:10.1089/end.2016.0895.

61. Zeng G, Traxer O, Zhong W, Osther P, Pearle MS, Preminger GM, et al. International Alliance of Urolithiasis guideline on retrograde intrarenal surgery. BJU Int. 2023 Feb;131(2):153-64. doi:10.1111/bju.15836.

62. Patel RM, Jefferson FA, Owyong M, Hofmann M, Ayad ML, Osann K, et al. Characterization of intracalyceal pressure during ureteroscopy. World J Urol. 2021 Mar;39(3):883-9. doi:10.1007/s00345-020-03259-z.

63. Bhojani N, Koo KC, Bensaadi K, Halawani A, Wong VKF, Chew BH. Retrospective first-in-human use of the LithoVue™ Elite ureteroscope to measure intrarenal pressure. BJU Int. 2023 Dec;132(6):678-85. doi:10.1111/bju.16173.

64. Doizi S, Letendre J, Cloutier J, Ploumidis A, Traxer O. Continuous monitoring of intrapelvic pressure during flexible ureteroscopy using a sensor wire: a pilot study. World J Urol. 2021 Feb;39(2):555-61. doi:10.1007/s00345-020-03216-w.

65. Sierra A, Corrales M, Kolvatzis M, Doizi S, Traxer O. Real time intrarenal pressure control during flexible ureterorenscopy using a vascular PressureWire: pilot study. J Clin Med. 2022 Dec 24;12(1):147. doi:10.3390/jcm12010147.

66. Huang J, Xie D, Xiong R, Deng X, Huang C, Fan D, et al. The application of suctioning flexible ureteroscopy with intelligent pressure control in treating upper urinary tract calculi on patients with a solitary kidney. Urology. 2018 Jan;111:44-7. doi:10.1016/j.urology.2017.07.042.

67. Han Z, Wang B, Liu X, Jing T, Yue WS, Wang Y, et al. Intrarenal pressure study using 7.5 French flexible ureteroscope with or without ureteral access sheath in an ex-vivo porcine kidney model. World J Urol. 2023 Nov;41(11):3129-34. doi:10.1007/s00345-023-04598-3.

68. Guan W, Liang J, Wang D, Lin H, Xie S, Chen S, et al. The effect of irrigation rate on intrarenal pressure in an ex vivo porcine kidney model – preliminary study with different flexible ureteroscopes and ureteral access sheaths. World J Urol. 2023 Mar;41(3):865-72. doi:10.1007/s00345-023-04295-1.

69. Zhang Z, Xie T, Li F, Wang X, Liu F, Jiang B, et al. Comparison of traditional and novel tip-flexible suctioning ureteral access sheath combined with flexible ureteroscope to treat unilateral renal calculi. World J Urol. 2023 Oct 11;41(12):3619-27. doi:10.1007/s00345-023-04648-w.

70. Qian X, Liu C, Hong S, Xu J, Qian C, Zhu J, et al. Application of suctioning ureteral access sheath during flexible ureteroscopy for renal stones decreases the risk of postoperative systemic inflammatory response syndrome. Int J Clin Pract. 2022 Mar 12;2022:9354714. doi:10.1155/2022/9354714.

71. Yekani S, Lazarus J, de Bruyn M, Kaestner L. A pilot study of a novel syphon ureteral access sheath shows potential to reduce renal pressures and improve irrigant flow. Urology. 2023 Jun;176:50-54. doi:10.1016/j.urology.2023.03.004.

72. Chen Y, Li C, Gao L, Lin L, Zheng L, Ke L, et al. Novel flexible vacuum-assisted ureteral access sheath can actively control intrarenal pressure and obtain a complete stone-free status. J Endourol. 2022 Sep;36(9):1143-8. doi:10.1089/end.2022.0004.

73. Ostergar A, Wong D, Shiang A, Ngo S, Venkatesh R, Desai A, et al. Intrarenal pressure with vacuum-assisted ureteral access sheaths using an *in situ* cadaveric porcine model. J Endourol. 2023 Mar;37(3):353-7. doi:10.1089/end.2022.0573.

74. John J, Wellman M, Dixon C, Kellermann T, Wisniewski P, Kopeć K, et al. Introducing an isoprenaline eluting guidewire: report on its design and the results of the dose-determining pilot study. J Endourol. 2024 Jun;38(6):590-7. doi:10.1089/end.2023.0745.

75. John J, Wellman M, Kellermann T, Kopeć K, Ciach T, Fieggen G, et al. Pharmacological modulation of intrarenal pressure in a porcine model using a novel isoprenaline-eluting guidewire. J Endourol. 2024 Jul 29. doi:10.1089/end.2024.0348.

76. Chung KJ, Kim JH, Min GE, Park HK, Li S, del Giudice F, et al. Changing trends in the treatment of nephrolithiasis in the real world. J Endourol. 2019 Mar;33(3):248-53. doi:10.1089/end.2018.0667.

77. Turney BW, Reynard JM, Noble JG, Keoghane SR. Trends in urological stone disease. BJU Int. 2012 Apr;109(7):1082-7. doi:10.1111/j.1464-410X.2011.10495.x.

78. Nelson CP, Pace KT, Jr VMP, Pearle MS, Ph D, Preminger GM, et al. Surgical management of stones: American Urological Association/Endourological Society Guideline, Part II. J Urol. 2016;196(1161). doi: 10.1016/j.juro.2016.05.091

79. Cho SY. Current status of flexible ureteroscopy in urology. Korean J Urol. 2015 Oct;56(10):680-8. doi:10.4111/kju.2015.56.10.680.

80. Skolarikos A, Gravas S, Laguna MP, Traxer O, Preminger GM, de la Rosette J. Training in ureteroscopy: a critical appraisal of the literature. BJU Int. 2011 Sep 25;108(6):798-805. doi:10.1111/j.1464-410X.2011.10337.x.

81. Linda K, Janet C, Molla D. To err is human. Washington, DC: National Academies Press; 2000.

82. Cameron JL. William Stewart Halsted. Ann Surg. 1997 May;225(5):445-58. doi:10.1097/00000658-199705000-00002.

83. Subramonian K, Muir G. The 'learning curve' in surgery: what is it, how do we measure it and can we influence it? BJU Int. 2004 Jun;93(9):1173-4. doi:10.1111/j.1464-410X.2004.04891.x.

84. Fung G, Sha M, Kunduzi B, Froghi F, Rehman S, Froghi S. Learning curves in minimally invasive pancreatic surgery: a systematic review. Langenbecks Arch Surg. 2022 Sep;407(6):2217-32. doi:10.1007/s00423-022-02470-3.

85. Botoca M, Bucuras V, Boiborean P, Herman I, Cumpanas A, Miclea F. 543 The learning curve in ureteroscopy for the treatment of ureteric stones. How many procedures are needed to achieve satisfactory skills? Eur Urol Suppl. 2004 Feb;3(2):138. doi:10.1016/S1569-9056(04)90538-6.

86. Cho SY, Choo MS, Jung JH, Jeong CW, Oh S, Lee SB, et al. Cumulative sum analysis for experiences of a single-session retrograde intrarenal stone surgery and analysis of

predictors for stone-free status. PLoS One. 2014 Jan 14;9(1):e84878. doi:10.1371/journal.pone.0084878.

87. Da Cruz JAS, Thiago C, Barros U de Q, de la Roca RLF, Lima JPC, di Migueli R. The learning curve for retrograde intra-renal surgery (RIRS): how many cases are necessary? J Urol. 2016 Apr;195(4):e443. doi:10.1016/j.juro.2016.02.1374.

88. Komori M, Izaki H, Daizumoto K, Tsuda M, Kusuhara Y, Mori H, et al. Complications of flexible ureteroscopic treatment for renal and ureteral calculi during the learning curve. Urol Int. 2015;95(1):26-32. doi:10.1159/000368617.

89. Zendejas B, Brydges R, Hamstra SJ, Cook DA. State of the evidence on simulation-based training for laparoscopic surgery. Ann Surg. 2013 Apr;257(4):586-93. doi:10.1097/SLA.0b013e318288c40b.

90. Zendejas B, Brydges R, Wang AT, Cook DA. Patient outcomes in simulation-based medical education: a systematic review. J Gen Intern Med. 2013 Aug;28(8):1078-89. doi:10.1007/s11606-012-2264-5.

91. White MA, DeHaan AP, Stephens DD, Maes AA, Maatman TJ. Validation of a high fidelity adult ureteroscopy and renoscopy simulator. J Urol. 2010 Feb;183(2):673-7. doi:10.1016/j.juro.2009.10.013.

92. Orecchia L, Manfrin D, Germani S, del Fabbro D, Asimakopoulos AD, Finazzi Agrò E, et al. Introducing 3D printed models of the upper urinary tract for high-fidelity simulation of retrograde intrarenal surgery. 3D Print Med. 2021 Jun 7;7(1):15. doi:10.1186/s41205-021-00105-9.

93. Emiliani E, Motta GL, Llorens E, Quiróz Y, Kanashiro AK, Angerri O, et al. Totally fluoroless retrograde intrarenal surgery technique in prestented patients: tips and tricks. J Pediatr Urol. 2019 Oct;15(5):570-3. doi:10.1016/j.jpurol.2019.06.017.

94. Mahmood SN, Toffeq H, Fakhralddin S. Sheathless and fluoroscopy-free retrograde intrarenal surgery: an attractive way of renal stone management in high-volume stone centers. Asian J Urol. 2020 Jul;7(3):309-17. doi:10.1016/j.ajur.2019.07.003.

95. Subiela JD, Kanashiro A, Emiliani E, Villegas S, Sánchez-Martín FM, Millán F, et al. Systematic review and meta-analysis comparing fluoroless ureteroscopy and conventional ureteroscopy in the management of ureteral and renal stones. J Endourol. 2021 Apr;35(4):417-28. doi:10.1089/end.2020.0915.

96. Lee KH, Lee DW, Kang BC. The 'R' principles in laboratory animal experiments. Lab Anim Res. 2020 Dec 9;36(1):45. doi:10.1186/s42826-020-00078-6.

97. Smith KA. Edward Jenner and the small pox vaccine. Front Immunol. 2011 Jun 14;2:21. doi:10.3389/fimmu.2011.00021.

98. Cooper DK. Christiaan Barnard—the surgeon who dared: the story of the first human-to-human heart transplant. Glob Cardiol Sci Pract. 2018 Jun 30;2018(2):11. doi:10.21542/gcsp.2018.11.

99. Bushi D, Assaf Y, Grad Y, Nishri B, Yodfat O, Tanne D. Similarity of the swine vasculature to the human carotid bifurcation: analysis of arterial diameters. J Vasc Interv Radiol. 2008 Feb;19(2 Pt 1):245-51. doi:10.1016/j.jvir.2007.09.022.

100. Wernersson R, Schierup MH, Jørgensen FG, Gorodkin J, Panitz F, Stærfeldt HH, et al. Pigs in sequence space: a 0.66X coverage pig genome survey based on shotgun sequencing. BMC Genomics. 2005 May 10;6:70. doi:10.1186/1471-2164-6-70.

101. Smith AC, Swindle MM. Preparation of swine for the laboratory. ILAR J. 2006;47(4):358-63. doi:10.1093/ilar.47.4.358.

102. Gómez FA, Ballesteros LE, Estupiñán HY. Anatomical study of the renal excretory system in pigs: a review of its characteristics as compared to its human counterpart. Folia Morphol (Warsz). 2017;76(2):262-8. doi:10.5603/FM.a2016.0065.

103. Sampaio FJB, Pereira-Sampaio MA, Favorito LA. The pig kidney as an endourologic model: anatomic contribution. J Endourol. 1998 Feb;12(1):45-50. doi:10.1089/end.1998.12.45.

104. Jakobsen JS, Jung HU, Gramsbergen JB, Osther PJ, Walter S. Endoluminal isoproterenol reduces renal pelvic pressure during semirigid ureterorenoscopy: a porcine model. BJU Int. 2010 Jan;105(1):121-4. doi:10.1111/j.1464-410X.2009.08678.x.

105. Raison N, Poulsen J, Abe T, Aydin A, Ahmed K, Dasgupta P. An evaluation of live porcine simulation training for robotic surgery. J Robot Surg. 2021 Jun;15(3):429-34. doi:10.1007/s11701-020-01113-3.

106. Glodny B, Unterholzner V, Taferner B, Hofmann KJ, Rehder P, Strasak A, et al. Normal kidney size and its influencing factors – a 64-slice MDCT study of 1.040 asymptomatic patients. BMC Urol. 2009 Dec 23;9:19. doi:10.1186/1471-2490-9-19.

107. Karami M, Rahimi F, Tajadini M. The evaluation and comparison of kidney length obtained from axial cuts in spiral CT scan with its true length. Adv Biomed Res. 2015 Jan 30;4:19. doi:10.4103/2277-9175.149850.

108. Emamian SA, Nielsen MB, Pedersen JF, Ytte L. Kidney dimensions at sonography: correlation with age, sex, and habitus in 665 adult volunteers. AJR Am J Roentgenol. 1993 Jan;160(1):83-6. doi:10.2214/ajr.160.1.8416654.

109. Arenas-Sarmiento F, Rincón-Uribe JS, Álvarez-Peña JC, Gómez-Torres FA, Cortés-Machado LS. Contribution to the anatomical study of urinary system in pigs. Spei Domus. 2015 Jun 1;11(22):17-24. doi:10.16925/sp.v11i22.1153.

110. Gómez FA, Ballesteros LE, Estupiñan HY. Morphological characterization of the renal arteries in the pig: comparative analysis with the human. Int J Morphol. 2017 Mar;35(1):319-24. doi:10.4067/S0717-95022017000100050.

111. Kalucki SA, Lardi C, Garessus J, Kfoury A, Grabherr S, Burnier M, et al. Reference values and sex differences in absolute and relative kidney size: a Swiss autopsy study. BMC Nephrol. 2020 Jul 20;21(1):289. doi:10.1186/s12882-020-01946-y.
112. Smit JHA, Leonardi EP, Chaves RHdeF, Furlaneto IP, da Silva CMS, Abib SdeCV, et al. Image-guided study of swine anatomy as a tool for urologic surgery research and training. Acta Cir Bras. 2021 Jan 20;35(12):e351208. doi:10.1590/ACB351208.
113. Talhar SS, Waghmare JE, Paul L, Kale S, Shende WR. Computed tomographic estimation of relationship between renal volume and body weight of an individual. J Clin Diagn Res. 2017 Jun 1;11(6):AC04-AC08. doi:10.7860/JCDR/2017/25275.10010.
114. Pereira-Sampaio MA, Favorito LA, Sampaio FJB. Pig kidney: anatomical relationships between the intrarenal arteries and the kidney collecting system. Applied study for urological research and surgical training. J Urol 2004 Nov;172(5 Pt 1):2077-81. doi:10.1097/01.ju.0000138085.19352.b5.
115. Satyapal KS, Haffejee AA, Singh B, Ramsaroop L, Robbs JV, Kalideen JM. Additional renal arteries: incidence and morphometry. Surg Radiol Anat. 2001;23(1):33-8. doi:10.1007/s00276-001-0033-y.
116. Evan AP, Connors BA, Lingeman JE, Blomgren P, Willis LR. Branching patterns of the renal artery of the pig. Anat Rec. 1996 Oct;246(2):217-23. doi:10.1002/(SICI)1097-0185(199610)246:2<217::AID-AR8>3.0.CO;2-Y.
117. Sampaio FJB, Aragao AHM. Anatomical relationship between the intrarenal arteries and the kidney collecting system. J Urol. 1990 Apr;143(4):679-81. doi:10.1016/s0022-5347(17)40056-5.

118. Tunc L, Resorlu B, Unsal A, Oguz U, Diri A, Gozen AS, et al. In vivo porcine model for practicing retrograde intrarenal surgery. Urol Int. 2014;92(1):64-7. doi:10.1159/000351420.

119. Shehata R. A comparative study of the urinary bladder and the intramural portion of the ureter. Acta Anat (Basel). 1977;98(4):380-95. doi:10.1159/000144817.

120. Ozturk NK, Kavakli AS. Use of bladder volume measurement assessed by ultrasound to predict postoperative urinary retention. North Clin Istanb. 2016;3(3):209-216. doi:10.14744/nci.2016.03164.

121. Dalmose AL, Hvistendahl JJ, Olsen LH, Eskild-Jensen A, Djurhuus JC, Swindle MM. Surgically induced urologic models in swine. J Invest Surg. 2000 May-Jun;13(3):133-45. doi:10.1080/08941930050075829.

122. Swindle MM, Makin A, Herron AJ, Clubb FJ Jr, Frazier KS. Swine as models in biomedical research and toxicology testing. Vet Pathol. 2012 Mar;49(2):344-56. doi:10.1177/0300985811402846.

123. Farag M, Timm B, Davis N, Wong LM, Bolton DM, Jack GS. Pressurized-bag irrigation versus hand-operated irrigation pumps during ureteroscopic laser lithotripsy: comparison of infectious complications. J Endourol. 2020 Sep;34(9):914-8. doi:10.1089/end.2020.0148.

124. Jakobsen JS, Holst U, Jakobsen P, Steen W, Mortensen J. Local and systemic effects of endoluminal pelvic perfusion of isoproterenol: a dose response investigation in pigs. J Urol. 2007 May;177(5):1934-8. doi:10.1016/j.juro.2007.01.020.

125. Danuser H, Weiss R, Abel D, Walter B, Scholtysik G, Mettler D, et al. Systemic and topical drug administration in the pig ureter: effect of phosphodiesterase inhibitors alpha1, beta and beta2-adrenergic receptor agonists and antagonists on the

frequency and amplitude of ureteral contractions. J Urol. 2001 Aug;166(2):714-20. doi:10.1016/s0022-5347(05)66049-1.

126. Butruk B, Trzaskowski M, Ciach T. Fabrication of biocompatible hydrogel coatings for implantable medical devices using Fenton-type reaction. Mater Sci Eng C Mater Biol Appl. 2012 Aug 1;32(6):1601-9. doi:10.1016/j.msec.2012.04.050.
127. Königsberger E, Wang Z, Königsberger LC. Solubility of L-cystine in NaCl and artificial urine solutions. Monatshefte fuer Chemie. 2000;131(1):39-45. doi:10.1007/s007060050004.
128. Kazmierska K, Szwast M, Ciach T. Determination of urethral catheter surface lubricity. J Mater Sci Mater Med. 2008 Jun;19(6):2301-6. doi:10.1007/s10856-007-3339-4.
129. Luk A, Junnarkar G. Critical challenges to the design of drug-eluting medical devices. Ther Deliv. 2013 Apr;4(4):471-7. doi:10.4155/tde.13.17.
130. Koźlik M, Harpula J, Chuchra PJ, Nowak M, Wojakowski W, Gąsior P. Drug-eluting stents: technical and clinical progress. Biomimetics (Basel). 2023 Feb 9;8(1):72. doi:10.3390/biomimetics8010072.
131. Forman MB, Brewer EC, Brown ZR, Menshikova EV, Lowman AM, Jackson EK. Novel guidewire design and coating for continuous delivery of adenosine during interventional procedures. J Am Heart Assoc. 2021 Feb 2;10(3):e019275. doi:10.1161/JAHA.120.019275.
132. Szymanski MW, Singh DP. Isoproterenol. [Updated 2023 May 1]. In: StatPearls [Internet]. Treasure Island, Fla.: StatPearls Publishing; 2024 [cited 16 May 2024. Available from: https://www.ncbi.nlm.nih.gov/books/NBK526042/

133. Andersson KE, Wein AJ. Pharmacology of the lower urinary tract: basis for current and future treatments of urinary incontinence. Pharmacol Rev. 2004 Dec;56(4):581-631. doi:10.1124/pr.56.4.4.

134. Jung H, Nørby B, Frimodt-Møller PC, Osther PJ. Endoluminal isoproterenol irrigation decreases renal pelvic pressure during flexible ureterorenoscopy: a clinical randomized, controlled study. Eur Urol. 2008 Dec;54(6):1404-13. doi:10.1016/j.eururo.2008.03.092.

135. Ji C, Gan W, Guo H, Lian H, Zhang S, Yang R, et al. A prospective trial on ureteral stenting combined with secondary ureteroscopy after an initial failed procedure. Urol Res. 2012 Oct;40(5):593-8. doi:10.1007/s00240-012-0476-0.

136. Hubosky SG, Healy KA, Grasso M, Bagley DH. Accessing the difficult ureter and the importance of ureteroscope miniaturization: history is repeating itself. Urology. 2014 Oct;84(4):740-2. doi: 10.1016/j.urology.2014.06.029

137. Mogilevkin Y, Sofer M, Margel D, Greenstein A, Lifshitz D. Predicting an effective ureteral access sheath insertion: a bicenter prospective study. J Endourol. 2014 Dec;28(12):1414-7. doi:10.1089/end.2014.0215.

138. Viers BR, Viers LD, Hull NC, Hanson TJ, Mehta RA, Bergstralh EJ, et al. The difficult ureter: clinical and radiographic characteristics associated with upper urinary tract access at the time of ureteroscopic stone treatment. Urology. 2015 Nov;86(5):878-84. doi:10.1016/j.urology.2015.08.007.

139. Lildal SK, Sørensen FB, Andreassen KH, Christiansen FE, Jung H, Pedersen MR, et al. Histopathological correlations to ureteral lesions visualized during ureteroscopy. World J Urol. 2017 Apr 12;35(10):1489-96. doi:10.1007/s00345-017-2035-3.

140. Traxer O, Thomas A. Prospective evaluation and classification of ureteral wall injuries resulting from insertion of a ureteral access sheath during retrograde intrarenal surgery. J Urol. 2013 Feb;189(2):580-4. doi:10.1016/j.juro.2012.08.197.
141. Mortensen J, Bisballe S, Jørgensen TM, Tågehøj-Jensen F, Djurhuus JC. The normal pressure-flow relationship of pyeloureter in the pig. Urol Int. 1982;37(1):68-72. doi:10.1159/000280799.
142. Zhou J, Yin H, Ma H, Wei S, Wen E, Zhang W, et al. An efficient and selective analytical method for the quantification of a β-adrenoceptor agonist, isoproterenol, by LC-MS/MS and its application to pharmacokinetics studies. J Liq Chromatogr Relat Technol. 2017;40(13):699-705. doi:10.1080/10826076.2017.1348952.
143. Palombo P, Bürkle A, Moreno-Villanueva M. Culture medium-dependent isoproterenol stability and its impact on DNA strand breaks formation and repair. Chem Biol Interact. 2022 Apr;357:109877. doi:10.1016/j.cbi.2022.109877.
144. Park YC, Tomiyama Y, Hayakawa K, Akahane M, Ajisawa Y, Miyatake R, et al. Existence of a beta3-adrenoceptor and its functional role in the human ureter. J Urol. 2000 Oct;164(4):1364-70. doi:10.1016/S0022-5347(05)67200-X.
145. Waseda Y, Takazawa R, Kobayashi M, Fuse H, Tamiya T. Different failure rates of insertion of 10/12-Fr ureteral access sheaths during retrograde intrarenal surgery in patients with and without stones. Investig Clin Urol. 2022 Jun 28;63(4):433-40. doi:10.4111/icu.20220081.
146. Roberts WW, Cadeddu JA, Micali S, Kavoussi LR, Moore RG. Ureteral stricture formation after removal of impacted calculi. J Urol. 1998 Mar;159(3):723-6. doi:10.1016/S0022-5347(01)63711-X.

147. Chhettri P, Shrestha A, Basnet RB, Shrestha PM. Pre-stenting for retrograde intrarenal surgery – need and duration: a prospective randomized clinical study. Nepalese Med J. 2020;3(2):361-5. doi:10.3126/nmj.v3i2.33050.

148. Joshi HB, Stainthorpe A, MacDonagh RP, Keeley FX Jr, Timoney AG, Barry MJ. Indwelling ureteral stents: evaluation of symptoms, quality of life and utility. J Urol. 2003 Mar;169(3):1065-9. doi:10.1097/01.ju.0000048980.33855.90.

149. Lildal SK, Andreassen KH, Christiansen FE, Jung H, Pedersen MR, Osther PJS. Pharmacological relaxation of the ureter when using ureteral access sheaths during ureterorenoscopy: a randomized feasibility study in a porcine model. Adv Urol. 2016 Oct 20;2016:8064648. doi:10.1155/2016/8064648.

150. Hubrecht RC, Carter E. The 3Rs and humane experimental technique: implementing change. Animals (Basel). 2019 Sep 30;9(10):754. doi:10.3390/ani9100754.

151. Hinman F, Lee-Brown R. Pyelovenous back flow: its relation to pelvic reabsorption, to hydronephrosis and to accidents of pyelography. JAMA. 1924;82(8):607-613. doi:10.1001/jama.1924.02650340017006.

152. Whitehurst L, Jones P, Somani BK. Mortality from kidney stone disease (KSD) as reported in the literature over the last two decades: a systematic review. World J Urol. 2019 May 27;37(5):759-76. doi:10.1007/s00345-018-2424-2.

153. Pauchard F, Bhojani N, Chew B, Ventimiglia E. How to measure intra-renal pressure during flexible URS: historical background, technological innovations and future perspectives. Actas Urol Esp (Engl Ed). 2024 Jan-Feb;48(1):42-51. doi:10.1016/j.acuroe.2023.10.007.

154. Shu X, Hua P, Xie L. An irrigation system for noninvasively estimating intrarenal pressure during flexible ureteroscopy. Int J Med Robot. 2021 Oct;17(5):e2306. doi:10.1002/rcs.2306.

155. Croghan SM, Somani BK, Considine SW, Breen KJ, McGuire BB, Manecksha RP, et al. Perceptions and practice patterns of urologists relating to intrarenal pressure during ureteroscopy: findings from a global cross-sectional analysis. J Endourol. 2023 Nov 1;37(11):1191-9. doi:10.1089/end.2023.0346.

156. Boston Scientific Corporation (Responsible Party). LithoVue Elite Registry (LVE). 2023 [cited 28 September 2024]. Available from: https://clinicaltrials.gov/ct2/show/NCT05201456

# Appendix 1 – Ethical clearance certificate 1

**UNIVERSITY OF CAPE TOWN**
**Faculty of Health Sciences**
**Animal Ethics Committee**

**Room E53-46 Old Main Building**
**Groote Schuur Hospital**
**Observatory 7925**
**Website**: www.health.uct.ac.za/fhs/research/animalethics/forms

27 July 2020

**Prof J. Lazarus**
Department of Urology
E26 GSH
Faculty of Health Sciences
University of Cape Town

Dear Prof Lazarus

**PROTOCOL TITLE:** Isoprenaline eluting guidewire project in white Landrace porcine model "Isowire"

**FHS AEC REF NO: 020_010**

Thank you for submitting your protocol to the Faculty of Health Sciences (FHS) Animal Ethics Committee (AEC) for review.

I am pleased to inform you that the FHS AEC has **approved** your protocol, which will terminate on **31 July 2023.**

Number of animals & species: 22 Pigs

**Please quote the FHS AEC REF NO (above) in all future correspondence.**

Please note that the approval of this protocol imposes the following obligations on the principal investigator (PI):

1. To submit an annual mandatory progress report. The first annual report for this protocol is due on **28 February 2021**. The forms can be accessed from http://www.health.uct.ac.za/fhs/research/animalethics/forms
2. To submit a final mandatory report on the **31 March 2023**, please access the final report form from: http://www.health.uct.ac.za/fhs/research/animalethics/forms
3. Ensuring that all study participants perform within the confines of the procedures and experimental design of the protocol as approved, or as amended.
4. Ensuring that all study participants comply with all applicable national legislation, UCT policies, FHS AEC policies and standard operating procedures (SOPs) and national standards (SANS 10386: 2008).

5. Ensuring that you as the PI immediately alert the FHS AEC to any event involving the welfare of the animals which has occurred during the course of the study, as well as the actions that were taken to respond to these events.
6. Ensuring that you as the PI alert the FHS AEC to any new or unexpected ethical issues that arose during the course of the study, and how these issues were addressed.
7. Ensuring that all study participants are registered with or have been authorised by the South African Veterinary Council (SAVC) to perform the procedures on animals or will be performing the procedures under the direct and continuous supervision of SAVC-registered veterinary professionals or SAVC-registered para-veterinary professionals.
8. If the PI or any study participant is in any way uncertain how to respond to any of these obligations or deal with any of the issues referred to above, they must consult with FHS AEC.
9. All animals found dead must be reported to the RAF on the appropriate form: http://www.health.uct.ac.za/fhs/research/animalethics/forms
10. All animals found in distress must be reported to the RAF on the appropriate form.

My best wishes for successful research and /or teaching endeavour.

Yours sincerely

Signed by candidate

**PROF G. LOUW**
**CHAIR, FHS AEC**

# Appendix 2 – Ethical clearance certificate 2

## EASTERN CAPE PROVINCE

DEPARTMENT OF HEALTH ISEBE LEZEMPILO

**CECILIA MAKIWANE AND FRERE HOSPITALS RESEARCH ETHICS COMMITTEE**
**NHREC PROVISIONAL REGISTRATION NUMBER: REC-260219-056**

**DEPARTMENT OF INTERNAL MEDICINE**
**PRIVATE BAG X 9047**
**EAST LONDON**
**5200**

Assoc Prof AG Parrish
Cell: 082 5765930
E-mail: andygp@mweb.co.za

Enquiries:

**18 August 2023**

**Protocol Title: Introducing the FIST (Frere Intrarenal Surgery Trainer) – a novel 3D-printed trainer for RIRS**
**Protocol Reference Number: FCMHREC/A0175/2023**
**Protocol Status: Approved**

**To Dr John**

**Dear Jeff**

The proposed study takes the form of a survey of clinicians, and as such does not entail clinical risk. Compliance with standards of Good Clinical Practice in terms of anonymizing information and data security are still essential in terms of collection, storage and publication of results.

**Explanation of protocol status:** 'approved' – the study may proceed with the conditions listed below; 'amendments required' – the suggested amendments are needed before the study will be approved and in the interim the study may not proceed; 'study not approved' – the study protocol was felt to contain substantive issues which will be spelt out below and the study may not proceed.

**Period of approval:** one year from the date of this letter. At the end of the approval period, please notify the committee of the status of the project (completed, discontinued or need for a further approval period). Also notify the committee at completion of the project on how you intend to feedback results to the local clinical and/or patient community.

**Conditions of approval:** Please inform the FCMREC in writing on the appropriate form if any of the following occurs: proposed protocol changes (FCMHREC/F056/2021); serious or unexpected adverse events (FCMHREC/F046/2021); unforeseen events that may affect the continuing ethical acceptability of the project. Urgent issues should also be communicated promptly either electronically or telephonically.

If you wish to appeal a decision of the FCMHREC, please do so using form FCMHREC/F047/2021.

Please note that the clinical governance structure of the institution(s) in which you intend to perform this study still need to be contacted both for permission to work within their clinical domain, and also so that they are aware of your activity on site.

**Yours sincerely**

Signed by candidate

**Assoc Prof AG Parrish**
**MBChB, DA(SA), MMed(Med), MMedSci, FCP(SA)**
**Chair, CMH and Frere Research Ethics Committee**

# Appendix 3 – Evaluating the FiST model: Participant consent form and questionnaire.

## Evaluating the FiST

## Participant Information/Consent Sheet

| | |
|---|---|
| Participant Number | |
| University | |

**What is the study about?**
To shorten the retrograde intrarenal surgery (RIRS) learning curve, various models – such as the Coloplast K-box and Cook Endourology Model, have been developed. While both have been validated – they are produced internationally and associated with high costs. We have designed a novel, the FiST (Frere Intrarenal Surgery Trainer) – a 3D printed training model.

**What will happen to me in the study?**

As with routine RIRS, you will first insert the scope into the bladder, identify and cannulate the ureteric orifice and insert the guidewire into the kidney. Thereafter, a ureteric access sheath will be inserted. A flexible, disposable ureteroscope will be inserted into the kidney through the ureteric access sheath. A nephroscopy to navigate the various calyces, and thereafter, laser lithotripsy was performed. Stone fragments will be removed using a standard stone basket.
There are no financial implications for taking part in this research.

**Why is the study being done?**

To conduct an assessment and validation study of the FiST model against real-life experience.

**Where will the study take place?**

The study will be done at the Karl Storz Offices, Homestead Place, Corner 12 Rivonia, Sandton.

**When will the study begin and possibly finish?**

The study will be performed during the weekend of 18 - 20th August 2023. Each participant will have a dedicated time slot to perform the procedure, assess and evaluate the FiST Model. me.

**Why have I been selected?**
You are one of the participants of the annual South African Urology Association (SAUA) Registrar masterclass. We invite all participants to participate in the study. You can ask questions about the study before deciding whether or not you would like to participate, and you may freely withdraw yourself/data from the study at any time.

**Who will lead the study?**
For any concerns and clarifications, please contact Dr Jeff John (jeffveenajohn@gmail.com), Professor John Lazarus or the Ethics Committee of the University of Cape Town.

---

**PARTICIPANTS CONSENT**

I, _____ do hereby consent to take part in the study.

Email: _____

Signature: _____ Date: _____

# Evaluating the FiST


| | |
|---|---|
| Participant Number | |
| University | |

| | | | | | |
|---|---|---|---|---|---|
| Position | Consultant | | | Yes ☐ | No ☐ |
| | Registrar | Yes ☐ | No ☐ | Year of Study | |
| | When do you plan on writing FC Urol (SA) finals? | | | | |
| | Would you consider yourself a "super-user" (i.e., more than 75 RIRS)? | | | Yes ☐ | No ☐ |

**Kindly evaluate the FiST model based on the Likert scale rating from 1 (strongly disagree) to 10 (strongly agree).**

Value of FiST in understanding RIRS-related procedures?

| | | | | | | | | | |
|---|---|---|---|---|---|---|---|---|---|
| 1 ☐ | 2 ☐ | 3 ☐ | 4 ☐ | 5 ☐ | 6 ☐ | 7 ☐ | 8 ☐ | 9 ☐ | 10 ☐ |

Value of FiST in stimulating contextual anatomy?

| | | | | | | | | | |
|---|---|---|---|---|---|---|---|---|---|
| 1 ☐ | 2 ☐ | 3 ☐ | 4 ☐ | 5 ☐ | 6 ☐ | 7 ☐ | 8 ☐ | 9 ☐ | 10 ☐ |

How realistic was it in cannulating the ureteric orifice?

| | | | | | | | | | |
|---|---|---|---|---|---|---|---|---|---|
| 1 ☐ | 2 ☐ | 3 ☐ | 4 ☐ | 5 ☐ | 6 ☐ | 7 ☐ | 8 ☐ | 9 ☐ | 10 ☐ |

How realistic is it to insert the ureteric access sheath?

| | | | | | | | | | |
|---|---|---|---|---|---|---|---|---|---|
| 1 ☐ | 2 ☐ | 3 ☐ | 4 ☐ | 5 ☐ | 6 ☐ | 7 ☐ | 8 ☐ | 9 ☐ | 10 ☐ |

How realistic is it to perform a nephroscopy and evaluate the calyces?

| | | | | | | | | | |
|---|---|---|---|---|---|---|---|---|---|
| 1 ☐ | 2 ☐ | 3 ☐ | 4 ☐ | 5 ☐ | 6 ☐ | 7 ☐ | 8 ☐ | 9 ☐ | 10 ☐ |

How realistic is it to perform laser lithotripsy?

| | | | | | | | | | |
|---|---|---|---|---|---|---|---|---|---|
| 1 ☐ | 2 ☐ | 3 ☐ | 4 ☐ | 5 ☐ | 6 ☐ | 7 ☐ | 8 ☐ | 9 ☐ | 10 ☐ |

How realistic is it to perform manual stone retrieval with a stone basket?

| | | | | | | | | | |
|---|---|---|---|---|---|---|---|---|---|
| 1 ☐ | 2 ☐ | 3 ☐ | 4 ☐ | 5 ☐ | 6 ☐ | 7 ☐ | 8 ☐ | 9 ☐ | 10 ☐ |

How realistic was the FiST model overall?

| | | | | | | | | | |
|---|---|---|---|---|---|---|---|---|---|
| 1 ☐ | 2 ☐ | 3 ☐ | 4 ☐ | 5 ☐ | 6 ☐ | 7 ☐ | 8 ☐ | 9 ☐ | 10 ☐ |

FiST model's perceived ability to enhance the trainee's confidence in performing RIRS?

| | | | | | | | | | |
|---|---|---|---|---|---|---|---|---|---|
| 1 ☐ | 2 ☐ | 3 ☐ | 4 ☐ | 5 ☐ | 6 ☐ | 7 ☐ | 8 ☐ | 9 ☐ | 10 ☐ |